Charles University in Prague
Faculty of Mathematics and Physics

DOCTORAL THESIS

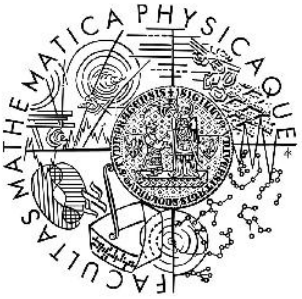

Hana Hromčíková

Modelling of radiobiological mechanisms in cells and tissues

Supervisor: RNDr. Miloš Lokajíček, DrSc.
Institute of Physics of the ASCR, v. v. i.
Prague

Study program: Physics of molecular and biological structures

First and foremost, my deepest thanks and gratitude are addressed to my supervisor RNDr. Miloš Lokajíček, DrSc. His guidance, comments and support were fundamental for all my work. I appreciate his endeavor to give me a motivation and comprehension for the problem domain.

Furthermore, I would like to express my gratitude and thanks to my colleague RNDr. Pavel Kundrát, PhD. His suggestions, discussions and inspiration were a real support to complete this doctoral thesis. Im very glad for his proofing of this text.

I would like to thank also the Institute of Physics, Academy of Sciences of the Czech Republic, for giving me the possibility to join numerous meetings and conferences, that were very helpful and inspirative for my research and study.

I am also thankful to RNDr. Pavel Ranocha, PhD. and Mgr. Václav Flaška for help with some mathematical problems and Mgr. Michal Reiter for discussing many aspect of writing in LaTeX.

Last, but definitely not least, I am very grateful to my family and friends and especially to my fiancé Ing. Josef Pisak for their support and encouragement.

I certify that I have written my thesis by myself and only using the references cited. I agree with lending my thesis.

Prague, November 21, 2008

Hana Hromčíková

Title: Modelling of radiobiological mechanisms in cells and tissues

Author: Hana Hromčíková

Department: Institute of Physics of the ASCR, v. v. i.

Supervisor: RNDr. Miloš Lokajíček, DrSc.

Supervisor's e-mail address: lokaj@fzu.cz

Abstract: The probabilistic two-stage model of cell inactivation enables to derive the characteristics of DNA damage induction and repair by analyzing published experimental survival data. To analyze in detail the cell inactivation effects of different ions at various energies, damage induction and repair processes in several hamster and human cell lines have been studied. Published survival data for Chinese hamster CHO-K1 cells and their radiosensitive mutants xrs5 irradiated by carbon ions and normal human fibroblasts irradiated by several light ions have been analyzed using the probabilistic two-stage model. The special attention is paid to studying the cellular repair processes. The comparison with two common used radiobiological models, the Linear quadratic model and the Local Effect Model, will be presented, too.

Keywords: irradiation, damage to DNA, cell survival curves, cell repair, radiobiological model

Contents

Part I

Theoretical background

Chapter 1

Introduction

1.1 Cancer diseases and treatment

Cancer is global term for more than 100 diseases, that have in common uncontrolled division of cells and their ability to attack other tissues. These abnormal cells can damage neighboring tissues by direct growth (invasion) or they can spread to distant places by transporting through the bloodstream or lymphatic system (metastases). The unregulated growth is induced by damage to DNA that causes mutations in genes that encode proteins controlling cell division.

More than 11 million people worldwide are diagnosed with cancer every year and it is estimated that this number will increase to 16 million new cases by 2020. Now cancer causes approximately 7 million deaths every year, that is 12.5% of deaths worldwide [http://www.who.int/en]. According to Institute of Health Information and Statistics [http://www.uzis.cz], Czech republic as compared to the rest of the world belongs to countries with high occurrence of tumors (especially colorectal and lung cancer).

Cancer is treated by surgery, chemotherapy, radiotherapy and biologic therapy or their combinations. In case the tumor is close to vital organs is radiotherapy often the only way to cure. The choice of optimal therapy type is depending on the location and phase of the tumor growth, as well as on the general condition of the patient.

During the last years, a big progress in modern techniques in all fields of cancer treatment has been made. This thesis is concerned with radiotherapy, particularly with a new promising method, hadron therapy. Classical radiotherapy is based on using X-rays to target tumor, but there is grow-

ing interest in using protons and ions instead. Beams of particles, such as protons and light ions, provide considerable advantages in comparison with X-ray radiotherapy. However, they have not been commonly used in clinical practice yet.

1.2 Radiotherapy

At the present time, radiotherapy is one of most effective methods used in cancer treatment. The aim of this treatment modality is to eliminate cells in tumor by irradiation with the smallest damage to normal tissues. Radiation therapy has been applied as a cancer treatment for more than 100 years, from the discovery of x-rays in 1895. The first concept of therapeutic radiation was suggested in fact by Wilhelm Conrad Röntgen when he discovered that the x-ray was a powerful and effective tool to kill cells. The x-ray radiation as a cancer treatment became the subject of medical research in the 1920s. In 1971 Godfrey Hounsfield invented a computed tomography (CT) [Ambrose et Hounsfield *et al* 1973, Hounsfield *et al* 1973], a very powerful modality for three-dimensional scanning of patient's body that make possible planning and measuring the dose delivered to the tumor based on axial tomographical images.

The development of new imaging technologies, e.g., magnetic resonance imaging (MRI) in the 1970s and positron emission tomography (PET) in the 1980s, new irradiation techniques as IMRT (Intensity-Modulated Radiation Therapy) and eventually IGRT (Image Guided Radiation Therapy) as well as using protons and heavier ions have led to better treatment outcomes and less side effects. Advancements in radiotherapy research have made it possible to cure cancers that had previously been regarded as incurable.

In next sections there is a very brief summary of radiotherapy methods used for treatment of oncological diseases.

1.2.1 Conventional therapy

Conventional radiotherapy is based on delivery of photons or electrons in two-dimensional beams using linear accelerator to shrink or destroy a tumor. It is usual to deliver the complete radiation dose in many sessions (fractions). This procedure spares normal tissues because of repair of sublethal damage between dose fractions and repopulation of cells [Hall *et al* 2006]. The damage of tumor cells increases, because of reoxygenation and reassortment of cells into radiosensitive phases of the cycle between dose fractions.

Brachytherapy

In contrast to external beam therapy, in which x-ray beams are focused at the tumor from outside the body, brachytherapy (also called internal radiation therapy) is based on placing a radioactive material directly inside or next to the tumor volume [Mazeron 2005]. The greatest advantage of this type of treatment is a possibility to use a higher total dose of radiation to treat a smaller area and faster than in the case of external radiation treatment.

There are two types of brachytherapy - temporary or permanent. In the case of temporary brachytherapy, the radioactive material is placed inside or near a tumor for a limited time and then removed. Temporary brachytherapy can be realized as a low-dose rate (LDR) or high-dose rate (HDR) treatment. Low-dose rate brachytherapy is also used in the treatment of coronary artery disease to prevent restenosis after angioplasty [Wolfram *et al* 2006]. Permanent brachytherapy (also called seed implantation) consist in placing radioactive seeds or pellets (about the size of several milimeters) in or near the tumor and leaving them in place permanently. The radioactivity level of the implants gradually decreases and after several months diminishes. The seeds then remain in the body, with no persisting effect on the patient [http://www.radiologyinfo.org].

3D Conformal Radiotherapy and Intensity-Modulated Radiation Therapy

Three dimensional conformal radiation therapy is a modern technique where the multiple x-ray beams are shaped exactly to the contour of the tumor volume. By using computed tomography treatment planning to image and model the tumor and its vicinity in three dimensions, 3D conformal radiation therapy allows to spare normal tissue much better than using classical irradiation.

Intensity-modulated radiation therapy (IMRT) is an advanced mode of three-dimensional conformal radiotherapy. It uses specialized software and computer controlled x-ray accelerators to model the intensity of radiation delivered to the treatment volume. Treatment is planned by using 3D computed tomography (CT) images of the patient following by dose calculations to choose the radiation intensity pattern that will best cover the tumor shape. The shaping is achieved by combinations of several intensity-modulated fields coming from different beam directions. Because the dose delivered to normal tissue is significantly lower in comparison to conventional techniques, markedly higher and therefore more effective doses can be delivered to treatment volume with fewer side effects.

Currently, IMRT is being used to cure tumors nearby organs at risk, like

cancers of the prostate, head and neck, thyroid, lung, as well as liver and brain tumors, lymphomas and sarcomas. In these days, it is one of the most precise forms of external beam radiation therapy available.

1.2.2 Hadron radiotherapy

The first proposal for using ions in radiotherapy was brought by Robert R. Wilson in 1946 [Wilson *et al* 1946]. He suggested to conform the dose to the tumor volume by using the Bragg peak, that is typical for penetration of charged hadrons in matter. The first treatments were done at proton accelerators built for physics research at Berkeley Radiation Laboratory in 1954 and at Uppsala in Sweden in 1957. The first radiotherapy proton center was opened in Loma Linda, California, and the heavy-ion therapy facility was completed in 1984 at Chiba in Japan. The summary of present particle therapy facilities is included in Appendix A.

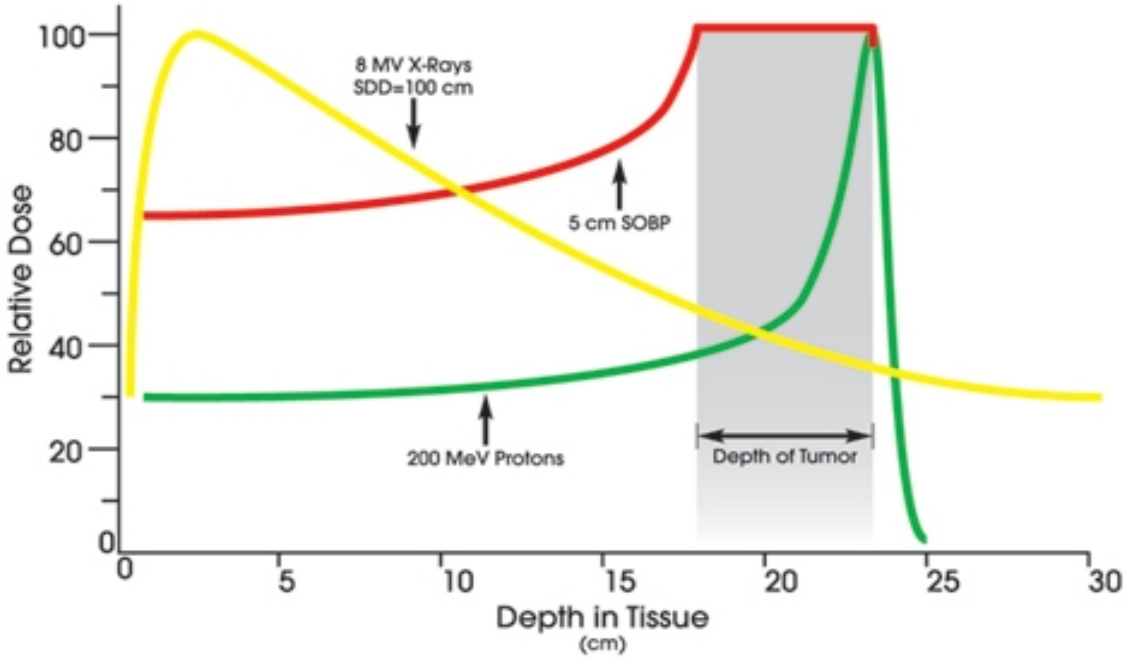

Figure 1.1: The comparison of the percentage of the absorbed dose in water for different radiotherapic sources: 8 MV X-Ray beam, monochromatic 200 MeV proton beams (Bragg curve), an a "modulated" proton beam, the so-called Spread Out Bragg Peak (SOBP) [Hall *et al* 2006]

The main difference between x-rays and ionizing particles is their different biological effect and depth-dose distribution. For x-rays the dose decreases

exponentially in dependence on penetration depths (Figure 1.1). Therefore tumors located in greater deep have to be irradiated from many sites in order to distribute the unwished dose in front of the tumor over a large volume when delivering a lethal dose to the tumor [Kraft 2007]. Contrary, for protons and ions is typical a steep increase of energy deposition at the end of the particle range. This ascension of energy given to the matter is called *Bragg peak* and it has been measured in 1903 by William H. Bragg. The sharp region of Bragg peak can be extended using special techniques into required shape, so-called Spread Out Bragg Peak - SOBP (see the red line in Figure 1.1). The another possibility to achieve covering of the tumor is active scanning of the volume by a thin "pencil" beam. In last decade the multiple beam irradiation (Intensity-Modulated Proton Therapy - IMPT) is available, too. Using this technique, the tumor can be shaped in all its contours with a precision of 2 - 3 mm. At present time, there are many proton and ion radiotherapy center all over the world (for detail review of hadrontherapy facilities see Appendix)

The comparison between conventional and hadron radiotherapy

The very modern techniques in conventional therapy, IMRT, achieves the excellent tumour control although a large volume of normal tissues is irradiated (see Figure 1.2 right panels). The major problem of this therapy is the induction of secondary tumours, especially in case of pediatric patients with long expected survival. Compared to an x-ray beam, a proton beam that is delivered with corresponding energy has a low dose in front of the tumor, a high-dose Bragg peak region that is designed to cover the entire tumor, and practically no dose beyond the tumor. Proton and especially heavier ions are characterized by high relative biological effectiveness (RBE) as a result of ionization density increase in the individual tracks of the particles, where DNA damage becomes clustered and therefore more difficult to repair. The RBE is defined as a comparison between two types of radiations to produce the same effect, therefore it is possible to say that in case of protons and ions lower dose is necessary to cause a certain result. The RBE depends on the possibility of repairing the damage caused by radiation. This is relevant in case of slowly growing tumors, which have a great repair capacity and therefore they are very radioresistant [Kraft 2007]. Moreover, carbon ion beams also have a smaller lateral scattering and range straggling compared to protons [Tobias *et al* 1979]. The dose distribution and primarily the biological effects of ions is often significantly better when compared to protons but also when compared to the IMRT. Another advantage of carbon ion therapy is the production of positron emitting carbon isotopes ^{10}C and ^{11}C that can be used for PET monitoring. The advantages of proton and ion therapy are

compensated by some limitations: the most important disadvantage is fact, that hadron therapy facilities are very expensive. Carbon therapy is even more expensive than proton, because for carbon ions are required greater energies, the accelerators are more expensive and for beam transport are used larger magnets. Because of greater RBE of protons and ions, for good utilization all benefits of this type of treatment is necessary very accurate treatment planning.

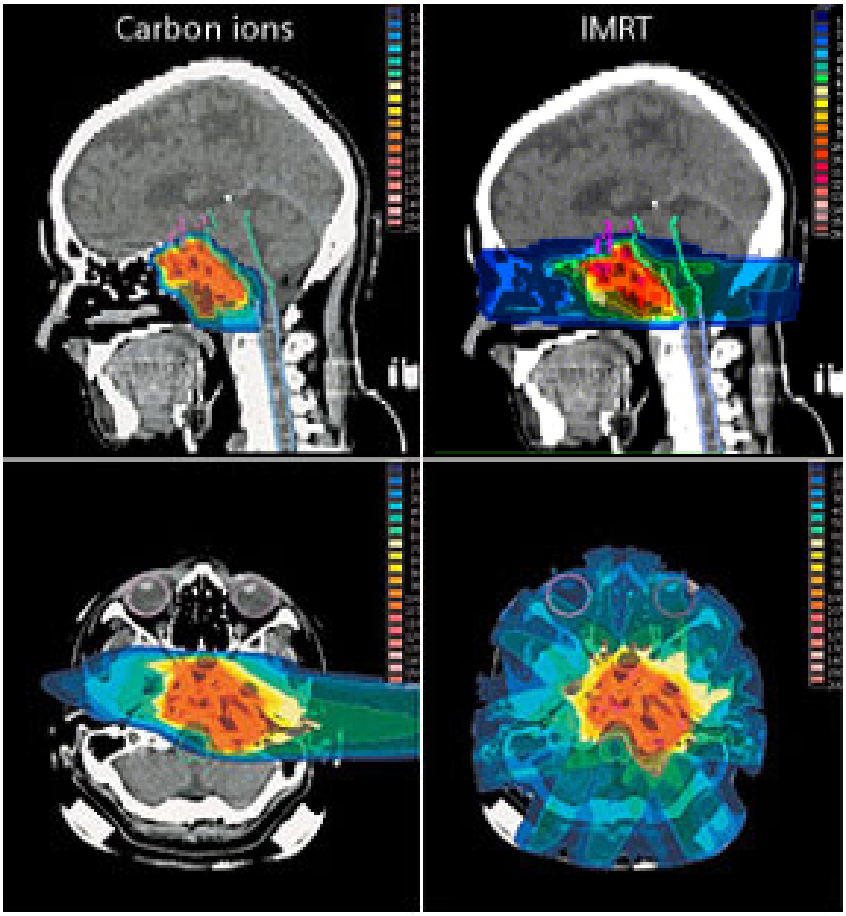

Figure 1.2: The comparison between dose distribution in hadron therapy (irradiation by carbon ions) and IMRT.
Picture from [http://www.medical.siemens.com]

1.2.3 Neutron therapy

Neutron beam therapy

Neutron therapy is based on the use of neutron beams, generated in proton or deuteron accelerators. Neutrons are high linear energy transfer particles and their effects to cells is done primarily by nuclear interactions [Montour *et al* 1974]. Fast neutrons are very suitable for treatment of very large tumors, because with increasing LET of particles the oxygen effect diminishes [Steel 1993]. This effect is significant in case of low-LET radiation, where for hypoxic cells the dose for inactivation certain ratio of cells is lower than for oxic cells (for details see section Oxygen effect and Oxygen Enhancement Ratio on the page 17). Moreover, the biological effectiveness of neutrons is not influenced by the stage in the life cycle of cancer cells. Because the biological effectiveness of neutrons is so high, the required number of fractions is approximately one third of the low LET radiation fractions. This type of treatment is suitable for broad spectrum of tumors, including palliative treatment of large tumors and their metastases. Neutron radiotherapy is offered at the Northern Illinois University Institute for Neutron Therapy at Fermilab (NIUINT at Fermilab) [http://www-bd.fnal.gov].

Boron Neutron Capture Therapy

After the discovery of the neutron by J. Chadwick in 1932, the ability of the boron nuclei to capture thermal neutrons has been measured. Boron Neutron Capture Therapy (BNCT) utilizes thermal or epithermal neutrons to irradiate tumors previously filled with the isotope ^{10}B. Neutrons interact with ^{10}B and produce alpha particle and lithium nuclei. The first step consist in intravenous injection of chemically modified ^{10}B, that binds to tumor cells in preference to normal ones. The neutrons are produced in reactors, or created in particle accelerators by impacts of protons into lithium or beryllium targets. After that, the energy spectrum of neutrons are adjusted by moderator and shaped by a collimator. In tissue they react with the ^{10}B, creating a excited isotope ^{11}B which immediately disintegrates to alpha particle and ^{7}Li. In place of decay the alpha particle and lithium ion create ionizations within a range of several micrometers. Therefore, the damage caused by radiations is limited only on a short range and normal tissues are spared. BNCT has been experimentally tested as an alternative treatment for some types of malignant brain tumors [Morris 1991].

1.3 Mathemical models in radiobiology and cancer treatment

At the present time, mathematical models are an integral part of radiobiological research. It is often necessary to compare various radiobiological data and set up a consistent and detailed theory of radiation mechanism in cells and tissues. One of the fundamental requirements in radiotherapy is a model describing relationships between given dose and cell survival. There is a need for reliable predictions of radiobiological effects caused by irradiation of defined radiation quality. For such predictions a mathematical formalism is necessary, often based on some underlying biophysical model. The modelling of radiobiological effect in cell is important for better understanding of the mechanisms in cells, for cancer treatment as well as for studying the radiation protection. The mathematical models should represents not only the qualitative attributes of the radiobiologic mechanism but also the quantitative parameters obtained in various experiments.

The most commonly used tool at the present time is the linear-quadratic (LQ) formalism, which describes cell survival through a parabolical curve in semi-logarithmic scale with two parameters (for details see Section Linear Quadratic Model on page 53). The LQ model also provides a approximate estimation of biological effects of fractionated irradiation [Steel 1993]. Although LQ model is relatively simple, it is possible to say that experimental data describes relatively satisfactory. At present time there are a tendencies to represent experimental data by models more related with physical and biological parameters. Because the cell and all processes after irradiation are very complicated system, the models involved often many parameters and relations. It is necessary to remember, that all models are only a simplified approach, although some of them are very precise. The review of main models used at the present time in radiobiology is described in chapter Modeling of radiobiological effects.

Chapter 2

Physics and radiobiology

2.1 Cell death and survival curve

A cell survival curve describes the dependence of radiation dose and a surviving fraction of cells. The survival fraction are usually plotted in a logarithmic scale because survival is almost an exponential function of dose and a logarithmic scale more easily allows to see and compare effects at very low survival rate [Steel 1993]. The difference between survival curve plotted in a linear and in a logarithmic scale is evident in the Figure 2.1.

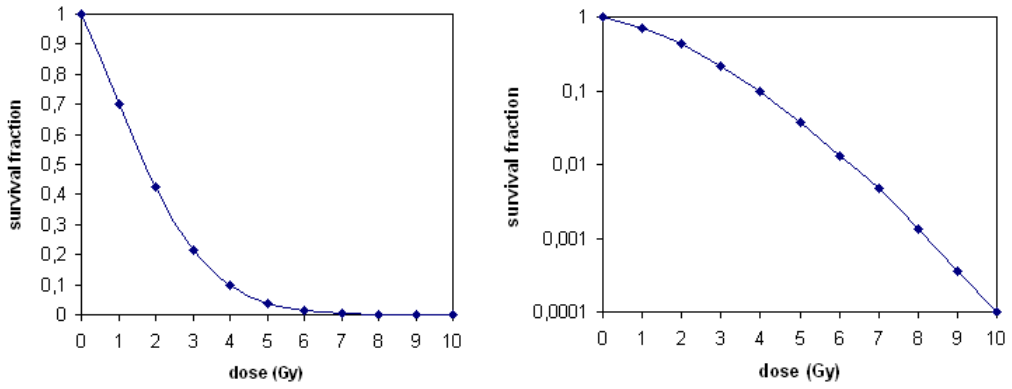

Figure 2.1: Comparison between survival curves plotted in non-logarithmic and logarithmic scale of axis y (s(D) means the surviving fraction of cells)

For this purpose it is necessary to define cell survival, or its reverse, cell death. For differentiated cells, such as nerve or muscle cells, that cannot

undergo a cell division, cell death means loss of their specific functions. For proliferating cells, like stem cells or squamous epithelial cells, cellular death is defined as the to loss of capability of sufficient proliferation. This is sometimes called *reproductive death* [Hall *et al* 2006]. After irradiation, cells may keep their function, may be able to synthetize proteins and DNA and can pass through one or two mitoses, but they do not have the capability of dividing and producing a large colony of daughter cells. In the commonly used terminology, these cells are not called "surviving". A cell that has kept its reproductive capability and is able to produce a large colony of progeny is said to be *clonogenic* [Hall *et al* 2006]. In laboratory routine as surviving cells are usually scored those which produce colonies of more than 50 cells.

2.1.1 Mechanisms of cell death

Cell may die by different mechanisms, the two main types of cellular death are apoptosis and necrosis. Apoptosis can be defined as an orderly and natural form of cell death that is sometimes programmed. Contrary, necrosis is always inappropriate or accidental, and usually occurs under adverse environmental conditions.

Apoptosis

Apoptosis was first described by Kerr [Kerr *et al* 1972] as a series of changes at the microscopic level leading to cell death. For apoptotic cells it is characterized by a special sequence of morphological modification. First, the cell shrinks because of cytoplasmic condensation, deforms and looses contacts to its adjacent cells. Chromatin condenses at the nuclear membrane, and finally the cell separates into a number of compact membrane-enclosed structures of differing sizes, called *apoptotic bodies* which contain cytosol, the condensed chromatin, and organelles. The apoptotic bodies are then absorbed by macrophages and thus are removed from the tissue without causing damage. Those morphological events are an effect of activation of proteolytic enzymes which finally cause the cleavage of DNA at specific sites between nucleosomes into oligonucleosomal packets as well as the fragmentation of protein substrates which determine the integrity and shape of the cytoplasm and organelles [Saraste *et al* 2000].

Necrosis

In contrast to apoptosis, liquidation of cell remains by phagocytes of the immune system is generally more difficult, because disorderly dying cells

generally send no molecular signals which tell adjacent phagocytes to engulf them. For the immune system it is hard to locate and recycle dead cells which have died through necrosis than if the cell had undergone apoptosis. There are four major types of necrosis: coagulative, caused by ischemia; liquefactive, usually caused by bacterial infections; caseous, that is distinct form of coagulative necrosis seen in mycobacterial infections; and fat necrosis, caused either by release of pancreatic enzymes from pancreas or intestine. Generally, necrosis is characterized by cell swelling and mitochondrial damage leading to rapid breakdown of homeostatic control. Cell membrane lyses and the release of the intracellular contents causes an inflammatory response, with oedema and damage to the surrounding cells [Majno *et al* 1995].

Mitotic death

The major form of cell death from irradiation is mitotic death [Hall *et al* 2006]. Death may occur in the first or second division after irradiation. It is hypothesized that mitotic cell death is a consequence of specific chromosomal aberrations such as asymmetric exchange-type abberations [Cornforth *et al* 1987].

Bystander effect

By-stander effect is defined as the induction of biologic effects in cells that are not directly traversed by a charged particle [Hall *et al* 2006]. According to many experiments, irradiated cells secrete a signalling molecules into the culture medium that is capable of killing adjacent unirradiated cells. On the other hand, medium irradiated without cells has no killing effect. Further experiments demonstrate that not all cells are capable of producing the toxic factor, nor all cells are able to receive the secreted signal [Mothersill *et al* 1997, Mothersill *et al* 2001]. The latest possibility to study this effect is the use of sophisticated single particle microbeams, which allow irradiating specific cells and studying biological effects at their neighbors [Randers-Pehrson *et al* 2001, Stewart *et al* 2002, Hall 2003].

2.2 Dose

Dose absorbed in matter is an amount of energy deposited by ionizing radiation. It is equal to the energy deposited per unit mass of medium (unit J/kg, called Gray (Gy)). Generally, the absorbed dose is not a good indicator of produced biological effect in cells and tissues. For example, 1 Gy of alpha particle irradiation is much more biologically effective than 1 Gy of photon

radiation. Suitable weighting constants can be used taking into account the different relative biological effects to find *the equivalent dose*.

Equivalent dose (H_T) is absorbed dose (D_T) multiplied by an appropriate constant, so called *the radiation weighting factor* (W_R):

$$H_T = D_T \, W_R \tag{2.1}$$

The radiation weighting factor W_R (dimensionless coefficient) depends on the pattern in which the energy of the radiation is distributed along the path of particle through the tissue. The value of w_R is 1 for x-rays, gamma rays and beta particles, but higher for protons, neutrons, alpha particles etc.

The equivalent dose is an estimation of the radiation dose given to the tissue where the different relative biological effects of various types of radiation are considered. The unit of equivalent dose is the sievert (Sv). Another unit (used mainly in USA) is Roentgen equivalent man (REM), 1 REM = 1/100 Sievert.

The response of individual tissues to irradiation is not equal. Therefore, another quantity, called *the effective dose* [Sv], is established. The equivalent dose is multiplied by a coefficient expressing the differing radiosensitivities of individual tissues.

The information about radiation weighting factor and other quantities in radiation protection can be found in [ICRP 1992].

2.3 Linear Energy Transfer

The linear energy transfer is an amount of the energy dE which a particle loses at a distance dl in matter. The International Commission on Radiological Units (ICRU) defined this term as follows [ICRU 1980]:

> The linear energy transfer (L) of charged particles in medium is the quotient of dE/dl, where dE is the average energy locally imparted to the medium by a charged particle of specified energy in traversing a distance of dl.

$$L = \frac{dE}{dl} \tag{2.2}$$

The unit of linear energy transfer is keV/μm. The LET is an average value because at the microscopic level, the energy per unit length enormously varies over such a wide range in dependence on the particle speed and other parameters [Hall *et al* 2006]. Another complication of LET determination consists in various possibilities to measure it. The most commonly used way

is to assess the track average, which is given by dividing the track length into equal sections, calculating the energy deposited in each segment and finding the mean. The second possibility is to divide the track into equal energy increments and averaging the lengths of track segments. These two methods give similar results for x-rays or monoenergetic charged particles, but for example for heavier particles the results can be very different [Hall *et al* 2006].

Generally speaking, relatively slowly moving alpha particles and heavier ions have a much higher LET than gamma rays and beta particles. The bigger biological effect of high LET particles is caused by depositing most of their energy within small range and the damage to the cell DNA is therefore larger.

2.4 Relative biological effectiveness

Radiobiological effect of given particles depends on many parameters, mainly on the particle type and energy. Densely ionizing radiation, e.g. high-Z low energy particles such as ions are expected to cause the highest biological effect. The differences in biological effects are given by diverse energy deposition at the microscopic level. Relative biological effectiveness, RBE, is defined as the ratio of doses of two ionizing radiations to produce the same effect:

$$RBE = \frac{\text{dose of reference radiation to produce a given effect}}{\text{dose of test radiation to produce a given effect}} \tag{2.3}$$

In comparing different types of radiation, it is usual to use x-ray radiation as the standard. In the case the two radiations do not give the same shapes of survival curve (e.g. x-ray survival curve have an initial shoulder and the carbon dose-survival being an exponential function of dose), the resultant RBE depends on dose. Figure 2.2 represents the definition of the RBE.

Generally speaking, RBE is a very complex quantity, depending on many parameters [Hall *et al* 2006]:

- **The radiation quality (LET)**
  The RBE increases with LET slowly and then steeper up to a maximum value, where the inactivation of cells by radiation is most effective. For higher LET, the energy is greater than is sufficient to kill the cell because the ionizing events are too close together (so called *overkill efect*), and RBE decreases (see Figure 2.3). RBE maxima for various particles are shown in Figure 2.4.

- **Dose and number of dose fractions**
  In general, the RBE is greater for lower doses. This is caused by

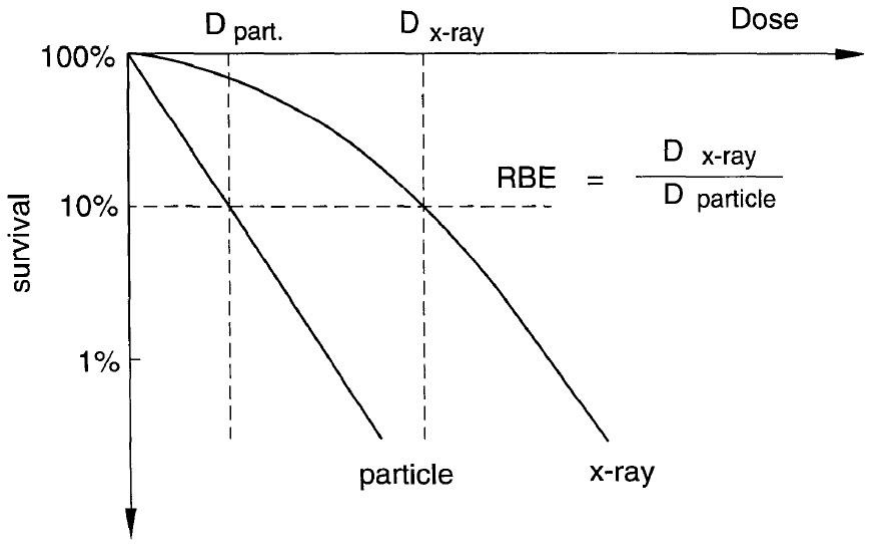

Figure 2.2: Relative biological effectiveness; picture from [Kraft 2001]

different shapes of survival curves for ions and X-rays: X-ray curves have an initial shoulder, whereas ions curves are straight lines in semi-logarithmical scale. The different heights of RBE maxima for a different survival fractions (SF) are seen in Figure 2.3. RBE for a fractionated irradiation is greater than for a single dose exposure, because fractions are set of small doses and the RBE is greater for small doses [Hall *et al* 2006].

- **Biological system, endpoint of biological measurement**
  The RBE is not very dependent on chosen endpoints if a particle beam of the same atomic number is used (relatively very different endpoints like DNA damage or cell inactivation have the RBE maximum at almost the same LET value [Kraft 2001]). However, the RBE varies critically for different cells and tissues. Tissues with great repair capability have a large RBE peak in contrast to systems with small or absent repair capacity, which have only a negligible or no RBE maximum [Kraft 2001].

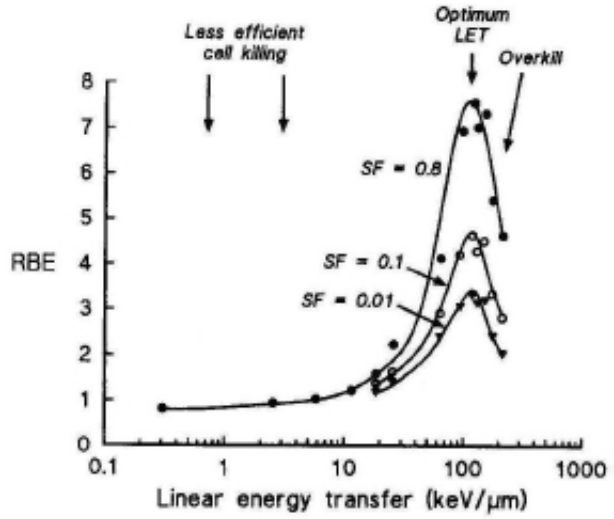

Figure 2.3: Dependence of relative biological effectiveness (RBE) on linear energy transfer (LET); taken from [Steel 1993]

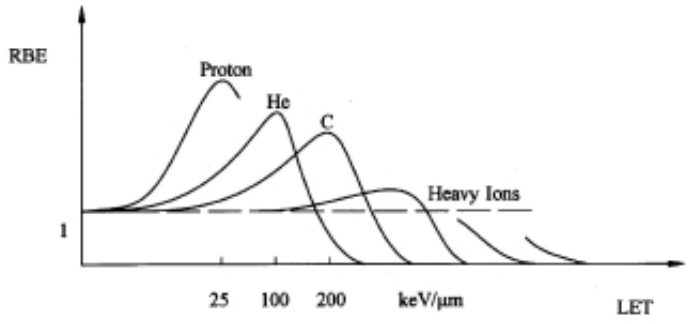

Figure 2.4: Relative biological effectiveness in dependence on particle type; taken from [Kraft 2001]

2.5 Oxygen effect

The inactivation effect of ionizing radiation is strongly dependent on presence of oxygen - cells are much more radiosensitive if they are aerated than those in hypoxic state [Steel 1993, Gray *et al* 1953]. This phenomenon was first described in 1923 by Petry in a study of the irradiation of vegetable seeds [Petry 1923]. Analogous to RBE, Oxygen Enhancement Ratio (OER) is a relation of radiation dose for hypoxic cells to the dose for oxic cells needed to achieve the same biological effect [Steel 1993]. Survival curves for oxic and hypoxic cells is presented in Figure 2.5.

$$OER = \frac{dose_{anoxic}\ to\ produce\ a\ given\ effect}{dose_{oxic}\ to\ produce\ a\ given\ effect} \tag{2.4}$$

There is an experimental evidence [Michael *et al* 1973] that the oxygen effect is observed only if oxygen is present during the irradiation or within a few milliseconds after. Measurable sensitization has been observed with oxygen added after 5 ms after irradiation [Hall *et al* 2006].

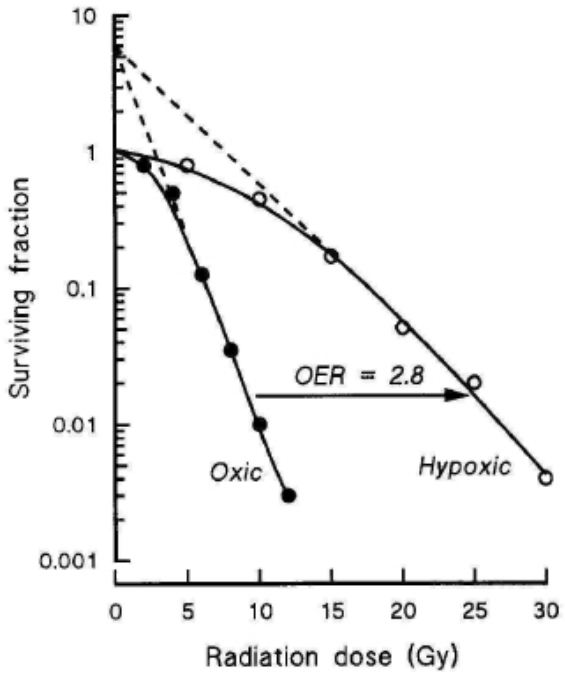

Figure 2.5: Oxygen Enhancement Ratio: Survival curves for mammalian cells exposed to x-rays under oxic and hypoxic conditions; picture from [Steel 1993]

One possible explanation of the oxygen effect mechanism gives the oxygen fixation hypothesis proposed on the basis of the model by [Alper *et al* 1956]. After irradiation in chemical phase, DNA reacts with the free radicals. The DNA radical can be chemically transformed to its reduced form through reaction with an SH group. If molecular oxygen is present in cells, non-restorable $RO_2\cdot$ (organic peroxide) is created. This reaction cannot proceed in the absence of oxygen. Therefore it is possible to say that oxygen fixates the radiation lesions [Hall *et al* 2006]. On the other hand, some recent analyzes [Ewing 1998, Lokajíček *et al* 2000] indicate that the oxygen fixation hypothesis does not satisfactorily explain why oxygen is a sensitizer. The basic chemistry proposed in the oxygen fixation hypothesis is correct, but the hypothesis does not explain why the reaction products mean a special risk to the cell. Attention must also be given to enzymatic DNA repair and to its success.

The question of oxygen effect is important in the radiation response of tumors. The solid tumors need a blood supply, so they induce creation of new blood vessel (angiogenesis) by secreting various growth factors. This new vessel system is usually primitive and not sufficient for the whole growing tumor. Therefore, tumor cells are located in a very different oxygen concentrations, ranging from very good oxygen supply in cells nearby the vessel to practically anoxic conditions in cells very far from vessel. The region of oxygen-deprived (hypoxic) cells that are radioresistant, is usually in the center of tumor.

The OER is strongly dependent on LET and the type of particle. The oxygen effect is more apparent for lower LET (< 50 keV/μm) and sparsely ionizing radiation, like x-rays (see Figure 2.6). Figure 2.7 illustrates the comparison of RBE and OER maxima dependence on LET. The increase of radiobiological efficiency of given radiation correlates with the decrease of the oxygen effect in tissues.

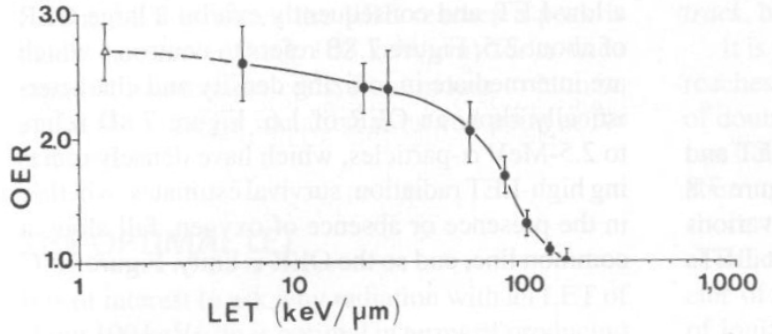

Figure 2.6: OER in dependence on LET. Measurements was done with human cultured cells, irradiation by monoenergetic charged particles (full symbols) and x-rays (open symbol) with an supposed LET value 1.3 keV/μm [Barendsen *et al* 1966]. Picture taken from [Hall *et al* 2006]

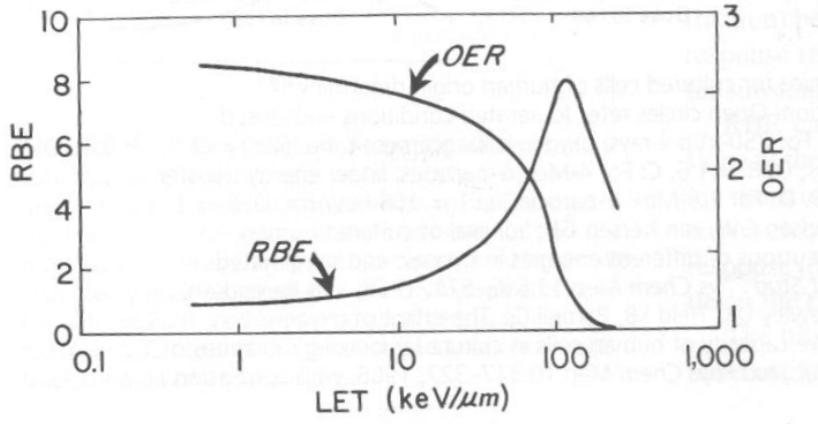

Figure 2.7: OER and RBE maxima in dependence of LET; picture taken from [Hall *et al* 2006]

Chapter 3

Biological effects of radiation

Irradiation of biological systems causes a sequence of different processes, which can be separate into three phases [Steel 1993] (see Figure 3.1):

- **Physical phase (0 -** 10^{-8} **s)** involves interactions between ionizing radiation and atoms in cells.
- **Chemical phase(**10^{-12} **- 10 s)** is the period in which excited and ionized atoms and molecules react with other cellular components in rapid chemical reactions.
- In **biological phase (**$10^{-1} - 10^{9}$ **s)** the response of cells, tissues and organism to irradiation is in progress.

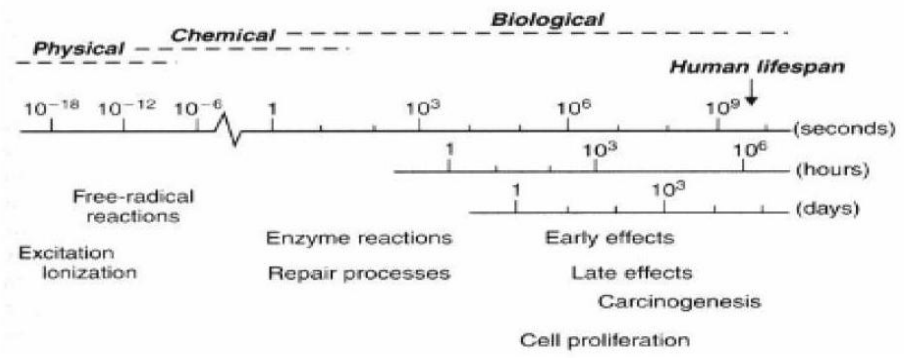

Figure 3.1: Time scale of radiation effects on biological systems; picture from [Steel 1993]

3.1 Physical phase

The physical phase begins with interaction of the radiation with atoms in cells. Radiation causes ejecting of orbital electrons from atoms (*ionization*) or raising electrons to higher energy levels within an atom or molecule (*excitation*). Secondary electrons may excite or ionize other atoms on the way which they pass, giving rise to a cascade of ionization events.

3.1.1 Types of radiations

Electromagnetic radiations - photons

The electromagnetic radiations x-rays and γ-rays are of the same nature, they differ only in the ways they are produced and their energy.

- **x-rays**
  X-rays are a form of electromagnetic radiation with the wavelength in the range 10^{-8} - 10^{-10} m. X-rays are emitted by charged particles (usually electrons) in changing atomic energy levels. They are produced in accelerator by colliding of electrons with a metal target. In medical applications, this is usually tungsten or its composite 5% rhenium and 95% tungsten. For specialized applications like mammography, molybdenum is used.

- **γ-rays**
  γ-rays (wavelength $< 10^{-10}$ m) are emitted from atomic nuclei during radioactive decay. Usually their emission is accompanied by the emission of an electron (beta ray) from the nucleus.

Particulate radiations

- **Charged particles**
  - *Electrons*
    Electrons are negatively charged particles. They may be accelerated to high energy (their speed is then close to the velocity of light) using betatron or linear accelerator. Electrons are widely used for cancer treatment [Hall *et al* 2006].
  - *Protons*
    Protons are positively charged, almost 2000 times heavier than electrons. For the sake of their mass, they must be accelerated

in larger devices than electrons - cyclotrons or synchrotrons are used.

- *α particles*
  These particles consist of two neutrons and two protons bound together (helium nucleus). Similarly as protons, they can be accelerated in cyclotrons or synchrotrons. Alpha particles are ejected from radioactive nuclei (uranium or radium) in an alpha decay. α particles are the main source of natural background radiation in nature [Hall *et al* 2006].
- *Heavy charged particles*
  Heavy charged particles are ions of elements such as carbon, oxygen, neon and others. They are positively charged and they have usually high kinetic energy ($\sim$ 100 MeV).

- **Uncharged particles**
  - *Neutrons* Neutrons are electrically neutral particles with mass a little bit larger than that of a proton. Neutrons for medical uses are usually produced by bombarding a beryllium target with protons.

3.1.2 Interactions of radiation with matter

Radiation may be classified as *ionizing* or *non-ionizing*. Non-ionizing radiation does not have enough energy to produce ions in the irradiated matter. Instead of producing charged ions, the non-ionizing radiation has adequate energy only for excitations. The examples of non-ionizing radiation are ultraviolet radiation, visible light, infrared radiation. Ionizing radiation has sufficient energy to break chemical bonds and eject electrons from the atoms. Ionizing radiation can be divided to *directly ionizing* and *indirectly ionizing* radiation. Directly ionizing particles are charged particles (electrons, protons, ions) with energy sufficient to disrupt the atomic structure of the matter and produce ions. The indirectly ionizing particles (uncharged particles like neutrons, photons) do not produce chemical and biological changes by themselves, but can eject directly ionizing charged particles from atoms in matter [Carlsson 1978].

Photons

The photon beam intensity is attenuated in matter due to absorption, scatter and pair production. The intensity of beam decreases exponentially with

depth:

$$I(d) = I_0 \, e^{-\mu d}, \tag{3.1}$$

where I_0 stands for initial value of intensity, $\mu = n\sigma$ is the absorption coefficient [m^{-1}]; here n is the number of atoms per m^3 in the material, σ means the absorption cross section (in m^2).

Generally, there are several types of interactions between photons and matter; most important are Compton effect, photoelectric effect and pair production [Attix 1986]. The relative occurrence of these processes is schematically shown in Figure 3.2.

- *Compton effect*
  This effect has been first measured by A. H. Compton in 1923. An x-ray photon of wavelength λ collides with an electron of an atom and a photon of wavelength λ' emerges at an angle θ. The energy given to the orbital electron is sufficient to its ejection from the atom. This recoil electron can interact with other electrons in the surroundings. The amount of energy which the photon gives to the orbital electron is determined by the initial energy of the photon and by the geometry of the collision [van der Plaats 1969].

- *Photoelectric effect*
  In this case, the x-ray photon ejects an orbital electron from the atom and completely looses all its energy (photon is totally absorbed). A part of the photon energy is used for liberation the electron, the rest of the energy is received by the electron as kinetic energy. The ejected electron is traversing through the surrounding matter and is slowed down by other collisions. The empty place which the photoelectron leaves is then filled by an electron of a higher energy level and the redundant energy is emitted as characteristic x-radiation [van der Plaats 1969]

- *Pair production*
  Pair production is an absorption process in which a photon disappears and an electron and a positron are created. This process may occur if the energy of x-ray photon is greater than 1.02 MeV (because electron and positron so formed each have a mass equivalent to 0.51 MeV). The energy over 1.02 MeV is given to the electron-positron pair as kinetic energy. Pair production increases with higher atomic number and with increasing x-ray energy [Attix 1986, van der Plaats 1969].

- *Rayleigh (coherent) scattering*
  In this case, the photon is scattered by the combined action of the whole atom. The photon loses practically negligible amount of its energy

and the atom moves just enough to conserve momentum. After the collision, the photon is usually deflected by only a small angle. Rayleigh scattering contributes nothing to dose, because there is no ionization or excitation. The relative importance of Rayleigh scattering is only a few percent of the beam attenuation coefficient [Attix 1986].

- *Photonuclear reactions*
  Photon of great energy (about a few MeV) enters the nucleus, may cause its excitation and a proton or neutron is emitted. The neutron produced in this process may lead to problems in radiation protection during the treatment. Although the effects caused by neutrons in radiotherapy are insignificant in comparison with the predominating photon beam, there are limitations on neutron levels in radiotherapy beams [Attix 1986].

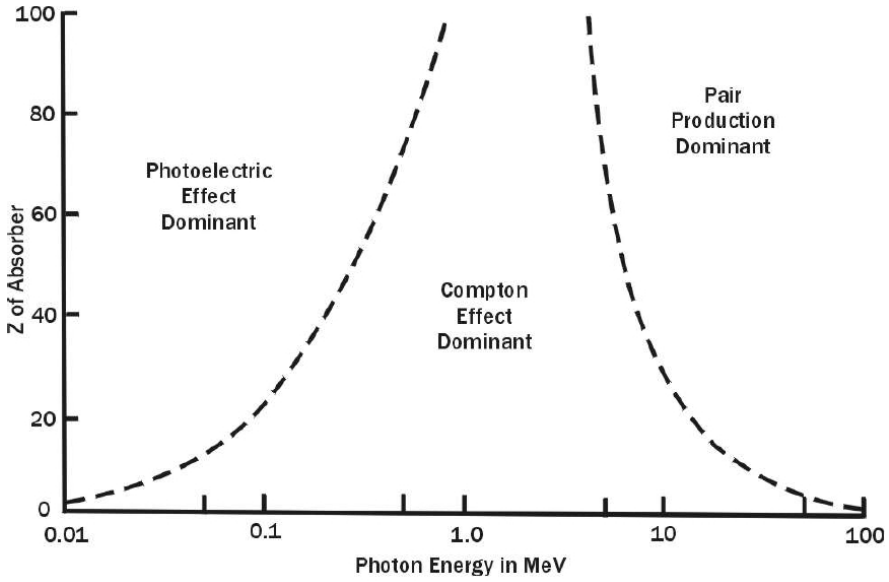

Figure 3.2: Relative occurrence of three most important types of photon interactions; picture taken from [Attix 1986]

Charged particles

There is a big difference between charged and uncharged particles and in a manner in which they lose their energy. An individual photon or neutron may traverse in matter practically with no interaction and lose its energy in

one or a few events. In contrast, the charged particles are surrounded by Coulomb electric force field and interact practically with all atoms that they have passed [Attix 1986]. If only the interactions given by coulombic forces are considered, there are four types of interactions of charged particles with matter:

- *Inelastic collision with electrons*
  This is the main process of energy transfer, especially if the velocity of the particle is lower and bremsstrahlung is not very significant. Charged particles cause excitations of the atomic electrons and ionizations.

- *Inelastic collision with nucleus*
  The charged particle causes the excitation of the nucleus or the particle may radiate (bremsstrahlung). Bremsstrahlung is electromagnetic radiation produced by the deceleration of a charged particle, when deflected by atomic nucleus. Bremsstrahlung increases with kinetic energy of the incident particle and with atomic number of the nucleus.

- *Elastic collision with nucleus - Rutheford scattering*
  The charged particles lose its energy only by recoil by the nucleus. There is no radiation and no ionization.

- *Elastic collision with electrons*
  The recoil of charged particles on atomic electrons is significant only for low energy electrons.

The transfer of energy in matter is given mainly by inelastic collision of charged particles with atomic electrons. This energy loss describes the *Bethe-Bloch formula* [Bethe 1930, Bloch 1933]:

$$-\frac{dE}{dx} = \frac{4\pi}{m_e c^2}\frac{nZ^2}{\beta^2}\Big(\frac{e^2}{4\pi\varepsilon_0}\Big)^2\Big[ln\Big(\frac{m_e c^2\beta^2}{I(1-\beta^2)}\Big) - \beta^2\Big], \tag{3.2}$$

where β = v / c
v ... velocity of the particle
E ... energy of the particle
x ... distance travelled by the particle
c ... speed of light
Z ... particle charge
e ... charge of the electron
ε_0 ... vacuum permittivity
m_e ... rest mass of the electron

n ... electron density of the target, $n = \frac{N_A Z^* \rho}{A}$; N_A stands for Avogadro number, Z^* is atomic number, A means mass number and ρ describes the density of the matter

I ... excitation potential of the target

From this equation it follows that energy given to a mass is inversely proportional to velocity of the particle squared, thus protons and ions deliver majority of its energy in the end of range. The energy loss in dependence on depth (x) (including also effects like energy-loss straggling) can be depicted as so-called *Bragg curve*, see Figure 3.3.

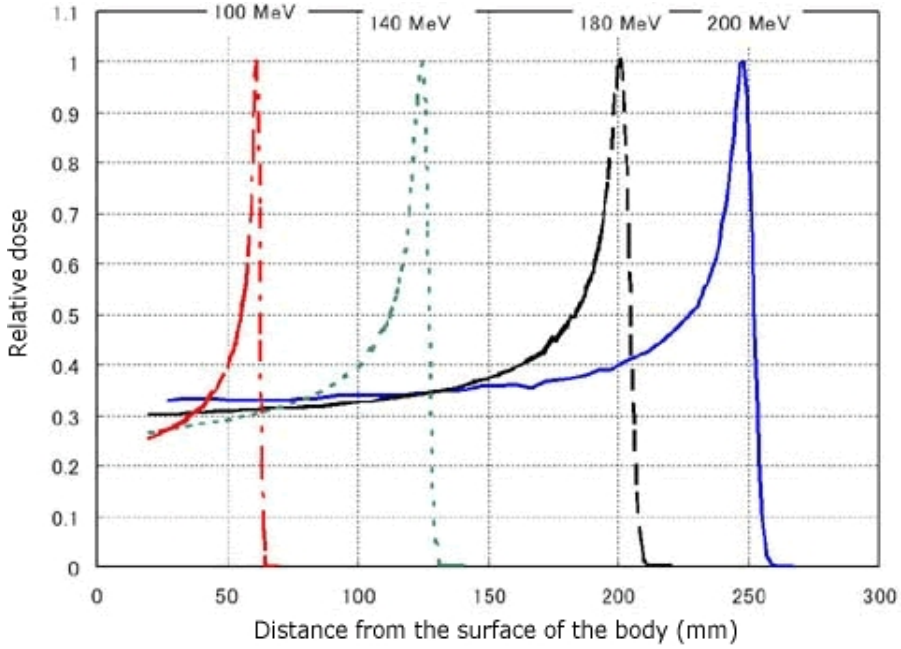

Figure 3.3: Depth-dose curve for different energy of protons, picture taken from [http://www.werc.or.jp]

In the literature, energy loss of different particles in different materials were calculated with various refinements such as shell correction, Bloch corrections from the first Born approximation, the density-effect correction and others. These calculations are discussed in detail for example in [Attix 1986, ICRU 1993, Ziegler 1999, Ulmer 2007]. Because the ionization energy loss are of stochastic nature, large fluctuations may emerge in the amount of energy deposited by a particle traversing the matter. The Bethe-Bloch formula gives only the average value of energy loss. The individual energy losses are distributed with various probability around the mean value. This distribution may be considered as Gaussian in the first approximation [Kundrát 2004].

To calculate the range, diffusion and slowing down of charged particles it is necessary to use the complete set of differential cross sections for energy losses and angular deflections in all collisions. There are two widely used approximations [ICRU 1993]:

- *Continuous slowing down approximation - CSDA*
  In this approximation charged particles are assumed to transfer their energy continuously along their tracks. The CSDA range mean the path length that a particle would traverse when slowing down from its original energy E_0 to a stop, if its rate of energy loss along the track were equal to the mean rate of energy loss [Attix 1986].

- *Straight ahead approximation*
  The charged particle is being scattered during its path throughout material (multiple scattering). In this case, the angular deflections caused by multiple scattering are omitted and track of the particle are assumed to be straight. For charged particles, this approximation is very good except the very end of particle track.

The range of a charged particle is the distance it travels before it stops, i.e. it looses all its kinetic energy by interacting with atoms in matter. The distance traveled per unit energy loss is given by the reciprocal value of the stopping power S(E)= $-\frac{dE}{dx}$. The mean range R(T) of a particle of kinetic energy T is the integral of reciprocal stopping power down to zero energy [Turner 1995]:

$$R(T) = \int_0^T (-\frac{dE}{dx})^{-1} dE. \tag{3.3}$$

The distribution of individual ranges around mean value can be considered as Gaussian, similarly as for the energy losses. The range depends on the type of the particle, on its initial energy and on the material which it traverses. Because of stochastic nature of individual energy transfers, the range of particle is a stochastic quantity, too.

The scattering and energy loss straggling blur the Bragg peak. Heavier ions (carbon, oxygen, neon etc.) have less lateral scattering than protons and sharper Bragg maximum, but fragmentations of nuclei caused by nuclear reactions especially for high energy induce a "tail" beyond the Bragg peak (see Figure 3.4). Fragmentation limits the use of absorber material in the beam (i.e. for passive beam shaping). Especially for heavier ions like neon an unacceptable amount of fragments is created. In case of carbon ions the number of fragments is tolerable when the beam energy is set up by the accelerator without passive beam shaping devices [Kraft 2001].

The fragmentation of ions gives a possibility of PET verification of treatment plans. In case of carbon irradiation, the small amount of the incident

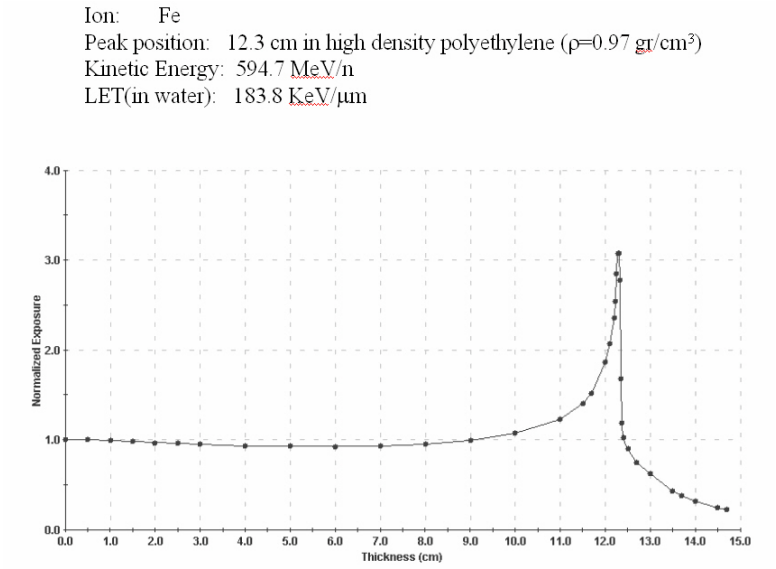

Figure 3.4: Bragg curve for Fe, picture taken from [http://www.bnl.gov]

ions undergoes nuclear fragmentation. They break up to one or two neutrons, that may convert the stable ^{12}C to isotopes ^{10}C and ^{11}C. These isotopes have almost the same velocity and ends at the almost same place as the main beam. These isotopes decay into e^+ and e^- and while annihilating they radiate γ-rays, that can be observed by PET scanner. Therefore, the location of the irradiating volume can be made visible [Hall *et al* 2006].

Neutrons

Because of zero electrical charge in comparison with charged particles the neutrons are highly penetrating. They cause indirect ionization and they are absorbed in matter mainly by elastic or inelastic scattering. In contrast to photons, which interact with orbital electrons, neutrons interact with the nuclei and give rise to recoil protons, α particles and nuclear fragments.

Neutrons can be classified into three energy categories: *thermal neutrons* (E $<$ 0.5 eV), *intermediate-energy neutrons* (E = 0.5 eV - 10 keV) and *fast neutrons* (E $>$ 10 keV). The typical interaction of thermal neutrons with tissue is neutron capture by nitrogen or by hydrogen. The dominating process for intermediate fast neutrons is elastic scattering, where the neutron collides with the nucleus and its kinetic energy is partly given to the nucleus and partly is retained by the reflected neutron. In soft tissue, the main interaction is between hydrogen nuclei and neutrons because hydrogen is most abundant

atom in tissues. For fast neutrons, inelastic scattering dominates. If neutron of high energy collides with the carbon or oxygen nucleus, three or four α particles are created (so called *spallation products*). The α particles so created are densely ionizing and may markedly contribute to biological effect of neutrons [Hall *et al* 2006].

3.2 Chemical phase

Ionization and excitation lead to the breakage of chemical bonds and the formation of free radicals. These are highly reactive and they can damage important molecules in the cell, especially DNA.

3.2.1 Radiolysis of water

The vast majority of biological molecules occur in an aqueous milieu; approximately 75-80 % of cells is composed of water [Hall *et al* 2006]. Therefore, the products of water radiolysis are the main factors in radiation-induced damage to DNA. The direct effect of excitations and ionizations of water by the secondary electron is the dominant reaction in cells for low LET irradiation [Alpen 1998]. The simplified scheme of water radiolysis is depicted in Figure 3.5. If the water molecule is excited by radiation, it may dissociate immediately to $H^\bullet$ and $OH^\bullet$:

$$H_2O^* \rightarrow H^\bullet + OH^\bullet. \tag{3.4}$$

As a result of ionization, the ion radical H_2O^+ is created:

$$H_2O \rightarrow H_2O^+ + e^-. \tag{3.5}$$

The excited water molecule H_2O^*, radicals $H^\bullet$ and $OH^\bullet$ and product from direct ionization of water, H_2O^+ and e^- are the *primary products* of water radiolysis. The *immediate products* are results of their reactions with water or other molecules [Alpen 1998]. H_2O^+ is charged and has an unpaired electron in the outer shell; this makes it highly reactive. The lifetime of $H_2O^+$is only about 10^{-10}s. The ion radical reacts with water molecule and forms reactive hydroxyl radical $OH^\bullet$:

$$H_2O^+ + H_2O \rightarrow H_3O^+ + OH^\bullet, \tag{3.6}$$

or dissociates

$$H_2O^+ \rightarrow H^+ + OH^\bullet. \tag{3.7}$$

The free electron produced by ionization interacts with H_2O to create H_2O^- or can form a cluster with water molecules e^-_{aq} (*solvated* or *hydrated electron*), compare [Alpen 1998, Platzman 1953]. The hydrated electron reacts with water molecule to produce OH^- and $H^\bullet$:

$$e^-_{aq} + H_2O \rightarrow OH^- + H^\bullet. \tag{3.8}$$

In the first 10^{-11} s there are created $H^\bullet$, $OH^\bullet$ and e^-_{aq}. In reactions of these early products is diffusion practically negligible.

Hydroxyl radicals reacts together and give rise the highly reactive hydrogen peroxide:

$$OH^\bullet + OH^\bullet \rightarrow H_2O_2. \tag{3.9}$$

If free oxygen is presented in cell, radicals are created:

$$e^- + O_2 \rightarrow O^- + O^\bullet, \tag{3.10}$$

and consequently

$$\begin{aligned} O^\bullet + H_2O &\rightarrow H^\bullet + HO^\bullet_2, \\ O^- + H_2O &\rightarrow H^\bullet + HO^-_2. \end{aligned} \tag{3.11}$$

As equations (3.10), (3.10) shown, the abundance of oxygen in cells leads to creation of highly reactive oxygen radicals, which may leads to further DNA damage (for details, compare section Oxygen effect at page 17).

3.2.2 Reactions with DNA

The radicals produced by radiolysis of water may damage the DNA molecule in many different ways [Alpen 1998]:

- *Extraction of hydrogen atoms*

$$R - H + H^\bullet \rightarrow R^\bullet + H_2, \tag{3.12}$$
$$R - H + OH^\bullet \rightarrow R^\bullet + H_2O. \tag{3.13}$$

- *Dissociative reactions*

$$R - NH^+_3 + e^-_{aq} \rightarrow R^\bullet + NH_3, \tag{3.14}$$
$$R - NH_2 + H^\bullet \rightarrow R^\bullet + NH_3. \tag{3.15}$$

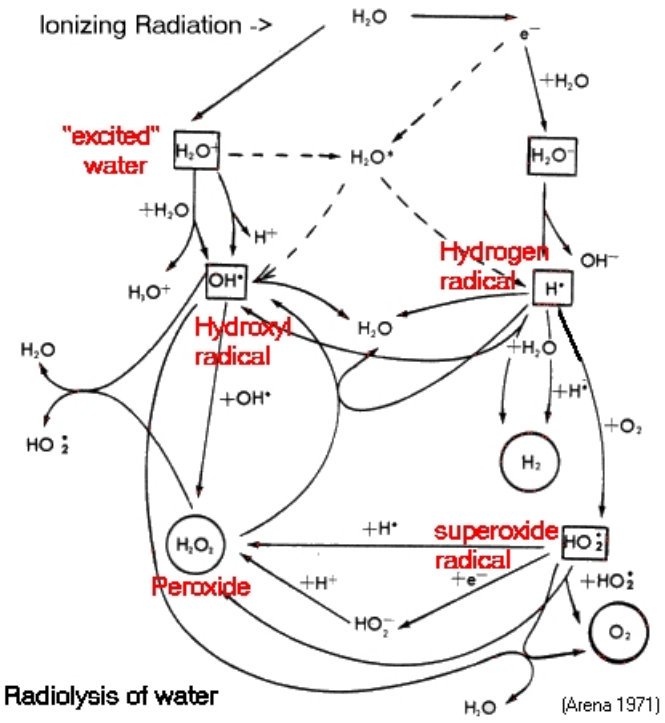

Figure 3.5: Scheme of the radiolysis of water. Taken from [Arena 1971]

- *Addition reactions*

$$R - CH = CH - R + OH^{\bullet} \rightarrow RCHOH - CH^{\bullet} - R. \tag{3.16}$$

- *Restitution*

$$R^{\bullet} + R - SH \rightarrow R - H + R - S^{\bullet}. \tag{3.17}$$

- *Damage fixation in oxygen effect*

$$R^{\bullet} + O_2 \rightarrow R^{\bullet} - peroxide. \tag{3.18}$$

Not all these reactions have the same importance for cell inactivation. There is a possibility to measure the relative contribution of individual radiation products to DNA damage in radical scavenging studies. According to experimental evidence, $OH^{\bullet}$ is the major agent in DNA damage [Alpen 1998, Chatterjee and Holley 1993]. The measured reaction rate constant for $OH^{\bullet}$ + DNA is approximately 3 x 10^8 mol.s^{-1} whereas for $H^{\bullet}$ + DNA just 1.4 x 10^8 mol.s^{-1} and for e^-_{aq} + DNA only 8 x 10^7 mol.s^{-1} [Alpen 1998].

There are a large number of possible reactions of the radicals produced in water radiolysis with molecules in cells. Detailed list of these reaction can be found e.g. in [Chatterjee and Holley 1993]. The water radiolysis by heavy charged particles is discussed in [Gervais *et al* 2006, Uehara and Nikjoo 2006, Yamashita *et al* 2008].

3.2.3 Chemical modification of radiation response

Radiosensitizers

Radiosensitizers are chemical compounds which enhance the response of cells to radiation. For practical use in radiotherapy, radiosensitizers must selectively sensitize tumor cells while having no effect on healthy tissues. At the present time, two kinds of compounds are being used in cancer treatment [Hall *et al* 2006]:

- *The halogenated pyrimidines*
  The halogenated pyrimidines are incorporated into DNA molecule in place of thymine. The differential effect is based on the idea that the tumor cells have faster cycle than normal tissues and consequently incorporate more of the radiosensitizer than normal cells. Detailed discussion about the radiosenzitizing effect of halogenated pyrimidines can be found e.g. in [Iliakis and Kurtzman 1991].

- *Hypoxic cells sensitizers*
  This method is based on the fact that in tumors hypoxic cells are present. The electron-affinic compounds selectively sensitize these hypoxic cells without effect on oxygenated cells. The clinically applicable compound must be able to selectively sensitize tumor hypoxic cells with tolerable toxicity to normal tissue, must be highly soluble in water and lipids and capable to diffuse through cell mass to tumor. The widely used compounds are e.g. misonidazole, etanidazole and nimorazole. An extensive survey of chemical radiosensitization of hypoxic cells is given in [Adams 1973, Adams 1977]

Radioprotectors

Radioprotectors (scavengers) are the chemical agents, that react with the radicals or other reactive species. The important scavengers are compounds with sulfhydryl group -SH (thiols), such as reduced glutathione, which is present normally in most cells. The mechanism of radiation protection by

thiols is given by:

$$DNA^{\bullet} + R - SH \rightarrow R - S^{\bullet} + DNA. \tag{3.19}$$

The clinical use of radioprotectors in radiotherapy is very problematic due to potential tumor protection and lowering of treatment efficiency.

3.3 Biological phase

The biological phase describes the period in which all subsequent processes are in progress. Enzymatic reactions repair majority of lesions in DNA. Some lesions remain unrepaired and this fact can lead to eventual cell death or mutation. Cells can undergo several mitotic divisions before dying. Killing of stem cells and the subsequent loss of the cells causes tissue damages during the first weeks and months after radiation exposure (*early effects*). At later times after the irradiation the so-called *late reactions* appear, such as fibrosis, blood-vessel damage. Later secondary tumors (radiation carcinogenesis) may appear, thus illustrating the fact that the timescale of the observable effects of ionizing radiation may extend up to many years after exposure.

3.3.1 DNA as a target for radiation damage

At the present time, there is a general agreement that chromosomes, specifically the DNA molecules, are the target for damage caused by ionizing radiation (compare e.g. [Alpen 1998, Steel 1993, Hall *et al* 2006, Ward 1990]. The evidence may be summarized in several points:

1. For primitive organisms, such as viruses and bacteriophages, there is a quantitative relationship between the DNA damage and biological function. The amount of strand breaks in DNA correlates very well with loss of biological functions.

2. For higher organisms the relation between DNA damage and biological inactivation is not such simple, but certainly loss of function has been measured with DNA strand breaks.

3. For many organisms the DNA repair capability is closely connected with cell survival after irradiation and cells lacking in the repair ability are substantially more radiosensitive. The artificially prepared mutants, which differ from maternal line only in repair capacity, are much more radiosensitive.

4. The other cell organelles are usually in abundance and the destruction of some of them has no effect on the cell survival. On the contrary, the DNA is in cell usually only in one or two exemplars (for haploid or diploid cells) and the exact sequence of bases is crucial for cell survival.

3.3.2 Sources and types of DNA molecule damage

Various changes of DNA molecule are caused by replication errors, heat, normal metabolic processes, radiation and exposure to substances in the environment. The number of this events averages to about 1 000 to 1 000 000 molecular lesions per cell per day [Lodish *et al* 2004]. Only fewer than one thousandth of this amount results in a permanent change in DNA, the rest are mended by DNA repair enzymes [Alberts *et al* 2002].

Sources of DNA damage can be divided into two groups:

- *endogenous* - replication errors, attack by reactive oxygen radicals produced during normal cellular respiration (spontaneous mutation), especially the process of oxidative deamination
- *exogenous* - induced by external causes like radiation, toxins, mutagenic chemical agents etc.

The replication of damaged DNA before cell division can lead to the incorporation of wrong bases to DNA strand. Daughter cells can inherit these mutations from which the original DNA sequence is unrecoverable.

Types of DNA damage

- *modification of the base* - all four of the bases in DNA can be modified at various positions
- *mismatches of the normal bases* as a result of a failure of proofreading during DNA replication (the wrong DNA base is stitched into place in a newly forming DNA strand)
- *breaks in backbone*
  - single strand breaks (SSB)
  - double strand breaks (DSB)
- *crosslinks* - covalent linkages between bases
  - intrastrand - on the same DNA strand

– interstrand - on the opposite DNA strand

Moreover, in scale of days, irradiation of the cell can cause mutations and chromosome and chromatid aberrations.

The schematic description of DNA damage is given in Figure 3.6.

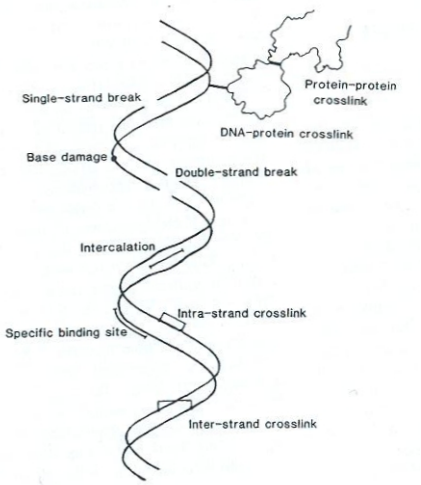

Figure 3.6: Types of DNA damage. Picture taken from [Steel 1993]

3.3.3 Other damages caused by radiation

Radiation-induced mutations

Some damage caused by irradiation is sufficient to change a cellular genetic information (*mutation*), but not enough to lead to stop cell division. Mutations come from a non-lethal modification of the base sequence in DNA. This alternation can be qualitative (bases are inserted, deleted or changed) or quantitative (genes are decreased or increased in number). Mutations lead to the expression of a different protein or may change amount of normal protein production. The frequency of radiation induced mutations usually increases proportionally with dose. At higher radiation doses lethal events in cells can prevail and the frequency of mutations decreases [Steel 1993].

Chromosome aberration

Chromosomal aberrations are disruptions in the normal chromosomal content of a cell. Damage to chromosomes is one of most common effect of ionizing

irradiation. The exposure of cells to ionizing radiations such as x-rays, γ-rays or charged particles causes a dose-dependent delay in the entering of cells into mitosis. When cells that were irradiated in interphase begin to divide, chromosome aberrations appear in some of them. Although the most serious chromosomal abnormalities lead to early cell death, some aberrations can be carried through many divisions [Steel 1993].

When cells are irradiated, breaks are produced in the chromosomes. Broken ends appear to be 'sticky' and can rejoin with any other sticky end. If breaks in DNA fibre are produced, different fragments may behave in a different ways:

- Breaks may reintegrate in their original state.
- Breaks may fail to rejoin and lead to a deletion.
- Broken ends may rejoin other broken ends and give rise to chromosomes that are deformed.

There are two main groups of abnormalities: *chromosome aberration* and *chromatid aberration*. Chromosome aberration results from irradiating cells early in interphase (G1 phase), before genetic material has been duplicated [Hall *et al* 2006]. Irradiation of cells later in interphase, after the DNA has doubled and the chromosomes consist of two strands of chromatin (G2 phase), leads to chromatid damage. Break that occurs in a single chromatid arm leaves the other arm of same chromosome undamaged. Irradiation in S phase can lead either to chromatid aberration or to chromosome aberration [Steel 1993]. The types of chromosome and chromatid aberrations and their occurrence in cell cycle are shown in Figure 3.7.

Many types of chromosome abnormalities are possible, not necessarily associated with cell inactivation.

- **Lethal aberrations**
  - *Dicentric or tricentric* (an interchange between two separate chromosomes)
  - *Formation of a ring* (a break is caused by irradiation in each arm of a single chromatid early in the cell cycle and the sticky ends may form a ring and a separate fragment)
  - *Anaphase bridge* (Breaks occur in both chromatids of the same chromosome, sticky ends rejoin incorrectly. In anaphase, when the two sets of chromosomes move to opposite poles of cell, the region of chromatin between the centromeres is stretched across between the poles and separation into new daughter cells is inhibited)

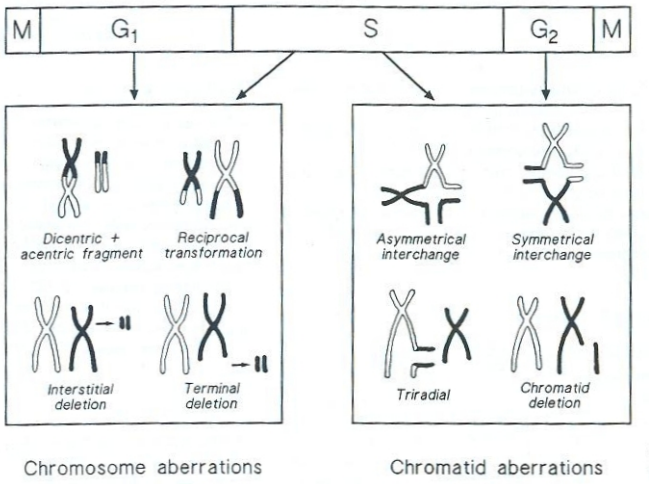

Figure 3.7: Scheme of radiation induced chromosome and chromatid aberrations. Picture taken from [Steel 1993]

- **Non-lethal rearrangements**
  - *Symmetric translocation* (radiation induces breaks in two different chromosomes since the replication has begun and the broken pieces are exchanged between these two chromosomes)
  - *Small interstitial or terminal deletion* (result from one or two breaks in the same arm of the same chromosome, leading to the loss of genetic information in the end of chromosome arm or between two breaks)

3.3.4 Detecting of DNA damage

Measurement of DNA double- and single-strand breaks frequency in mammalian cells is essential for the understanding of cell damage mechanisms by ionizing radiation and many DNA-reactive drugs. Many of these techniques can measure either SSB or DSB by manipulation of the pH.

Sucrose Gradient Sedimentation

In this technique [Steel 1993, Cox *et al* 1973], the solute is sucrose or some other not very dense substance that has perceptible viscosity. Solutions are prepared within centrifuge tubes with a sucrose concentration varying continuously from around 30 % at the bottom to 5 % at the top. Cells are

exposed to radioactive DNA precursors (^{3}H or ^{14}C thymidine) for labeling most of the DNA. After that, cells are mixed with solution that causes cell lysis and releases the DNA. The experimental substance is placed at top of the gradient, which is then centrifuged for up to 20 hours at about 20 000 - 30 000 rpm. The larger fragments migrate further and the distribution of fragment sizes is detected by piercing the bottom of the centrifuge tube, collecting fractions of the fluid and assaying for the modified thymidine.

Filter Elution Assay

The alkaline and neutral (or nondenaturing) filter elution assays are very useful methods for measuring DNA strand breakage [Rudinger *et al* 2002, Steel 1993]. In the 1970s Kohn developed these techniques [Kohn *et al* 1973], initially for total yield of strand breaks at pH sufficient to denature the strands (pH $>$ 12), then specifically for double strand breaks at near-neutral pH [Bradley and Kohn 1979]. Cells are lysed and DNA is prelabeled by radioactive ^{3}H or ^{14}C thymidine. The principle of filter elution is based on the fact, that the rate at which DNA fragments are carried through a microporous filter by a fluid flow depends on the size distribution of those strands.

Pulsed Field Gel Electrophoresis

This method is used to separate especially long strands of DNA by length, and for this reason it is very suitable for measuring of strand breakage produced by small radiation doses [Steel 1993]. Fragments of DNA are incorporated into a flat gel matrix of agarose and they generally migrate under an electric field. In case of normal electrophoresis, large DNA fragments (above 30-50 kb) migrate at similar rates, regardless of size. In this technique, the DNA molecules are forced to change direction of movement using pulsing electric field and alternating it (usually between directions 30 to the axis of motion). Consequently, fragments with different sizes begin to separate from each other. The theoretical basis of this effect is not clearly explained (numerous models have been proposed [Carle *et al* 1986, Birren *et al* 1993]), but generally speaking, the smaller fragments are able to re-orient to the new field more quickly than are larger ones. For calibrating this technique, DNA of known molecular weight (for example intact yeast chromosomes) is used [Steel 1993]. The detailed discussion about this technique and models that describes the behavior of DNA during PFGE can be found e.g. in [Chu 1990].

Single Cell Gel Electrophoresis assay

The single cell gel electrophoresis assay is a sensitive technique which detects DNA damage in individual cells. Individual cells or nuclei are placed in agarose, lysed under neutral buffer conditions to release the DNA and electrophoresed. The damage is represented by an increase of DNA fragments migrating out of the cell nucleus and creating the characteristic pattern resembling the comet with a head and a tail [Klaude *et al* 1996]. The image is visualized by ethidium bromide, silver stain or fluorescent dyes. If the cells are undamaged, under application of an electrical current their DNA does not migrate and the amount of migration DNA in the agarose is directly proportional to the quantity of damage [Hall *et al* 2006]. This method detects single-strand DNA breaks, alkaline-sensitive sites, incomplete excision repair sites and DNA crosslinks [Tice *et al* 1991, Tice *et al* 1995].

Fluorometric Analysis of DNA Unwinding

This method was invented by [Birnboim 1990] for detecting x-ray induced DNA damage in normal and repair-deficient mutants of mammalian cells. The method is based on the unwinding of DNA strand from break sites under alkaline conditions [Baumstark-Khan *et al* 2000]. Cells are lysed by addition of detergents and high salt concentrations and the DNA is denatured at pH 12,4. After neutralization using HCl the DNA is fragmented by ultrasound and after that stabilized by sodium lauryl sulfate. The solution that contains single- and double-stranded DNA, is applied to hydroxyapatite columns. By addition of increasing concentrations of potassium phosphate buffers single-stranded DNA and double-stranded DNA can be chromatographically separated. The eluate is incubated and the relative fluorescence (DNA content) of the sample is measured with a spectrofluorometer. Finally, the percentage of double-stranded DNA and the quantity of DNA breaks can be calculated [Ahnström *et al* 1981].

There are many other methods for detecting DNA damage: fragment length analysis using repair enzymes (FLARE) that enable base specific DNA damage detection [Chirikjian 1997], semi-artificial fluorescent molecular machine for DNA damage detection [Didenko *et al* 2004], acoustic waves [Hianik *et al* 2006], flow and laser scanning cytometry [Milner *et al* 1987, Darzynkiewicz *et al* 2006] etc.

3.3.5 DNA repair processes

Repair of damaged bases

Damaged or wrongly inserted bases can be repaired by several mechanisms:

- *direct chemical reversal of the damage*
- *excision repair*
  - Base Excision Repair (BER)
  - Nucleotide Excision Repair (NER)
  - Mismatch Repair (MMR)

Although direct chemical reversal is an efficient way of repair of some special types of DNA damage, excision repair is a more general way of dealing with a wide variety of DNA lesions. Therefore, the diverse kinds of excision repair play a crucial role in DNA repair mechanisms in both prokaryotic and eukaryotic cells. In excision repair, the damaged DNA base or bases are recognized primarily and after that removed by special set of enzymes. In place of missing bases the new DNA strand is then synthesized and the intact complementary bases act as a template. Three types of excision repair, Base Excision Repair, Nucleotide Excision Repair, and Mismatch Repair, each one with different sets of enzymes, enable cells to repair a variety of different types of DNA damages.

Direct chemical reversal of damage

Most damage to DNA molecule is repaired by some type of excision repair that consists in removal of the damaged bases and their new synthesis in the excised region. However, some specific kind of lesions in DNA can be repaired by *direct reversal of the damaged base*, which may be a more efficient way of repairing specific types of DNA damage that occur frequently [Cooper 2000]. But only a few types of DNA damage are repaired in this way, particularly pyrimidine dimers caused by exposure of DNA to ultraviolet light and alkylated guanine residues modified with methyl or ethyl groups at the O^6 position of the purine ring.

Pyrimidine dimers result from ultraviolet light absorbed by a double bond in pyrimidine bases, which causes opening of the bonds. If it is next to a second pyrimidine base on the same strand, the UV-modified bases set up a cyclobutane ring resulting from saturation of the double bonds between carbons C^5 and C^6. This formation deform the structure of the DNA molecule and blocks transcription or replication from this site on strand, so their repair

is closely correlated with the ability of cells to deal with UV irradiation. One mechanism of repairing UV-induced pyrimidine dimers is photoreactivation, a direct reversal of the dimerization reaction [Setlow 1966]. Energy derived from visible light is used to break the cyclobutane structure and the original pyrimidine bases remain in DNA, restored to the normal state. Photoreactivation repair of pyrimidine dimers is typical for a variety of prokaryotic and eukaryotic cells, including E. coli, yeasts, and some plants and animals. However, this mechanism of DNA repair is not universal for all species; many of them, including humans, lack this type of DNA repair.

The other type of direct chemical reversal in cells represents repair of alkylated guanine. O^6-methylguanine forms complementary base pairs with thymine instead of cytosine. This lesion can be repaired by an enzyme O^6-methylguanine methyltransferase that transfers the methyl group from to a cysteine residue in its active site and restore the normal state of guanine. This pathway of repair occurs in both prokaryotes and eukaryotes.

Base Excision Repair

In this type of repair, a single damaged base is recognized and removed from the DNA molecule and the correct one is replaced according to an undamaged template strand. The scheme of Base Excision Repair (BER) is demonstrated in Figure 3.8.

In the first step, a group of DNA glycosylases recognizes a modified base in DNA and catalyzes its hydrolytic removal. In the DNA molecule an apyrimidinic/apurinic (AP) or abasic site is, therefore, produced. There are at least six types of these enzymes, each intended for a special type of DNA damage, e.g. deaminated cysteins or adenines, different types of alkylated or oxidized bases, bases with opened rings and bases in which a double carbon-carbon bond is converted to a single one [Alberts *et al* 2002]. After that, AP endonuclease removes the sugar residue and the gap is filled with the correct nucleotide by DNA polymerase β. Finally, DNA ligase III restore the sugar backbone of the DNA strand. In case more that one nucleotide is to be replaced, the complex of RFC/PCNA/DNA polymerase δ/ϵ completes the repair synthesis, the overhanging flap structure is removed by the FEN1 endonuclease and DNA strands are sealed by ligase [Hall *et al* 2006]. BER is often responsible for correcting damages that occur spontaneously, due to replication errors, the inherent instability of DNA, or from alkylation of DNA. Defects in BER may caused an increased mutation rate, but usually do not lead to cellular radiosensitivity.

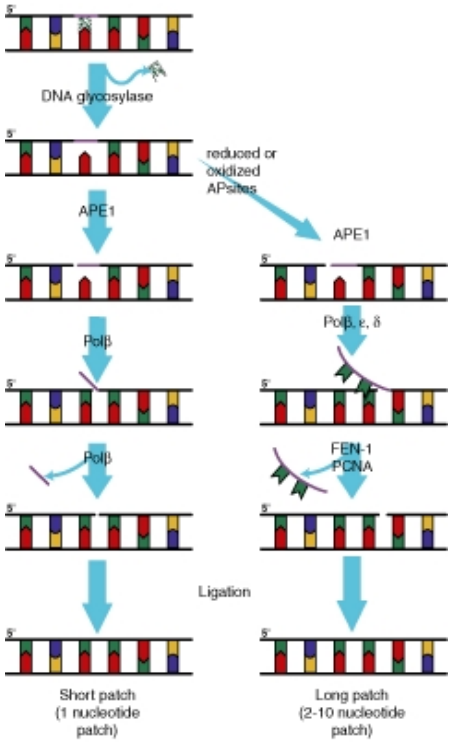

Figure 3.8: The scheme of two subpathways of BER. On the left is the repair of a single nucleotide (short patch), on the right is repair of two or more nucleotides (long patch).
Taken from [http://www.rndsystems.com]

Nucleotide Excision Repair

Nucleotide excision repair (NER) is a flexible repair pathway, involved in the removal of a wide variety of bulky DNA lesions, such as pyrimidine dimers. In this type of repair, the damaged bases (e.g., a thymine dimer) are removed as part of an oligonucleotide containing the lesion [Hall *et al* 2006]. There are two slightly different variants of NER: *global genomic NER* (GG-NER), which repairs damage in both transcribed and nontranscribed DNA strands in active and inactive genes in the genome, and *transcription coupled NER* (TC-NER), which proceeds on the actively transcribed areas of the DNA. These two forms of NER are practically identical except in their damage recognition mechanism. Successful NER involves the action of approximately 30 proteins and requires a stepwise execution of these events (see Figure 3.9):

1. Damage recognition by specialized enzymes.

2. Binding of a multi-protein complex at the damaged site. The subunits

of this complex have helicase activity and unwind the DNA locally in the damaged area.

3. Double incision of the damaged strand several nucleotides away from the damaged site, on both the 5' and 3' sides (the whole excision region is usually between 24 and 32 nucleotides in length) and displaced of the damage-containing oligonucleotide.

4. The gap is then filled by correct nucleotides by DNA polymerase δ/ϵ and the strand is sealed by a DNA ligase.

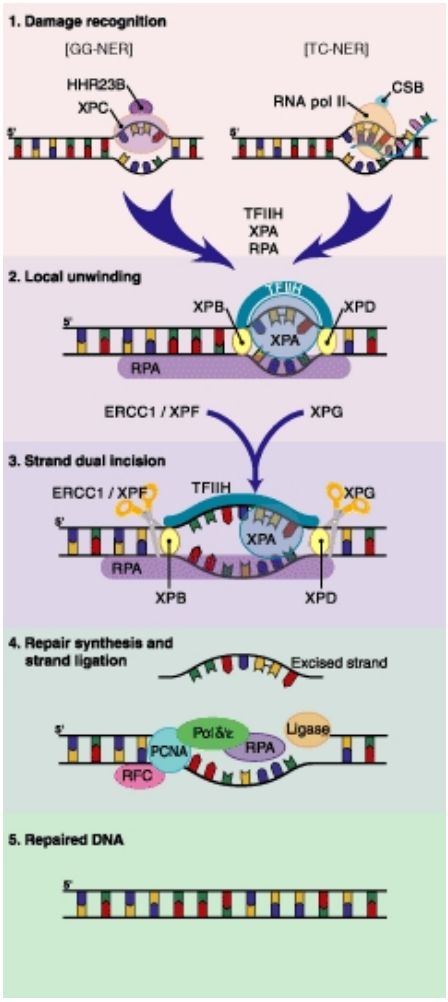

Figure 3.9: The scheme of nucleotide excision repair.
Picture from [http://www.rndsystems.com]

Mismatch Repair

The mismatch repair (MMR) mechanism repairs replication errors such as base-base mismatches, insertion and deletion loops resulting from DNA polymerase misincorporation of nucleotides and template slippage. The systems primarily repair mismatched, but undamaged, base pairs and small insertions or deletions. Some kind of modified bases, such as O-methylguanine are also detected. The mismatch repair is similar to the other excision repair pathways (BER and NER). Many mismatched bases are removed by the proofreading activity of DNA polymerases. The remaining wrong bases are repaired by the mismatch repair system, which scans newly replicated DNA molecule. The repair is initiated by recognition of the mismatch, insertion or deletion by specialized proteins (so-called MutS α β in mammalian cells).

Mismatch repair is strand specific, because only the newly synthesized DNA strand will contain errors and replacing bases in the original (template) strand would leads to errors. The mismatch repair mechanism have several systems which distinguish the newly synthesized strand from the parental. If a mismatch is found, the enzymes of this repair system identify and excise the mismatched base specifically from the newly replicated DNA strand. After that, the error is corrected and the proper base sequence is restored. In mammalian cells, it appears that the strand-specificity of mismatch repair is determined by the presence of single-strand breaks, which would occur in newly synthesized DNA strand. Similarly as for BER, there are two types of mismatch repair mechanisms; *long patch* and *short patch*. Long patch can repair all types of mismatched bases and can excise segments up to a few kilobases long. Short patch repair is dedicated only for specific mismatches caused by damage to the DNA, and removes regions of approximately 10 nucleotides [Alberts *et al* 2002]. In all organisms, mismatch repair involves the following steps (see Figure 3.10):

1. Detection of a single mismatch, in the newly synthesized DNA strand
2. Determining which of the two base pairs is incorrect
3. Correcting the error by excision repair

Mismatch repair is a highly conserved mechanism; it occurs widely in prokaryotes as well as in eukaryotes. The MMR mechanism is described in details e.g. in [Iyer *et al* 2006].

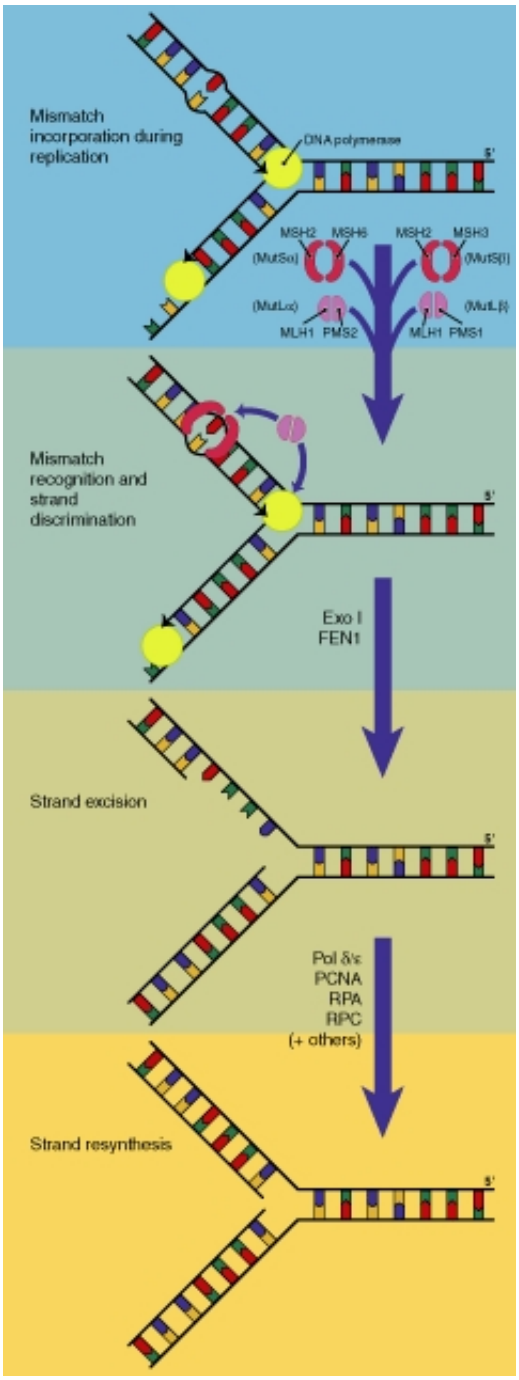

Figure 3.10: The scheme of mismatch repair.
Picture taken from [http://www.rndsystems.com]

Repairing of strand breaks

Ionizing radiation and certain chemicals can produce both single strand breaks (SSBs) and double strand breaks (DSBs) in the DNA backbone. In contrast to SSBs, which usually have insignificant effect to the cell survival, the DSBs may lead to chromosomal instabilities and consequent nonregulated gene expression, carcinogenesis or cell inactivation. DSBs differ from other types of DNA damage, because they influence both strands of the DNA molecule and therefore it is not possible to use the complementary strand as a template for their repair (compare BER, NER and MMR in previous sections).

Single strand breaks are repaired using the same enzymes as used in Base Excision Repair (BER). Complete interruption of DNA strands are repaired by two different types of mechanism:

- direct joining, also called *Non Homologous End Joining* (NHEJ)
- *Homologous Recombination* (HR)

The cellular decision which pathway to use to repair DSB is not understand; however, the choice seems to be influenced by the stage within the cell cycle at the time of damage induction [Takata *et al* 1999].

Non Homologous End Joining

The double strand break in DNA molecule is sealed by a simple ligation. This rejoining can be perfect, simply renewing the original sequence, or imperfect, adding a few nucleotides, or removing in region ranging from one nucleotide to a few kilobases. In mammalian cells, essential for the process of NHEJ is the DNA-dependent protein kinase complex and the Ku70 and Ku80 heterodimeric protein [Featherstone and Jackson 1999a]. The Ku proteins seem to be the first proteins that recognized a DNA double strand break and together bind to the broken site [Featherstone and Jackson 1999b]. After that, the Ku protein forms a complex with the DNA-dependent protein kinase catalytic subunit (DNA-PKcs; its function in NHEJ is not yet fully explained) and recruits other proteins (XRCC4, Artemis and DNA Ligase IV) to the damage site. Because the ends of most DSBs are induced by toxic agents, damaged sites are unable to be directly sealed. Therefore, before joining has started, the ends often must be processed by specialized nucleases and polymerases. After that, the DNA-PKcs is released from the Ku-bound DNA and Ku proteins join with LX complex at the DNA end. Then, the NHEJ protein complex ligates the DNA ends by Ligase IV [Caldecott 2004].

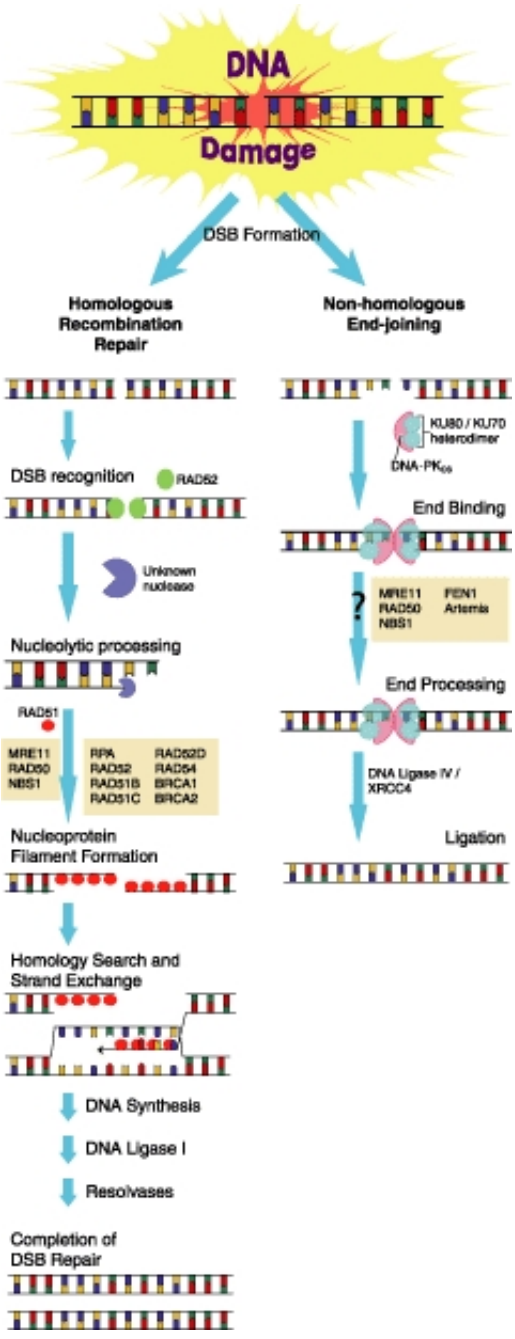

Figure 3.11: The scheme of two pathways of double strand break repair, Homologous Recombination on the left and Non Homologous End Joining on the right.
Picture taken from [http://www.rndsystems.com]

Homologous Recombination

Homologous recombination (HR) is the exchange (crossing over) or replacement (gene conversion) of a DNA region by its homologous DNA sequence from the undamaged homologous chromosome or the sister chromatid. In contrast to NHEJ, HR requires close proximity the repaired region and an undamaged chromatid or chromosome, which serves as a template. Therefore, the majority of homologous recombination repairs proceeds in late S and G2 phases of the cell cycle when the undamaged chromatid is available. Homologous recombination also occasionally occurs between similar DNA sequences on nonhomologous chromosomes or within a chromosome. A single gene conversion event changes one of the pair of homologous sequences without changing any other parts of the genome. The repair process is mediated by RAD52 group of proteins, which is supposed to be the initial sensor of the broken DNA sites. The free ends are processed by nucleases and the 3' single-stranded DNA (ssDNA) overhangs are created. The new ssDNA ends are bound by RAD51 proteins to form a nucleoprotein filament. The RAD51 nucleoprotein filament then seeks the undamaged DNA sequence on the sister chromatid for a homologous template. After the homologous DNA region has been recognized, DNA is unwind by ATPase activity of Rad54 protein. The two invading ends serve as primers for DNA synthesis and create the structure called *Holliday junction*. After that, the flanking sequences are isomerized and whole process is finished by ligation. The schema of homologous recombination is depicted in Figure 3.11.

3.3.6 Cellular and tissue response to radiation damage

As mentioned above, generally, DNA repair systems comprise these mechanisms: direct DNA damage reversal, DNA excision repair, mismatch repair and homologous recombination. The various kinds of DNA damage are summarized in Table 3.1. The basis, on which the choice of the DNA repair pathway is made, is not fully understand yet. There is general agreement that it depends on the inducing agent or process [Iliakis *et al* 2004].

Low-LET radiation mainly causes the base damage through the formation of reactive radicals in water radiolysis. During the repair of base damage, temporary single strand breaks (SSB) are created as intermediate products in the repair. Double strand breaks (DSBs) may be created by high doses of low-LET radiation from clusters of damaged bases. On the other hand, high-LET radiation may generate DSBs directly without the previous creation of base damage [Ward 1985]. The amount of single base damage is approximately two orders of magnitude bigger than the amount of DSBs.

The primary events caused by ionizing radiation, arranged by abundance, are: base damage > SSB >> DSB [Alberts *et al* 2002].

The DSBs may be repaired either by by non-homologous endjoining (NHEJ), or homologous recombination (HR). Determination of the relative contribution of NHEJ and HR specifically to the repair of ionizing radiation induced DSBs is important for understanding of the mechanisms leading to chromosome aberration formation. The biochemical studies confirm, that the process of main importance is NHEJ. Only a small fraction of ionizing radiation induced DSBs undergo the homologous recombination or HR comes after the initial end joining [Iliakis *et al* 2004].

The models of some repair processes in cells can be found e.g. in [Politi *et al* 2005] (BER), [Semenenko *et al* 2005, Semenenko and Stewart 2005] (BER, NER) and [Cucinotta *et al* 2008] (NHEJ).

DNA Damage	**Effect**	**Repairability**	**Reference**
Altered Bases	Primary	Easily Repaired	[Ward 1995]
SSB	Primary and secondary	Easily Repaired in most cases	[Ward 1985]
DSB	Primary and secondary	Not all accurately repaired	[Ikpeme *et al* 1995] [Löbrich *et al* 1995] [Taucher–Scholz 1995]
Fragmentation	Primary and secondary	Results from inability to repair primary damage	[Holley and Chatterjee 1996]
Deletions	Secondary	Results from inability to repair primary damage	[Kronenberg *et al* 1995]
Chromosomal Rearrangements	Secondary	Results from inability to repair primary damage	[Nagasawa and Little 1981]
Protein-DNA cross-link	Secondary	Not repaired	[Olinski *et al* 1992]

Table 3.1: Radiation induced damage.
Table from [http://hacd.jsc.nasa.gov/].

Chapter 4

Modelling of radiobiological effects

This chapter presents some models used for analyzing the relationship between cell survival and radiation dose. The attention is paid to formulating the basic assumptions and relations between physical characteristics of radiation (dose, LET), biological characteristics of cells (repair capacities, properties of the chromosomal system) and the biological output (survival, inactivation, mutation).

4.1 Target theory

The target theory explains the dose-response curves on the basis of a presumption that there are regions in the chromosomal system of a cell that are critical for the survival of the cell [Chadwick *et al* 1973]. The survival of the cell is assumed to depend directly on the number of these sensitive sites (targets) having been hit. In fact, the location of these sensitive targets in cell is at least problematical.

Generally, the model is applicable for high doses and is not suitable for lower, more clinically relevant doses.

There are several versions of this theory [Steel 1993]:

Single-target single-hit inactivation

In this approach, just one hit to a single sensitive target is sufficient to cell inactivation. Under the assumption that the impacts of individual particles

into cell are completely random, the distribution of traversing particle numbers may be represented by Poisson statistics. For each cell it is possible to write

$$p(survival) = p(no\ hits) = e^{-\frac{D}{D_0}}, \tag{4.1}$$

where D_0 stands for the dose that yields on an average one hit per target. Thus ratio D/D_0 represents the average number of hits per cell.

The survival curve is exponential, therefore linear in the semi-logarithmic plot (see Figure 4.1). This type of cell survival curve occurs for the inactivation of viruses and bacteria or some types of very sensitive mammalian cells and for very high-LET radiation [Steel 1993].

Multi-target single-hit inactivation

Let us assume that there are more important targets in a cell and one hit to each of n targets leads to cell inactivation. Using Poisson statistics:

$$p\left(no\ hits\ on\ a\ specific\ target\right) = e^{-\frac{D}{D_0}}, \tag{4.2}$$

Therefore,

$$p\left(at\ least\ one\ hit\ on\ a\ specific\ target\right) = \tag{4.3}$$

$$p\left(specific\ target\ inactivated\right) = 1 - e^{-\frac{D}{D_0}}, \tag{4.4}$$

and for n targets in the cell,

$$p(all\ targets\ inactivated) = (1 - e^{-\frac{D}{D_0}})^n. \tag{4.5}$$

Probability of survival is then given by

$$p(survival) = p(not\ all\ targets\ inactivated) = 1 - (1 - e^{-\frac{D}{D_0}})^n. \tag{4.6}$$

As shown the Figure 4.1, the survival curves approximate to a straight line for high doses and have a shoulder for low doses, in the region of the so called *quasi-threshold dose* (D_q) [Steel 1993].

Two-component model

The major drawback of the multi-target single-hit model is predicting a flat response for very low doses (see Figure 4.1 on the right side). Due to experimental evidence for a certain initial slope at low doses, the model may be adapted by adding a single-hit term:

$$p(survival) = e^{-\frac{D}{D_1}}(1 - (1 - e^{-D(\frac{1}{D_0} - \frac{1}{D_1})})^n). \tag{4.7}$$

Here the term $e^{-\frac{D}{D_1}}$ adjust the initial slope, i.e. D_1 represents the dose required to reduced survival from 1 to $\frac{1}{e}$ (see Figure 4.2).

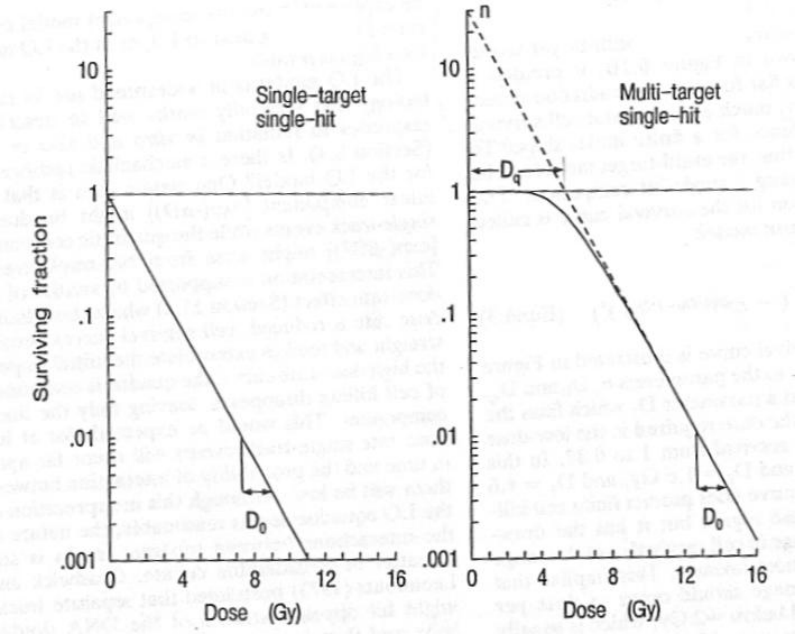

Figure 4.1: The two most common variants of target theory. The single-target single-hit (left); the multi-target single-hit (right); picture from [Steel 1993]

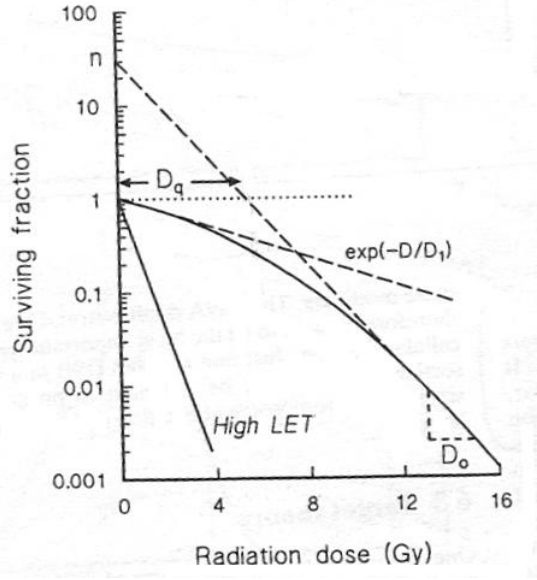

Figure 4.2: The two-component model; taken from [Steel 1993]

4.2 Linear-quadratic model

The linear-quadratic model (LQ model) [Chadwick *et al* 1973, Dale 1985, Thames 1985] is the most commonly used tool for describing cell radiation response in radiobiology. There is strong theoretical and experimental evidence for LQ model at low doses and low-LET radiation [Sachs *et al* 1997], but this model is unsuitable in predicting dose-response of high doses and high LET radiation (survival curves become more linear).

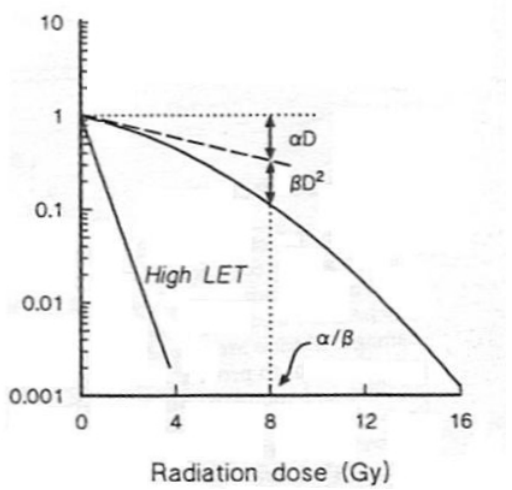

Figure 4.3: The linear quadratic model; picture from [Steel 1993]

The survival probability S is given by

$$S = e^{-\alpha D - \beta D^2}, \tag{4.8}$$

where α, β are parameters. This equation represents a continuously bending survival curve. The curvature is determined by the ratio α/β. The α/β ratio [Gy] describes the dose value at which the linear contribution to cellular damage (αD) is equal to the quadratic contribution (βD^2) [Steel 1993], see Figure 4.3. It results from equation 4.8:

$$\begin{aligned} \alpha D &= \beta D^2, \\ D &= \alpha/\beta. \end{aligned} \tag{4.9}$$

There is a possible interpretation of linear and quadratic terms: linear term $exp(-\alpha D)$ relates to the number of lethal lesions produced by a single radiation track (the single-track effect) and the quadratic component $exp(-\beta D^2)$

corresponds to the number of lethal lesions produced by two different radiation tracks (i.e. the two-track effect) [Steel 1993, Wang *et al* 2006].

[Chadwick *et al* 1973] proposed that two separate tracks might cause damage to opposite strands of the DNA molecule and induce a double strand break. However, at present time this hypothesis seems not very plausible, because the probability of such a close interaction of tracks at a few gray doses is too small. The more likely explanation is complex DNA damage and interaction between more widely-spaced regions in DNA [Steel 1993].

The linear quadratic model in fractionation radiotherapy

The linear-quadratic model is very useful for describing the relationship between the total isoeffective dose and the dose per fractions in fractionated radiotherapy [Steel 1993]. The survival after a dose d per one fraction is according to 4.8

$$S_d = e^{-\alpha d - \beta d^2}. \tag{4.10}$$

There is a experimental evidence that all fraction in a series have the same effect, so the biological effect E after n equal fractions of irradiation (here it is assumed that repair of sublethal lesions is finished) can be expressed as

$$E = -ln(S_d)^n = -n\, ln(S_d) = n(\alpha d + \beta d^2) = \alpha D + \beta d D, \tag{4.11}$$

where d means the dose per fraction and the total delivery dose $D = d\ n$. Thus the relationship between the total dose and the dose per fraction is described by equation

$$D = \Big(\frac{E}{\alpha}\Big) / \Big[1 + \frac{d}{\alpha/\beta}\Big]. \tag{4.12}$$

The α/β ratio is different for various types of tissues. For tissues with early reaction to irradiation the characteristic α/β value is about 7 - 20 Gy, for late-responding tissues it is in the range of 0.5 - 6 Gy. In tables 4.1 and 4.2 the values α/β for some types of acute- and late-responding normal tissues are reported.

There are several methods to calculate isoeffect relationships for radiotherapy on the basis of LQ model [Hall *et al* 2006]. The main approaches are *Extrapolated Tolerance Dose* (ETD) by [Barendsen 1982] and *Total Effect* (TE) suggested by [Thames and Hendry 1987]. Mathematically identical to ETD is *Biologically Effective Dose* (BED) [Dale 1985, Barendsen 1982]. These concepts seek for a fractionation specification, that have the same effect.

Tissue and effect	α/β	**References**
Skin - desquamation	11.2 (7.8-18.6)	Turesson and Thames (1989)
Skin - erythema	7.5 (5.4- 10.9)	Turesson and Thames (1989)
Lung (acute)	<8.8	Cox (1987)

Table 4.1: Values of α/β ratio for early responding tissues. Data from [Steel 1993].

Tissue and effect	α/β	**References**
Larynx - cartilage necrosis	<4.4	Horiot *et al* (1972)
	<4.2	Stell and Morrison (1973)
Lung - pneumonitis	<3.8	Cox (1987)
Cord - myelopathy	<3.3	Dische *et al* (1981)
Bowel - performation	2.2 - 8.0	Bennet (1978)

Table 4.2: Values of α/β ratio for late-responding tissues. Data from [Steel 1993].

From Eq. (4.11) it follows

$$\begin{aligned} E &= n\, d(\alpha + \beta d) \\ \frac{E}{\alpha} &= D[1 + \frac{d}{\alpha/\beta}] = \text{Biologically Effective Dose (BED)} \end{aligned} \tag{4.13}$$

The term $[1 + \frac{d}{\alpha/\beta}]$ is called *relative effectiveness*.

The LQ model described in Eqs. 4.9, 4.11 supposes that between fractions is enough time for cells to repair sublethal damages. This time is approx. 6 hours, but for some types of tissues (spinal cord) can be more than 24 hours. If the interval between irradiation is lower than this "full-repair time", residual unrepaired damage can interact with damages from the next fraction and the total tissue damage increases. The simple LQ model can be modified by adding a repair half-time ($T_{1/2}$) to take incomplete repair into account (so called *Incomplete repair model* [Thames 1985]). Repair half-time represents the time required for half of the maximum possible repair in tissues. In this approach, the quantity of unrepaired damage is described by a function H_m, which depends on the interval between fractions, the number of equally-spaced fractions and repair half-time. For fractionated radiotherapy, an extra

term is added to Eq. (4.13):

$$BED = D\left[1 + \frac{d}{\alpha/\beta} + \frac{H_m d}{\alpha/\beta}\right], \tag{4.14}$$

where m stands for number of fractions per day. In case of continuous very low dose rate radiotherapy ($<$ 5cG/hour), cells have opportunity to fully repair during irradiation. The corresponding modified BED formula is then

$$BED = D\left[1 + \frac{d}{\alpha/\beta} + \frac{g\,d}{\alpha/\beta}\right]. \tag{4.15}$$

Values of H_m and g are accessible for various repair half-times in publications [Thames and Hendry 1987, Steel 1993].

Nanodosimetry-based LQ model

In this approach the coefficients α and β of the LQ formula are explicitly expressed in terms of three physical quantities and three biological quantities [Wang *et al* 2006]. The physical parameters are related to energy depositions and the biological quantities are connected with lesion production, interaction probabilities and lesion repair rate. According to the model, DNA lesions may be divided into two types: *unrepairable* and *repairable* lesions. Unrepairable DNA damage is supposed to be irreversible (complex double strand breaks, lethal chromosome aberations), while repairable DNA lesion can be fully repaired with the exception of pairwise interaction between two repairable damages, which can lead to unrepairable damage, too.

The advantage of the new model is the possibility to relate parameters α and β to physical and biological characteristics and to estimate the iso-effect for radiotherapies that involve ionizing radiation of mixed LET.

4.3 Local Effect Model

In Local Effect Model (LEM), the biological effect of ionizing radiation is determined locally as a function of the local dose deposited by charged particle tracks [Scholz and Kraft 1996]. The inputs for this model are x-ray survival curves, the radial dose pattern inside the track and geometrical parameters of cell nucleus. LEM is able to cover special properties characteristic for charged particles, like the relative biological effectiveness (RBE) as a function of energy and atomic number of the particles and the transition from linear to shouldered survival curves (on semilogarithmical scale) depending on the size of the biological object and particle fluence.

The LEM is based on the premise that the biological effect of radiation is given by the spatial local dose distribution and thus there is no difference between local dose inactivation effect of charged particles and x-rays. According to [Barendsen 1990] and others, cell nucleus is the target volume for the cell inactivation and sensitive sites are homogenously located throughout the whole volume of nucleus. The track structure and dose distribution of photons and ions is evidently completely different, but the size of critical target is in the order of micrometers and integration of energy over such a volumes smears out the fine structure of dose distribution. On the other hand, x-ray survival curves are not linear and for lower doses there is a shoulder. It means, high doses are relatively more efficient in comparison with low doses. Using the same presumption in local doses, the certain amount of energy given as a high local dose into a small volume of the nucleus is more efficient than the same energy deposited as a low local dose in a larger volume. Integration of the energy over the nuclear volume would thus underestimate the biological effects created by the high local doses in the center of a track [Scholz and Kraft 1996].

Using Poisson distribution, one obtains for survival of cells:

$$S_{ion}(D) = e^{-N_X(D)}, \tag{4.16}$$

where D is the dose delivered by the X-rays and $N_X(D)$ represents the average number of lethal events produced by photon radiation in the cell nucleus. Lethal events are created by local dose deposition and cell nucleus is homogenously sensitive. For photon radiation the density of lethal events $\nu_X(D)$ in the cell nucleus can be written as

$$\nu_X(D) = \frac{N_X(D)}{V_{nucleus}} = \frac{-ln\ S_X(D)}{V}, \tag{4.17}$$

where $V_{nucleus}$ stands for the volume of the nucleus. The total number of

lethal events in the cell is the summation over sensitive volume:

$$\overline{N_X} = \int_x \int_y \int_z \nu_X(D(x,y,z))dx\,dy\,dz = \int_x \int_y \int_z \frac{-ln\ S_x(D(x,y,z))}{V} dx\,dy\,dz. \tag{4.18}$$

According to the main assumption of the LEM, the local biological effect is determined by the local dose, but is independent of the particular radiation type leading to a given local dose:

$$\nu_{ion}(D(x,y,z)) = \nu_X(D(x,y,z)), \tag{4.19}$$

and therefore

$$\overline{N_{ion,lethal}} = \int_x \int_y \int_z \frac{-ln\ S_x(D(x,y,z))}{V} dx\,dy\,dz. \tag{4.20}$$

Using Eqs. (4.16) and (4.18), taking into account the Eq. (4.19), the survival fraction is given by

$$S = e^{-\overline{N_{ion,lethal}}}. \tag{4.21}$$

In accordance to the principles of the model, the fundamental premise of the LEM is, that the local biological effect is determined by the local dose, but is independent of the particular radiation type leading to a given local dose, i.e. local density of lethal events $\nu(D)$ is equal for both the photons and ions supposing they delivered the same energy locally [Scholz and Elsässer 2007].

The x-ray survival curve is shouldered and therefore the number of lethal events caused by sum of the single dose depositions is lower than the sum of two dose depositions together (see Figure 4.4) :

$$N(D_1 + D_2) > N(D_1) + N(D_2). \tag{4.22}$$

Therefore for local doses, the efficiency of overlapping tracks is higher in comparison to single dose distributions. For that reason the biological efficiency has to be calculated from the total local dose at a given subvolume, taking into account local doses from all the particles contributing to a given point in the nucleus (Figure 4.4). Hence, if the track diameter is large enough and a sufficient part of energy is deposited by overlapping tracks, the shouldered survival curves are to be expected. On the other hand, exponential survival curves occur for very high LET particles and low fluences, where the overlapping is negligible, or for low LET particles and very high fluences, where the diameter of tracks is very small and there is a small probability for overlapping tracks.

For describing survival curves for photon irradiation, the authors of LEM have chosen a parametrization that is linear-quadratic in low dose range and

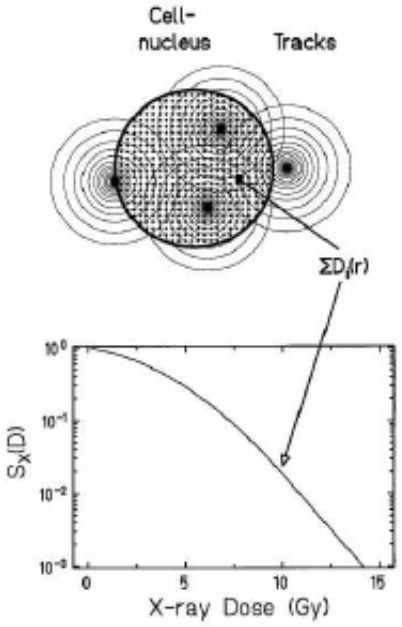

Figure 4.4: Overlapping of the tracks in nucleus. Taken from [Kraft *et al* 1999]

linear for doses above the threshold dose D_t [Scholz *et al* 1997, Scholz and Kraft 1996]. Cell survival is then determined by

$$\begin{aligned} S(D) &= e^{-aD-bD^2} \quad for\, D \leq D_t \\ S(D) &= S_t e^{-s(D-D_t)} \quad for\, D > D_t, \end{aligned} \tag{4.23}$$

where the coefficients a, b are analogous of α, β in LQ model, s determines the slope of the survival curve at threshold dose D_t and S_t stands for survival at the threshold dose.

Practically, for the prediction of survival after ionizing particle irradiation it is necessary to know [Scholz and Kraft 1996, Beuve *et al* 2007]:

- radial dose distribution $D(\mathbf{r})$ for determining the local dose distribution in certain position inside the track
- the sensitive volume V and geometrical parameters of the cell nucleus
- x-ray survival curve for calculating the number of lethal events *N(D)* and event density ν*(D)*

First, a lay-out of ion irradiation is generated randomly for an irradiation dose D_{ion} and after that the local dose is obtained from a track structure model. The number of lethal events is derived from Eq. (4.18), where $S(D(x, y, z))$ means survival after x-ray irradiation. Ion irradiation is a process of very stochastic nature, all procedure has to be repeated many times to decrease influence of statistical fluctuations on the calculated survival. The detailed description of computational procedure of LEM is given in [Scholz *et al* 1997].

The Local Effect Model describes experimental data quite satisfactory even thought some presumptions of the model are based on certain simplifications.

4.4 Kinetic models

4.4.1 Repair-Misrepair Model

This model [Tobias 1985, Tobias *et al* 1980] is based on distinguishing the initial submicroscopic lesions and macroscopic processes like cell repair and cell progression. For RMR model the so-called *uncommitted lesions* (U lesions) are relevant. After irradiation of cells by ionizing particles, the lesions are created and cells try to repair them. The quality and velocity of repair processes is dependent on the availability of repair enzymes. Moreover, the radiation may influence the repair processes in many ways - some present repair enzymes can be inactivated by radiation or more repair enzymes may be also created. In the RMR model it is supposed that the cell has a "memory" for previous irradiation. Some of the U lesions can interact with other U lesions created previously. After irradiation, the number of lesions per cell U_0 is proportional to dose D and to the yield coefficient δ:

$$U_0 = D\delta. \tag{4.24}$$

The time-dependence of the number of lesions per cell may be described by differential equation

$$\frac{dU}{dt} = -\lambda U - \kappa U^2, \tag{4.25}$$

where λ stands for linear self-repair coefficient and κ is a coefficient for cooperative repair, including the interference between pairs of U-lesions. For the sake of simplicity, the time saturation term $T = 1 - e^{-\lambda t}$ is used, single dose is delivered into a cell at t = 0 and it is assumed that there remain no *U(t)*

lesions when $t \to \infty$. With these assumptions, the solution of Eq. (4.25) is

$$U(t) = \frac{U_0 e^{-\lambda t}}{1 + \frac{U_0 T}{\epsilon}}, \tag{4.26}$$

where $\epsilon = \lambda/\kappa$.

Under the supposition that no new U-lesions are created during the repair process, the U_0 can be expressed as

$$U_0 = U(t) + R_L(t) + R_Q(t). \tag{4.27}$$

In this equation,
$R_L(t) = \int_0^t \lambda U dt = \epsilon \, ln \, (1 + \frac{U_0 T}{\epsilon})$ is the total number of self-repairs and
$R_Q(t) = \int_0^t \lambda U^2 dt$ is the total number of quadratic misrepairs. The authors suppose that all linear repairs lead to survival and all quadratic repairs are lethal misrepairs. The mean number of lethal lesions in cells, when $t \to \infty$ is

$$R_Q(t \to \infty) = U_0 - R_L(t). \tag{4.28}$$

The survival probability is equal to absence of lethal lesions in cell

$$S = e^{R_Q(t \to \infty)} = e^{-U_0}[1 + \frac{U_0}{\epsilon}]^{\epsilon} = e^{-\delta D}[1 + \frac{\delta D}{\epsilon}]^{\epsilon}. \tag{4.29}$$

This equation contains two independent parameters and it is composed of lesion term $e^{-\delta D}$ and repair term $[1 + \frac{\delta D}{\epsilon}]^{\epsilon}$. The model can be modified by further additional assumptions [Tobias 1985].

4.4.2 Lethal and Potentially Lethal Model

This model, proposed by [Curtis, 1986], involves many kinds of radiobiologic processes: lesion interaction, irreparable lesions created by single tracks, fixation of linear lesions and lesion repair and binary misrepair. The main presumptions of the model are:

- Irradiation leads to two different kinds of lesions, *lethal* and *potentially lethal*. The lethal damage is irreparable and causes inactivation of the cell. Potentially lethal lesions may be repaired by the cell repair system. This process is characterized by average rate constant ϵ_{PL} per unit time. PL lesions can also interact with each other (rate constant ϵ_{2PL} per unit time) causing a lethal lesion. This type of creating irreparable damage is called *binary misrepair*.

- Potentially lethal damages may be fixed in cell (i.e. made unrepaired, lethal) by trypsinization or other process.

- The numbers of lethal and potentially lethal lesions for a certain dose rate $\dot{D}$ per cell per unit time are given by $\eta_L \dot{D}$ and $\eta_{PL} \dot{D}$, where η_L is the rate of production of lethal lesions and η_{PL} is the rate of production of potentially lethal lesions per unit of absorbed dose.
- There is no saturation in the repair process, i.e. the rate of repair per lesion is not dependent on the present lesions in the cell.

The scheme of creating lethal and potentially lethal lesions in cells is described in Figure 4.5. Using the presumptions mentioned above, the time

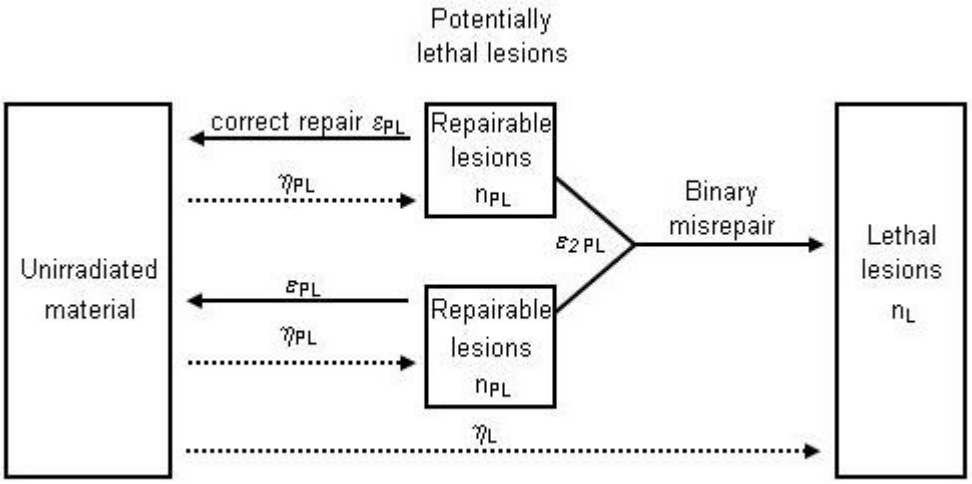

Figure 4.5: The scheme of LPL model; picture adapted from [Curtis, 1986]

rate of change in the numbers of potentially lethal lesions $n_{PL}(t)$ is given by

$$\frac{dn_{PL}(t)}{dt} = \eta_{PL}\dot{D} - \epsilon_{PL} n_{PL}(t) - \epsilon_{2PL} {n_{PL}}^2(t). \tag{4.30}$$

In this equation, the number of lesions caused by irradiation is changing in time by correct repair (term $\epsilon_{PL} n_{PL}(t)$) and by binary misrepair (term $\epsilon_{2PL} {n_{PL}}^2(t)$). The quadratic term for binary misrepair arises from the fact that the probability for interaction of the potentially lethal lesions per unit time is proportional to the number of pairwise interactions of lesions.

Similarly, for the number of lethal lesions it is possible to write:

$$\frac{dn_L(t)}{dt} = \eta_L \dot{D} + \epsilon_{2PL} {n_{PL}}^2(t). \tag{4.31}$$

Here, the initial number of lethal lesions is increasing by the binary misrepair term from Eq. (4.30). Because no lesions are present at the start of the irradiation (at time t=0), the initial conditions are $n_L = 0$, $n_{PL} = 0$.

The solution of Eqs 4.30 and 4.31 is given by

$$n_L(t) = \eta_L D + \epsilon ln\Big[\frac{2\epsilon_0}{\epsilon_0 + \epsilon_{PL} + (\epsilon_0 - \epsilon_{PL})e^{-\epsilon_0 t}}\Big] + \frac{(\epsilon_0 - \epsilon_{PL})^2 t}{4\epsilon_{2PL}} - n_{PL}(t) \quad (4.32)$$

$$n_{PL} = \frac{2\eta_{PL}\dot{D}(1 - e^{-\epsilon_0 t})}{\epsilon_0 + \epsilon_{PL} + (\epsilon_0 - \epsilon_{PL})e^{-\epsilon_0 t}}, \quad (4.33)$$

where ϵ_0 stands for

$$\epsilon_0 = \sqrt{{\epsilon_{PL}}^2 + 4\epsilon_{2PL}\eta_{PL}\dot{D}} \quad (4.34)$$

and

$$\epsilon = \frac{\epsilon_{PL}}{\epsilon_{2PL}}. \quad (4.35)$$

In real situations, the irradiation stops at time t = T and after time t_r all repair processes are finished and the outcome of irradiation is determined. In time t = T for numbers of lethal and potentially lethal lesions it is possible to write

$$\frac{dn_{PL}(t)}{dt} = -\epsilon_{PL} n_{PL}(t) - \epsilon_{2PL} {n_{PL}}^2(t) \quad (4.36)$$

$$\frac{dn_L(t)}{dt} = \epsilon_{2PL} {n_{PL}}^2(t) \quad (4.37)$$

where the initial conditions for these differential equations are

$n_{PL}(T)$ = the value of n_{PL} in Eq. (4.30) in time t = T
$n_L(T)$ = the value of n_L in Eq. (4.31) in time t = T
The solutions of these differential equations are:

$$n_{PL}(t) = \frac{N_{PL} e^{-\epsilon_{PL} t_r}}{[1 + N_{PL}/\epsilon(1 - e^{-\epsilon_{PL} t_r})]} \quad (4.38)$$

$$n_L(t) = N_L + \frac{N_{PL}(1 + N_{PL}/\epsilon)(1 - e^{-\epsilon_{PL} t_r})}{[1 + N_{PL}/\epsilon(1 - e^{-\epsilon_{PL} t_r})]} - \epsilon\, ln[1 + \frac{N_{PL}}{\epsilon(1 - e^{-\epsilon_{PL} t_r})}], \quad (4.39)$$

where $N_L = n_L(T)$ from Eq. (4.32) and $N_{PL} = n_{PL}(T)$ from Eq. 4.33 and t_r is time after that there is no repair present in cells.

The total number of lethal lesions at that time per cell is the sum of lethal and potentially lethal lesions, because all potentially lethal lesions present in

cell at the end of the repair time t_r are thought to be fixed, i.e. lethal. The total number of lethal lesions per cell in time $t = T + t_r$ is then

$$n_{TOT}(T + t_r) = n_L(T + t_r) + n_{PL}(T + t_r). \tag{4.40}$$

The survival of the cell is equivalent to the probability that no lethal lesions is present in cell:

$$S = e^{-n_{TOT}(T+t_r)} = e^{-n_L(T+t_r)-n_{PL}(T+t_r)}. \tag{4.41}$$

Using the terms from Eqs. (4.38) for n_L and (4.39) for n_{PL}, the survival is given by

$$\begin{aligned} S &= e^{-(N_L+N_{PL})+\epsilon ln[1+N_{PL}/\epsilon(1-e^{-\epsilon_{PL}t_r})]} = \\ &= e^{-N_{TOT}}[1 + N_{PL}/\epsilon(1 - e^{-\epsilon_{PL}t_r})]^{\epsilon}. \end{aligned} \tag{4.42}$$

In this equation,
N_L = number of lethal lesions after irradiation,
N_{PL} = number of potentially lethal lesions after irradiation,
$N_{TOT} = N_L + N_{PL}$.

The survival may be expressed as a function of absorbed dose D and dose rate $\dot{D} = D/T$:

$$S(D, \dot{D}, t_r) = e^{-N_{TOT}(D/\dot{D})}[1 + \frac{N_{PL}(D/\dot{D})}{\epsilon}(1 - e^{-\epsilon_{PL}t_r})]^{\epsilon}, \tag{4.43}$$

where $N_{TOT}(D/\dot{D}) = n_{PL}(T) + n_L(T)$ is the total number of lesions at the end of irradiation exposure time, $N_{PL}(D/\dot{D}) = N_{PL}(T)$ is the number of potentially lethal lesions at the end of irradiation exposure time.

If the available repair time t_r is sufficiently long, the term $(1 - e^{-\epsilon_{PL}t_r})$ may be neglected and the Eq. 4.43 can be simplified

$$S(D, \dot{D}, t_r = \infty) = e^{-N_{TOT}(D/\dot{D})}[1 + \frac{N_{PL}(D/\dot{D})}{\epsilon}]^{\epsilon}. \tag{4.44}$$

Practically, the parameters in the model η_L, η_{PL}, ϵ_{PL} and ϵ_{2PL} are to be determined for a given cell line. The parameter η_L is the reciprocal value of the D_0 for the exponential curve obtained at very low doses. The values of η_{PL}, ϵ_{PL} and ϵ_{2PL} were obtained by fitting the experimental data [Curtis, 1986].

4.4.3 Two-Lesion Kinetic Model

Kinetic models mentioned above, the LPL model and RMR model, are practically successful in describing the cell inactivation by radiation. On the other

hand, these models are not so good in relating cell killing to the creation and repair or misrepair of the double strand breaks, which are commonly accepted as the main reason for cell killing by radiation [Steel 1993, Sachs *et al* 1997]. The Two-lesion kinetic model (TLK) was proposed by R. D. Stewart to understanding better the relation between DSBs in cells and their killing [Stewart 2001].

This model is similar to former kinetic models like LPL and RMR model. Like in the LPL model, creation of DSBs is proportional to the absorbed dose. In contrast to LPL, where lethal and potentially lethal lesion are no further classified, simple and complex DSB types with unique characteristic of lesion repair are distinguished. The elementary version of DSB is the simple DSB (Type I), interpreted as a 10 - 20 bp long DNA section that contains a break in each strand. A complex DSB (Type II) contains elementary damage sites in addition to simple DSB (like base damage, base deletion, single strand breaks). The TLK model does not include direct lethal lesion production term that is included in the LPL model. Instead of this, the damage fixation mechanism and the linear misrepair of DSBs, similarly as in RMR model, are considered. In real situation, the misrepair of DSB causes a lethal or a nonlethal genetic change of the DNA molecule. In contrary, in the TLK this misrepair always leads to a lethal DNA damage. Formation of DSB, their repair and misrepair are described by two nonlinear differential equations:

$$\frac{d\bar{L}_1(t)}{dt} = 2\dot{D}(t)Y\Sigma_1 - (\varepsilon_1 + \lambda_1)\bar{L}_1(t) - \bar{L}_1(t)[\eta_1\bar{L}_1(t) + \eta_{1,2}\bar{L}_2(t)]$$
$$\frac{d\bar{L}_2(t)}{dt} = 2\dot{D}(t)Y\Sigma_2 - (\varepsilon_2 + \lambda_2)\bar{L}_2(t) - \bar{L}_2(t)[\eta_{1,2}\bar{L}_1(t) + \eta_2\bar{L}_2(t)]. \quad (4.45)$$

In this equation, $\bar{L}_1(t)$ is number of Type I DSBs and $\bar{L}_2(t)$ is number of Type II DSBs per cell. The Σ_1, Σ_2, λ_1,λ_2, η_1, η_2 and $\eta_{1,2}$ are parameters with biophysical interpretation, the parameters ε_1 and ε_2 describe the fixation of DSBs. The calculated cell survival curves are in very good agreement with experimental data (CHO 10B2 cells, irradiated by ^{137}Cs γ rays [Stewart 2001]).

4.5 Probabilistic two-stage model

The Probabilistic two-stage model, proposed in the Institute of Physics, is described in next chapter in detail.

Chapter 5

Probabilistic two-stage model

The model of biophysical mechanisms of cell inactivation by ionizing particles was proposed in 1980s by Dr. Lokajíček [Lokajíček 1981, Lokajíček 1986]. This earlier version of probabilistic two-stage model distinguishes two stages: physico-chemical phase (formation of double strand breaks - DSBs) and biological phase (cellular repair and survival or inactivation as the final response to irradiation). The DSBs are considered as the main reason for cell inactivation. In accordance with [Resnick 1976, Resnick and Martin 1976], the damages of chromosomes (in diploid cells) were divided into three groups [Lokajíček 1986]:

1. only one chromosome of a homologous pair is damaged,
2. at least one DSB is created in each chromosome of a homologous pair, but they are not in the same segment,
3. at least one DSB is formed in homologous segments of chromosomes.

In the model the survival probabilities for different damage kinds were derived.

The next approach [Judas *et al* 2001, Kundrát 2004] is mathematically similar to the Linear-Quadratic model. Briefly, the survival ratio in the LQ model is given by

$$\begin{aligned} S(D) &= e^{-\sigma(D)} \\ \sigma(D) &= \alpha D + \beta D^2. \end{aligned} \tag{5.1}$$

However, in the probabilistic two-stage model, the function $\sigma(D)$ was developed into the whole Taylor series:

$$\begin{aligned} \sigma(D) &= \sum_k \alpha_k D^k \\ S(D) &= e^{-\sum_k \alpha_k D^k} \end{aligned} \tag{5.2}$$

The polynomial expansion into the Taylor series gives an exact representation of the survival curve. This model has been used for analyzing survival curves of V79 cells irradiated by protons and deuterons [Hromčíková 2003]. However, due to its high computational complexity, the polynomial fitting procedure may be used only for low total particle numbers (maximum up to approximately 6 – 8 particles), i.e. for high-LET particles or in the low-dose region of survival curves [Kundrát 2004].

The current form of the probabilistic two-stage model (P2S) proposed in the Institute of Physics, Academy of Sciences of the Czech Republic [Kundrát *et al* 2005, Kundrát 2006] represents the damage induction caused by radiation and takes into account also repair processes in cells. This model enables to distinguish and describe two various types of lesions: lethal damage formed by a single track and less severe damage, where only the combination of at least two events may be lethal.

The probabilistic two-stage model has been used for analyzing several published data sets, for example two Chinese hamster cell lines with different radiosensitivity (data from [Weyrather *et al* 1999]). All these results can be found in Part "Results and analyses".

5.1 Basic concept of the model

In the probabilistic two-stage model, the "first stage" involves physical and chemical phase of the radiobiological mechanism, i.e. energy deposition to the cell (more precisely to the chromosomal system, which is generally accepted as the most sensitive target for radiation in cells; compare e.g. [Steel 1993, Sachs *et al* 1997, Hall *et al* 2006, Alpen 1998]). As described above in Chapter "Biological effects of radiation", charged particles cause ionization and excitation of atoms in cells. After that, the changed molecules react with others, the chemical bonds are broken and these processes lead to damage of important molecules (especially the DNA).

The "second stage" is characterized by the response of the irradiated cell to damage caused by radiation, i.e. biological phase. It involves enzymatic repair processes in the cell itself. All these biological mechanisms lead to the final cell response to irradiation - survival or inactivation.

Under the condition that the particles imparted to cells have approximately the same energy (monoenergetic ions), the average number of particles traversing the chromosomal system at given dose may be described by equation

$$h_D = \frac{A.D}{L}. \tag{5.3}$$

Here D stands for dose [Gy], L means linear energy transfer (LET) of given radiation [keV.μm] and

$$A = C_k.\sigma, \tag{5.4}$$

where $C_k = 6.24\,[keVGy^{-1}\mu m^{-3}]$ is a conversion constant corresponding to the standard choice of units and σ is the geometrical effective cross section of the cell nucleus (more precisely the sensitive area within the nucleus). The average number of particles that hit the nucleus is proportional to dose:

$$h_D = h\ D. \tag{5.5}$$

The number of particles having impacted to the given nucleus is random. The probability of hitting a cell nucleus by k particles is therefore given by Poisson statistics:

$$P_k(D) = \frac{(hD)^k}{k!}e^{-hD} \tag{5.6}$$

The probability of cell survival after k hits is

$$S(D) = 1 - \sum_k P_k(D)p_k(L), \tag{5.7}$$

where $p_{(k)}$ is the probability of cell inactivation after k hits. These probabilities fulfill the condition

$$p_0 = 0 \leq p_k \leq p_{k+1} \leq 1. \tag{5.8}$$

The equation (5.7) may be rewritten by replacing the term $(1 - p_k)$ by the survival probability q_k after k hits,

$$S(D) = \sum_k P_k(D)q_k(L). \tag{5.9}$$

5.2 Damage induction and repair

After irradiation, various types of DNA lesions are formed in cells. In the probabilistic two-stage model, three kinds of lesions are distinguished (see Figure 5.1):

- *Lesions negligible for the cell.* The cellular repair system can recondition this lesion type without problems.
  - single strand breaks, base loss, small deletions
- *Damage of lower severity.* They are repaired if they occur in cells separately. It must combine with at least another one to be lethal. Probability of this type of lesions is denoted as b in probabilistic two-stage model.
  - some type of double strand breaks, DSB pair misrejoining, some deletions
- *Severe lesions induced by a single track*, possibly lethal even if only one damage of this type is in a cell. Probability of forming a severe single-track lesion is named a in this model.
  - complex damaged sites, lethal dicentric or tricentric aberrations

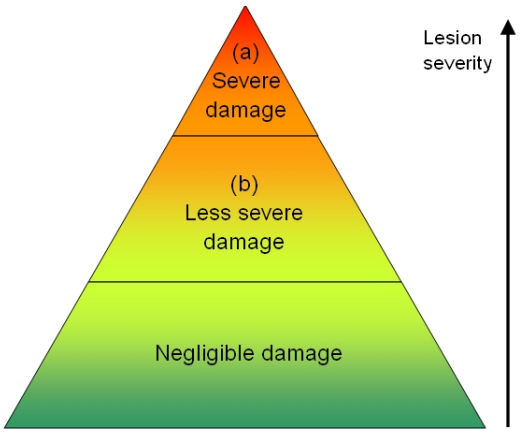

Figure 5.1: The schematic description of the damage type in cells, adapted from [Kundrát 2006]

5.2.1 Cell survival probability

The probability of not forming a severe damage or a less severe damage by one particle hit may be expressed as *(1-a)* or *(1-b)*, respectively. Therefore,

the probability of not forming a severe single-track lesion after k traversals of particles is given by

$$q_k^a = (1-a)^k, \tag{5.10}$$

and analogously for less severe b-type damage:

$$q_k^b = (1-b)^k. \tag{5.11}$$

Together, the probability of creating neither a single track lesion nor a single lesion is

$$q_k = q_k^a.q_k^b. \tag{5.12}$$

The cell survival probability after k particle traversals of the nucleus is given by [Kundrát 2006, Kundrát 2008]

$$q_k = \sum_{i=0}^{k} \binom{k}{i} a^i (1-a)^{k-i} \sum_{j=0}^{k-i} \binom{k-i}{j} b^j (1-b)^{k-i-j} r_{ij}^{ab}, \tag{5.13}$$

where r_{ij}^{ab} stands for corresponding repair probabilities of severe type of single track lesion and less serious "combined" damage, respectively. For i=0 $\wedge$ j=0 and i=0 $\wedge$ j=1 there is no effect for the cell, because at least one severe a-type damage or two "combined" b-type damage are necessary for cell inactivation. Therefore, $r_{00} = r_{01} = 1$.

The first term in Eq. (5.13), $\sum_{i=0}^{k} \binom{k}{i} a^i (1-a)^{k-i}$ describes the formation of i severe single-track lesions after k hits. Assuming that one particle can create only one kind of lesion, the b-type damage can be formed only from k-i hits. Thus, the term $\sum_{j=0}^{k-i} \binom{k-i}{j} b^j (1-b)^{k-i-j}$ describes the induction of less severe b-type damage from k-i hits. Therefore, the the modified probability $b^* = b.(1-a)$ express the probability of induction a less severe damage with taking into account the fact that if one particle create the a-type damage, it cannot create a b-type.

The cell survives if after repair processes in cell no a-type damage and at most a single b-type lesion remain unrepaired. Assuming the independent repair of individual lesions, the repair function is given by

$$r_{ij}^{ab} = r_a^i.\{r_b^j + j\, r_b^{j-1}(1-r_b)\}, \tag{5.14}$$

where r_a and r_b are repair success probabilities of a severe single particle a-type damage or a less severe "combined" b-type damage and i, j stand for the numbers of lesions formed. The cell survival probability after k hits of the nucleus can be rewritten as

$$q_k = \sum_{i=0}^{k} \binom{k}{i} a^i (1-a)^{k-i} r_a^i \sum_{j=0}^{k-i} \binom{k-i}{j} b^j (1-b)^{k-i-j} \{r_b^j + j\, r_b^{j-1}(1-r_b)\}, \tag{5.15}$$

where the first sum represents the induction and repair of i severe single-track lesions and the second one describes the induction of j less severe "combined" damages and their repair.

The Eq. (5.15) can be summed by dividing to two double series to form [Kundrát 2008]

$$q_k = [a r_a + (1-a)(1-b+b r_b)]^k + k(1-a)b(1-r_b)[a r_a + (1-a)(1-b+b r_b)]^{k-1}. \tag{5.16}$$

By denoting
$\Delta = a\, r_a + (1-a)(1-b+b\, r_b)$
$\gamma = (1-a)b\,(1-r_b)$,
Eq. (5.16) can be rewritten in a simple form

$$q_k = \Delta^k + k\,\gamma\Delta^{k-1}. \tag{5.17}$$

The terms γ and Δ, or $1-\Delta$ and $1-\Delta-\gamma$ respectively, may be interpret as follows [Kundrát 2007]:

$$\gamma = (1-a)\,b\,(1-r_b) = \text{(no a-type damage is created)} \tag{5.18}$$
and (b-type-damage is created) and (b-type damage is not repaired)

$$\begin{aligned} 1-\Delta &= 1 - a\, r_a + (1-a)(1-b+b\, r_b) = \\ &= a\,(1-r_a) + (1-a)\,b\,(1-r_b) = \\ &= \text{(a-type damage is created and not repaired)} \\ &\quad \text{or (b-type damage is created and not repaired)} \end{aligned} \tag{5.19}$$

$$1-\Delta-\gamma = a(1-r_a) = \text{(a-type damage is created and not repaired)} \tag{5.20}$$

In other words, γ mean the probability of creating the unrepaired b-type damage, $1-\Delta-\gamma$ represents the probability of creating the unrepaired a-type damage and $1-\Delta$ signifies the formation of unrepaired a-type damage or unrepaired b-type damage.

The cell survival probability q_k descends with the number k of hits to the nucleus. In Figure 5.2, q_k for several different values of repair probabilities r_a and r_b are displayed.

If repair processes are not taken into account as an independent term, i.e. only unrepaired damages are considered ($r_a = r_b = 0$), it is possible to rewrite the Eq. (5.16) in an even more simple form:

$$q_k = (1-a)^k[(1-b)^k + kb(1-b)^{k-1}]. \tag{5.21}$$

Using Eqs. (5.6), (5.9) and (5.17) the cell survival at dose D is given by

$$S(D) = \sum_k P_k\, q_k = \sum_k \frac{(hD)^k}{k!} e^{-hD}(\Delta^k + k\,\gamma\Delta^{k-1}), \tag{5.22}$$

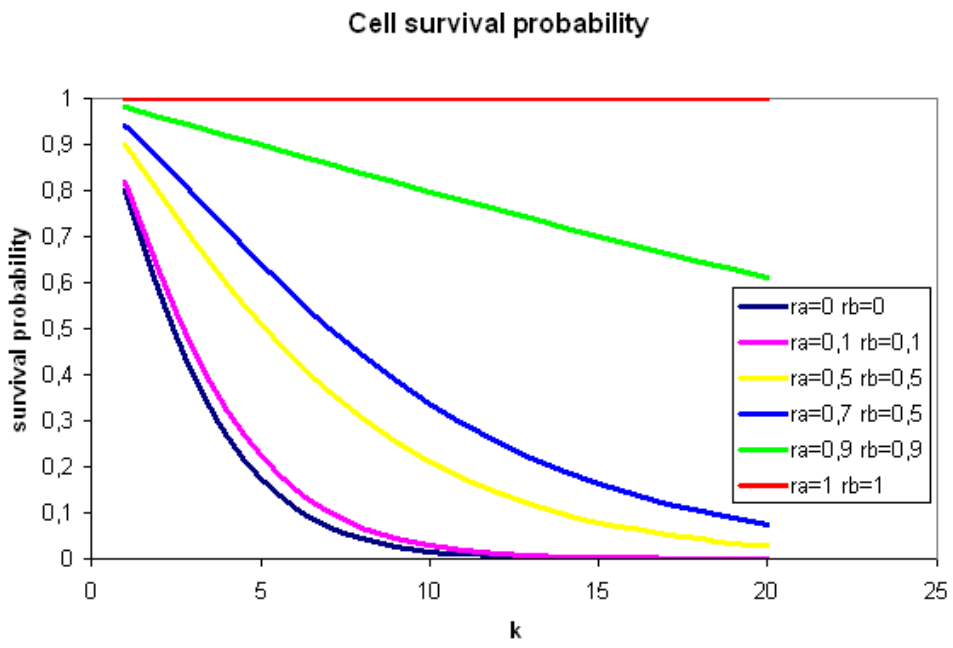

Figure 5.2: Survival probability q_k for various values of r_a and r_b. Values of a, b and h are fixed: a = 0.2, b = 0.3, h = 2.

which one may convert by summing to

$$S(D) = e^{-hD(1-\Delta)}(1 + \gamma hD). \tag{5.23}$$

This term is independent on k (number of the nucleus hits) and it is given only by dose and damage induction and repair probabilities. The behavior of function *S(D)* for various values of repair probabilities r_a and r_b is represented in Figure 5.3.

5.2.2 Parametrization

The damage induction probabilities a, b and repair probabilities r_a and r_b in Eqs. (5.10) - (5.15) depend on the radiation quality (i.e. type of particle and LET), as well as on biological characteristics (in particular, the repair capability of given cell line, the stage of cell cycle). For the analysis of experimental data, a, b and r are represented by functions depending on LET only. These functions must be smooth, continuous and sufficiently flexible to represent various types of behavior of cell survival curves. The functions *a(L)* and *b(L)* must be increasing with LET, because with increasing energy given to the cell the probability of creating a damage in DNA increases. We

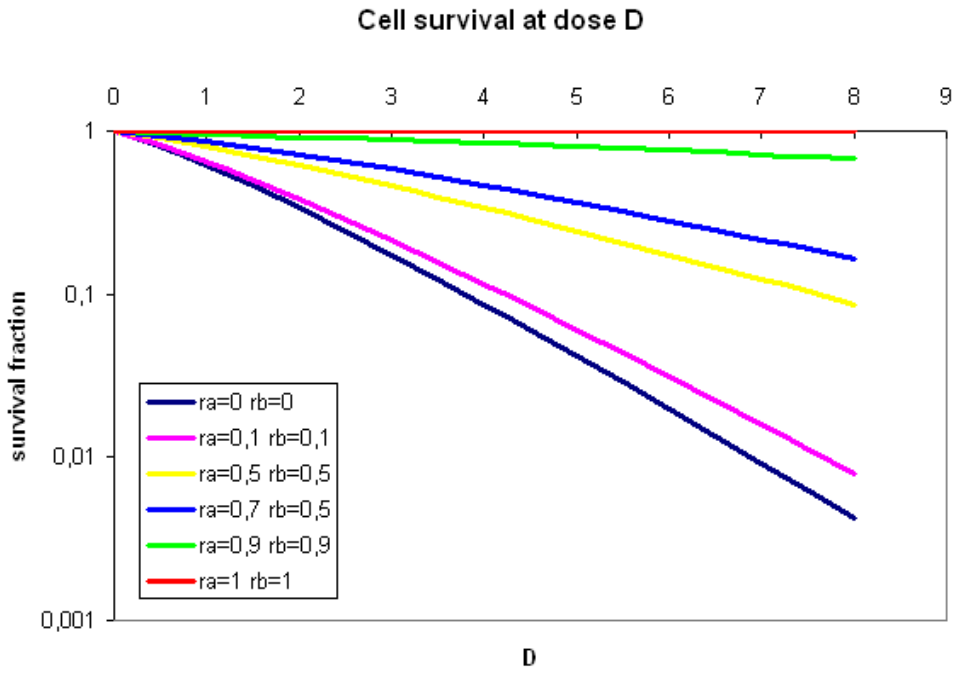

Figure 5.3: Survival ratio in dependence of dose for various values of r_a and r_b. Values of a, b and h are fixed: a = 0.2, b = 0.3, h = 2.

have assumed that $r(L)$ decreases with LET (the function $r(L)$ is decreasing with LET), but in analysis presented in part "Results and analyses" it will be shown that probability of successful repair is practically independent on LET. All these functions describe probabilities, therefore their values range between 0 and 1. The conditions mentioned above are fulfilled for example by test functions of this type:

$$\begin{aligned} a(L) &= a_0 \frac{(1 - e^{(-(a_1 L)^{a_2})})}{(1 + a_3\, e^{(-(a_4 L)^{a_5})})} \\ b(L) &= b_0 \frac{(1 - e^{(-(b_1 L)^{a_2})})}{(1 + b_3\, e^{(-(b_4 L)^{b_5})})} \\ r(L) &= 1 - r_0 \frac{(1 - e^{(-(r_1 L)^{r_2})})}{(1 + r_3\, e^{(-(r_4 L)^{r_5})})}. \end{aligned} \tag{5.24}$$

Every these functions is dependent on LET and six auxiliary parameters. For our analysis we have used this type of parametrization with $a_3 = 0$, $b_3 = 0$, $r_3 = 0$. This presumption reduces the number of parameters to three for each function, but the flexibility is still sufficient. In Figure 5.4 the behavior of function $a(L)$ is shown. This figure shows that a function with three

parameters allows satisfactory flexibility for describing various behavior of *a(L)*.

The values of parameters $a_0 - a_2$, $b_0 - b_2$ and $r_0 - r_2$ may be obtained by analyzing the experimental data (this will be subject of the Part "Results and analyses"). The fits are systematic in the sense that for all experimental curves of one cell line type irradiated by one type of particle the same parameters a_i, b_i, r_i are used.

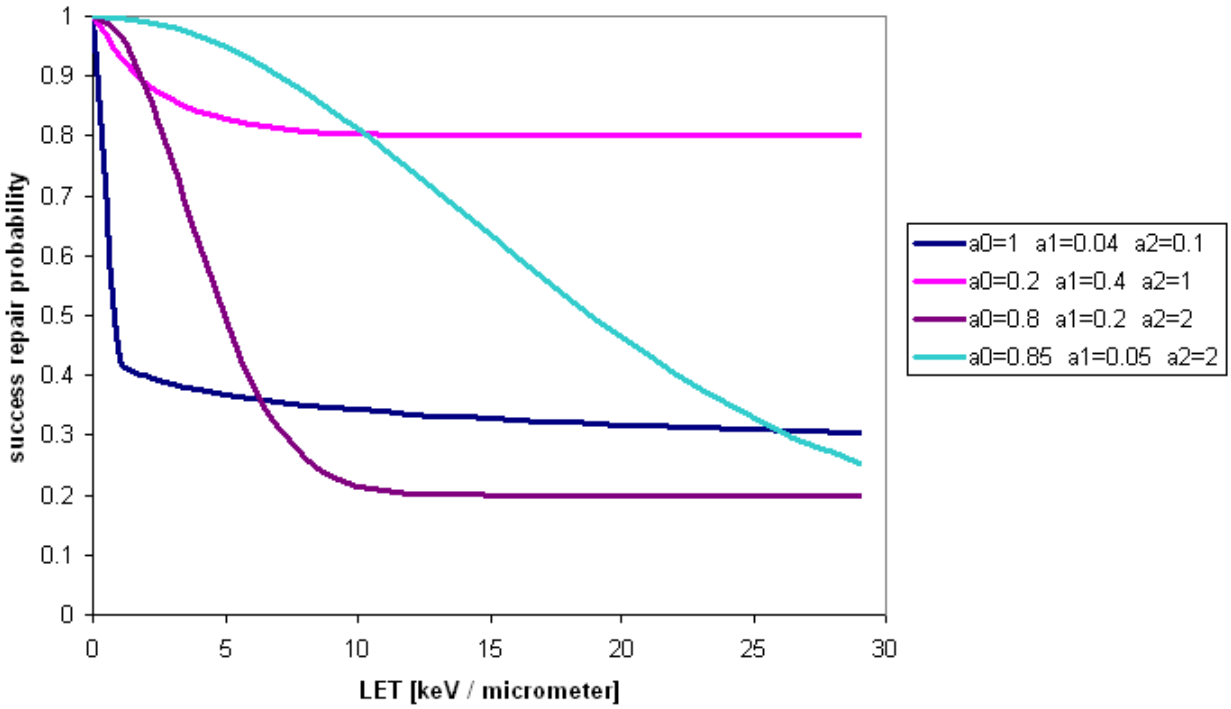

Figure 5.4: Function a(L) with various sets of auxiliary parameters $a_0 - a_2$

Chapter 6

Methods of calculation

6.1 FORTRAN

FORTRAN (abbreviation from *The IBM Mathematical Formula Translating System*) is a programming language that in the 1950s was developed for numeric computation and solving scientific problems. The FORTRAN code enables solving of computationally difficult problems like numerical weather prediction, computational physical and chemical analysis and others.

After the first version from 1956, FORTRAN has occurred in several latter versions with various extensions and compatibility with previous editions. The newer versions have supported processing of character-based data (FORTRAN 77), array programming and object-based programming (FORTRAN 90/95), object-oriented and generic programming (FORTRAN 2003) and parallel processing (the latest FORTRAN 2008).

The information about programming in FORTRAN can be found e.g. in [Etter 1990] or [McCracken 1961].

6.2 MINUIT

MINUIT routine was developed at CERN by Fred James as a tool designed to find the minimum value of a multi-parameter function and analyze the shape of the function around the minimum [http://seal.web.cern.ch]. The main application is statistical analysis using the chisquare or log-likelihood functions, computation of the best-fit parameter values including uncertainties and correlations between the parameters.

The MINUIT works upon a multi-parameter function named FCN, although the individual name may be changed by the user. The FCN function is defined by the user and depends on one or more variable parameters. The MINUIT routine then minimizes FCN with a view to maximum and minimum values of these parameters set by user, i.e. MINUIT find such a combination of parameters values that give the lowest value of chisquare. The chisquare is defined as follows:

$$\chi^2(\alpha) = \sum_{i=1}^{n} \frac{f_i(\alpha) - e_i}{\sigma_i^2}, \tag{6.1}$$

where α is the vector of free parameters being fitted, e_i individual measured values and the σ_i are the uncertainties in the individual measurement values e_i.

The parameter values and commands specifying the requested analysis are given either as a data file or they are written in special calling program in FORTRAN. The calling program needs to be compiled before execution, but gives a possibility of conditional execution, looping and other features available in FORTRAN. It is also possible to use calling program which use the input data file.

MINUIT routine is designed for finding the parameter values which minimize a function FCN defined by user. The shape of multi-parameter function FCN in proximity of the minimum determines the uncertainty in the best parameter values, the so called *parameter errors*. MINUIT gives a possibility to analyze the parameter errors in several different ways (calculation of Error Matrix, finding FCN contours and others).

The detailed information about MINUIT package can be found especially in [http://seal.web.cern.ch], various methods for finding the greatest or least value of function are given e.g. in [Nelder and Mead 1965, Rosenbrock 1960]

6.3 Data digitizing

Data were digitized from published papers by digitizing program WinDIG, which was created by D. Lovy at Dept. of Physical Chemistry in University of Geneva [http://www.unige.ch].

WinDIG is a free data digitizer for Windows, designed to get curves and points from scanned images of different formats. The programm enables manual or fast automatic curve digitalization, measuring and storing distances in a graph, basic bitmap edition functions for small corrections and many other functions.

6.4 Procedure of calculation

The first step consists in writing the initial parameters and their maximum and minimum values into a data file (see Figure 6.1). The parameter number is in the first column, followed by the name given by the user, in next column is required step size. In last two columns are maximum and minimum acceptable values.

```
Weyrather WK Int J.Biol.75,1357-1364(1999)
     1  Ac        .6730E+03    0.       1.         800.
     2  Ax        .7610E+03    0.       1.         761.
     3  a0        .9265E+00    0.01     0.         1.
     4  a1        .6016E-02    0.01     0.         1.00
     5  a2        .1869E+01    0.010    0.        15.00
```

Figure 6.1: The part of the input data file

The second step is compilation and start of the FORTRAN program calling the minimization routine MINUIT. The program acts on the input data file and the resulting parameter values are saved in to the output data file. In this file may be found information about the resulting FCN value, and also the values of parameters and their uncertainties (see Figure 6.2). The output values may serve as an input for next run of the minimization procedure.

```
FCN=   4249.217     FROM MIGRAD    STATUS=CALL LIMIT  2008 CALLS     2265 TOTAL
                    EDM=  0.16E-03  STRATEGY=1  ERROR MATRIX UNCERTAINTY= 47.1%

 EXT PARAMETER                 APPROXIMATE        STEP         FIRST
 NO.   NAME        VALUE           ERROR          SIZE      DERIVATIVE
  1      Ac        673.00        constant
  2      Ax        761.00        constant
  3      a0       0.92657        0.48066E-02  -0.51046E-05  -0.77599
  4      a1      0.60129E-02     0.37708E-04   0.10237E-06   -64.320
  5      a2       1.8652         0.16979E-01   0.26760E-05    29.191
```

Figure 6.2: A part of the output data file

Part II

Results and analyses

Chapter 7

Analysis of experimental data

7.1 Study of cellular repair

For our study of cellular repair two cell lines have been chosen: wild type CHO-K1 cells and their radiosensitive mutant xrs5 with lacking Ku80 component of the active DNA-PK complex that is important in double strand break repair. Twelve survival curves for xrs5 and CHO-K1 irradiated by carbon ions of different LET values measured by [Weyrather *et al* 1999] have been used. In accordance with experimental evidence [Dikomey *et al* 1998] we have supposed that these cell lines did not vary in the induced DNA damage and the difference in response to irradiation is only due to their different repair capacities. The results of this analysis were published in [Hromčíková *et al* 2007]

7.1.1 Cell lines

Chinese hamster ovary cells CHO (see Figure 7.1) are widely used in biological, farmaceutical and medical research and development. They have a very low chromosome number (2n = 22), and for their rapid growth and high protein production they are an ideal model for radiation and other research [http://www.microscopyu.com].

Chinese hamster ovary cells - CHO-K1
In 1957, T. Puck derived original Chinese hamster ovary (CHO) cell line from the female Chinese hamster (*Cricetulus griseus*) from Dr. Yerganian's laboratory at the Boston Cancer Research Foundation [Puck *et al* 1958].

Chinese hamster ovary cells - mutant line xrs5
The xrs5 are radiosensitive mutant of CHO-K1 cells, lacking in the Ku80 component of the active DNA-PK complex. This complex is important in double strand break repair and in V(D)J recombination [Feng *et al* 1996].

	CHO-K1	**xrs5**
Cultivation		
Medium	Ham's F12 medium with 10% fetal calf serum and 2mM glutamine	α-MEM medium with 5% fetal calf serum and 2mM glutamine
Antibiotics	50units/ml penicillin and 50μg/ml streptomycin	50units/ml penicillin and 50μg/ml streptomycin
Atmosphere	humidified air, 5% CO_2	humidified air, 5% CO_2
Temperature	37 $^{\circ}C$	37 $^{\circ}C$
Properties of the cells		
Doubling time	12h	12h
Plating efficiency	0.75 $\pm$ 0.11	0.43 $\pm$ 0.06
Average nuclear size	108 $\pm$ 4.15 μm^2	122 $\pm$ 8 μm^2

Table 7.1: Parameters of CHO-K1 and xrs5 cells. The data was taken from [Weyrather *et al* 1999].

The parameters of cell cultivation and biological properties are given in detail in Table 7.1.

Before irradiation, the cell population was grown as monolayer logphase cultures. In case of low energy experiments, the cells were plated in a small area at the center of Petri dishes (35 mm in diameter) at an amount of 8x10^4 cells per one dish 12 – 24 hour before irradiation. Low-energy irradiation (energy of the particles 3.5 – 18.4 MeV/u) was performed at the GSI Unilac and the Tandem van de Graaf accelerator at Max Planck Institut fur Kernphysik in Heidelberg, Germany. For high-energy experiments, the cells were plated in an area of 3 cm in diameter to 25 cm^2 culture flasks. The irradiation was done at the GSI synchrotron SIS in Darmstadt, Germany

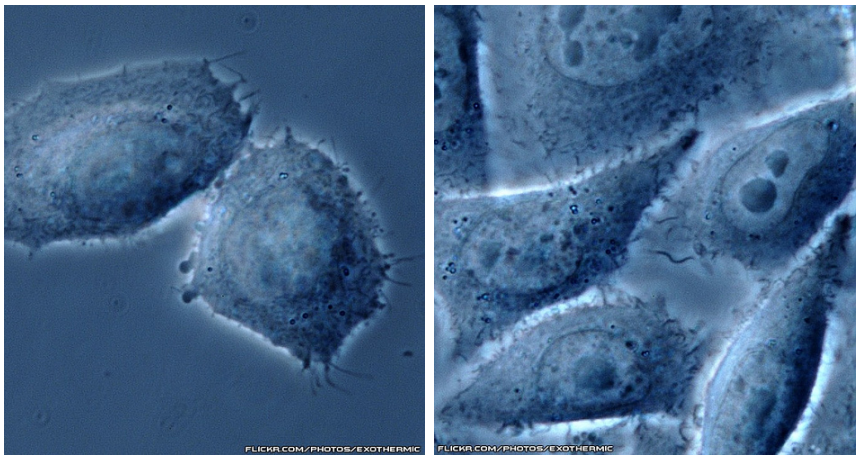

Figure 7.1: Live Chinese Hamster Ovary cells (CHO) in vitro viewed by a phase contrast microscope.
[http://flickr.com/photos/8928507@N02/2547162058]

[Weyrather *et al* 1999]. The physical parameters of the carbon beams used in irradiation are characterized in Table 7.2.

Cell survival after particle irradiation was measured by a colony assay in accordance with standard laboratory procedures [Wulf *et al* 1985]. All measurements were repeated 2-4 times; except 103.0 keV/μm, where the survival curve is the result of single experiment.

Energy [MeV/u]	**Energy on target [MeV/u]**	**LET [keV/μm]**	**Range in water (mm)**
270	266.4	13.7	140
195	190.7	16.8	80
85	76.9	32.4	15.9
18.4	18.0	103.0	1.2
11.4	11.0	153.5	0.5
6.12	5.4	275.1	0.15
5.0	4.2	339.1	0.1
3.5	2.4	482.7	0.05

Table 7.2: Parameters of carbon beams used in irradiation of CHO-K1 and xrs5 cells. The table is redrawn from [Weyrather *et al* 1999].

7.1.2 Assumptions

In our analysis of experimental data it has been supposed that damage formation characteristics are the same for both cell lines. Although the xrs5 cell line has no Ku80 component of the active DNA-PK complex and therefore is lacking in some repair pathways, the ability of repair is not totally blocked. Those repair processes that are common for both cell lines have been included in the damage induction probability (i.e., only unrepaired lesions for xrs5 cells are considered). Damage induction probabilities *a(L)* and *b(L)* are chosen in accordance with Eq. 5.24:

$$\begin{aligned} a(L) &= a_0(1 - e^{(-(a_1 L)^{a_2})}), \\ b(L) &= b_0(1 - e^{(-(b_1 L)^{b_2})}). \end{aligned} \tag{7.1}$$

Involving of repair processes for CHO-K1 is given by function:

$$\begin{aligned} r_a(L) &= 1 - r_{a0}(1 - e^{(-(r_{a1} L)^{r_{a2}})}), \\ r_b(L) &= 1 - r_{b0}(1 - e^{(-(r_{b1} L)^{r_{b2}})}); \end{aligned} \tag{7.2}$$

for xrs5 repair is not considered.

7.1.3 Results

Survival curves

In Figures 7.2 - 7.4 the theoretical and experimental survival curves for CHO-K1 and xrs5 cells are given. In Figure 7.5 the damage induction probabilities a and b are shown. Assuming that one particle can create only one kind of lesion, the b-type damage can be formed only in case that there was create no a-type damage. For the sake of clarity, there is modified function $b^* = b.(1-a)$ shown, too. In Figure 7.6 the repair probabilities in dependence on LET are displayed. In Figures 7.7 and 7.8 the functions $1-\Delta$ (creation of unrepaired a- or b-type damage), γ (formation of unrepaired b-type damage) and $1-\Delta-\gamma$ (creation of unrepaired a-type damage) in dependence on LET are shown.

For calculations of the average number of particles traversing the chromosomal system h_D (see Eq. (5.3)) the published values of nucleus area has been used [Weyrather *et al* 1999]:
$\sigma_{CHO} = 107{,}8\ \mu m^2, \quad \sigma_{xrs} = 122{,}0\ \mu m^2.$
For the sake of simplicity, it has been supposed that geometrical effective cross section of the chromosomal system σ is equal to whole nucleus area. The experimental data has been fitted by minimization routine MINUIT. For calculation of cell survival the Eq. (5.23) has been used.

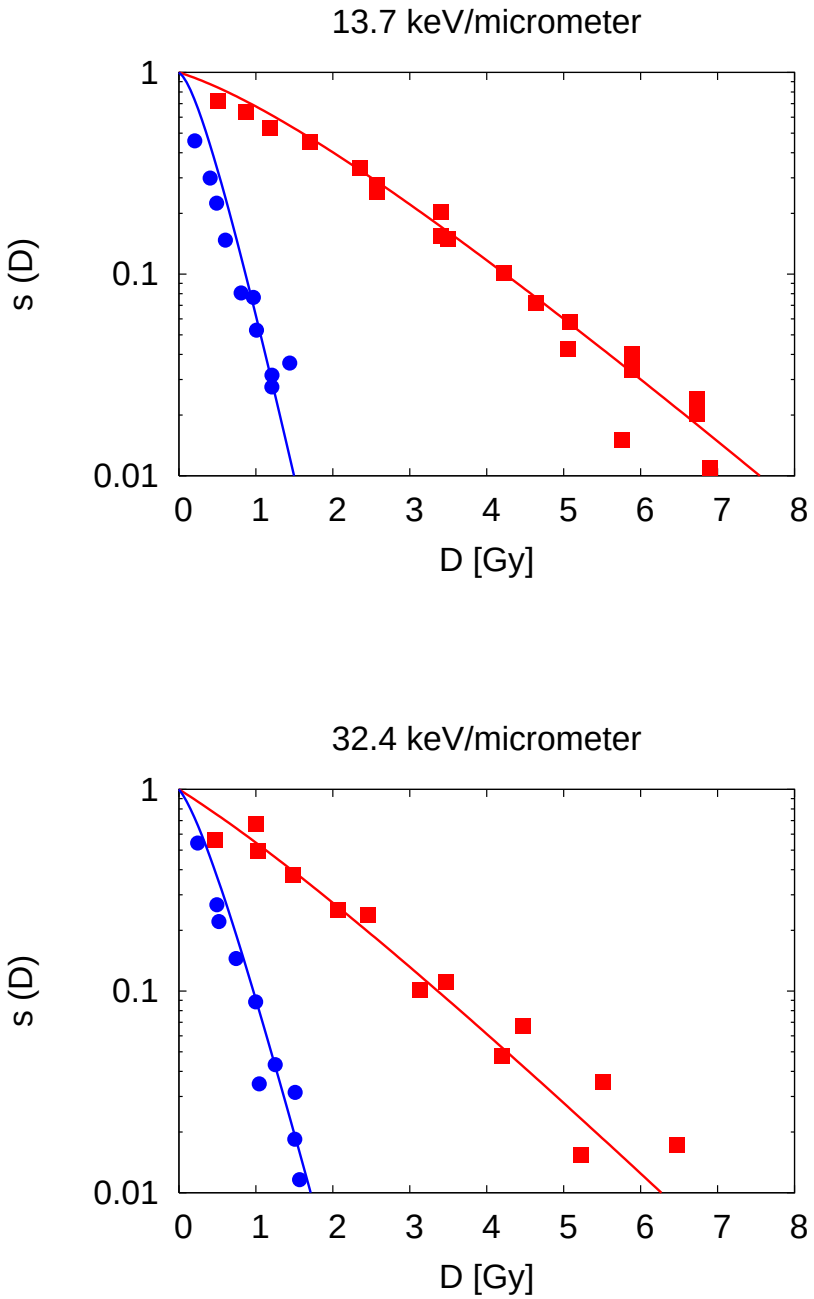

Figure 7.2: Survival curves for CHO-K1 (in red) and xrs5 cells (in blue) for 13.7 and 32.4 keV/μm

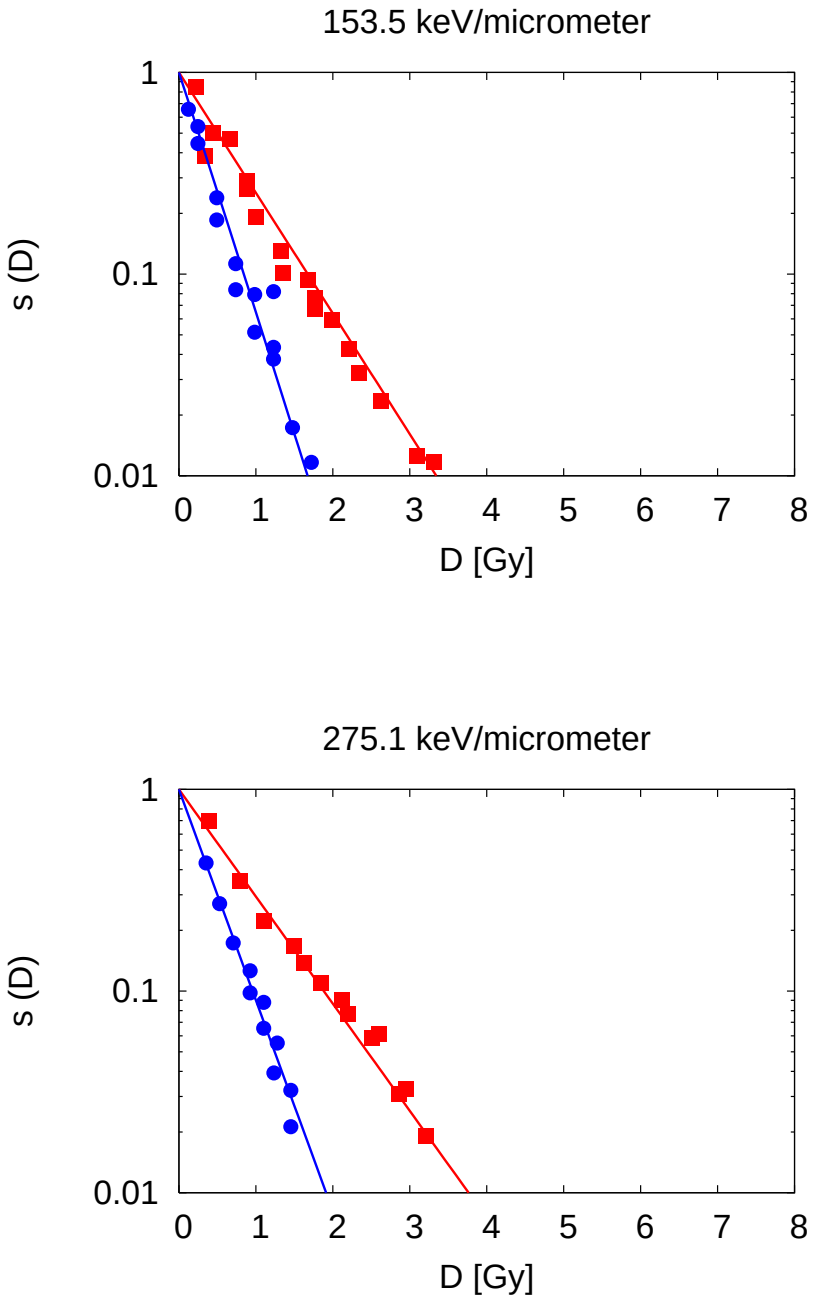

Figure 7.3: Survival curves for CHO-K1 (in red) and xrs5 cells (in blue) for 153.5 and 275.1 keV/μm

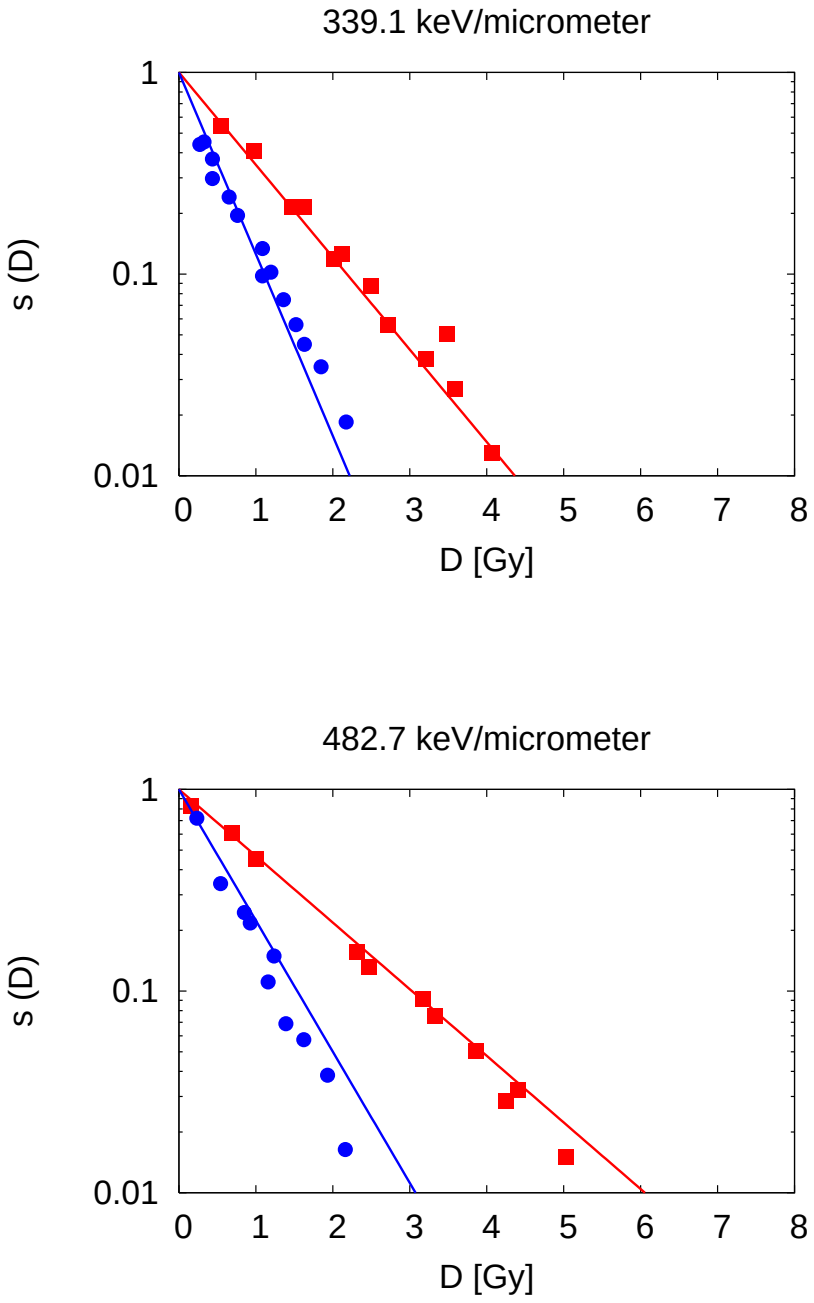

Figure 7.4: Survival curves for CHO-K1 (in red) and xrs5 cells (in blue) for 339.1 and 482.7 keV/μm

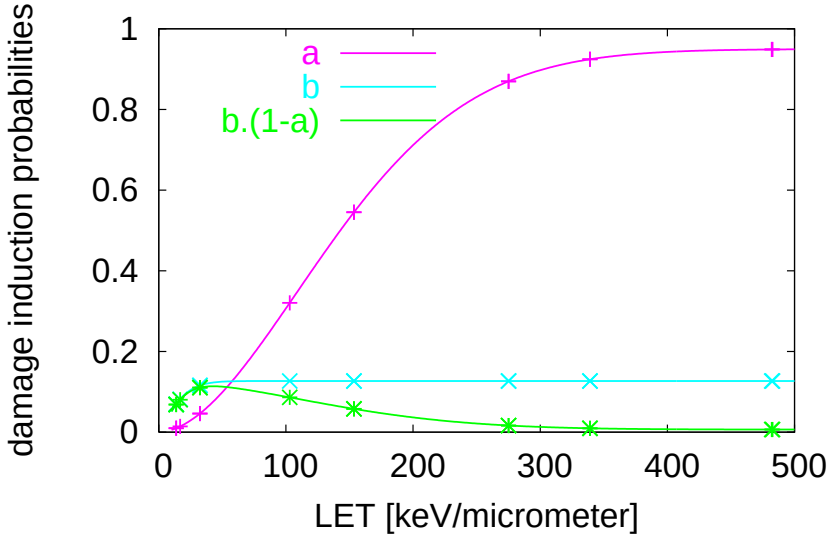

Figure 7.5: Damage induction probabilities in dependence on LET

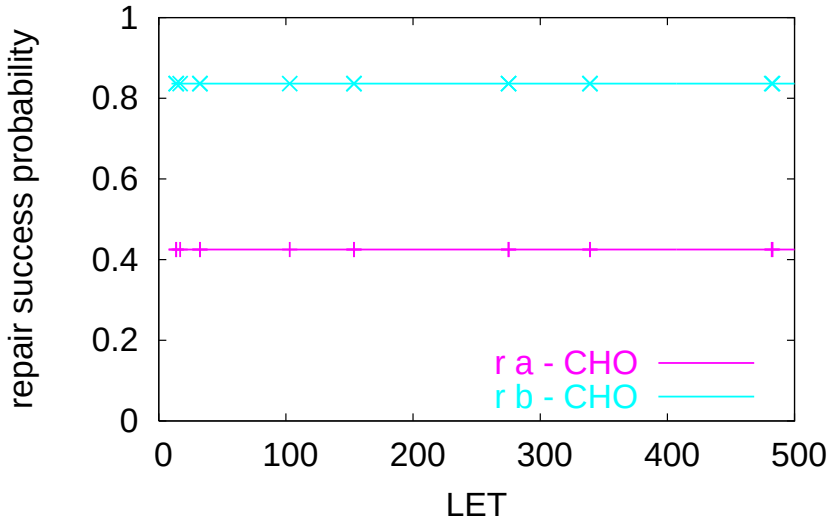

Figure 7.6: Repair success probabilities in dependence on LET

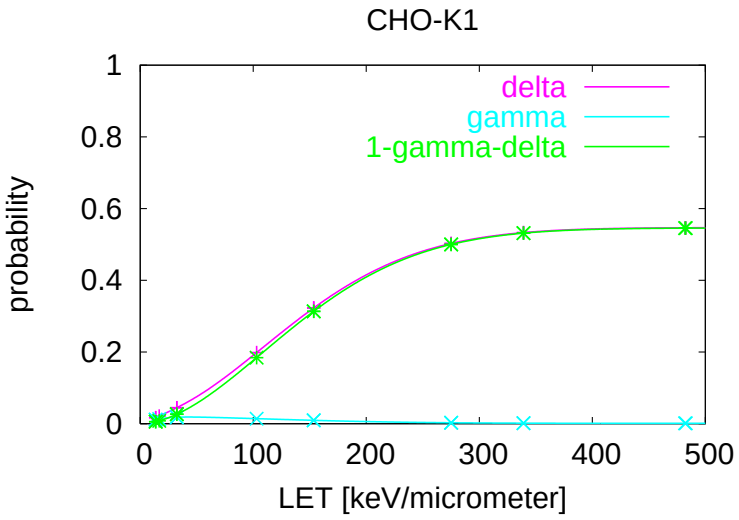

Figure 7.7: Functions $1-\Delta$, $1-\Delta-\gamma$ and γ in dependence on LET; CHO-K1 cells

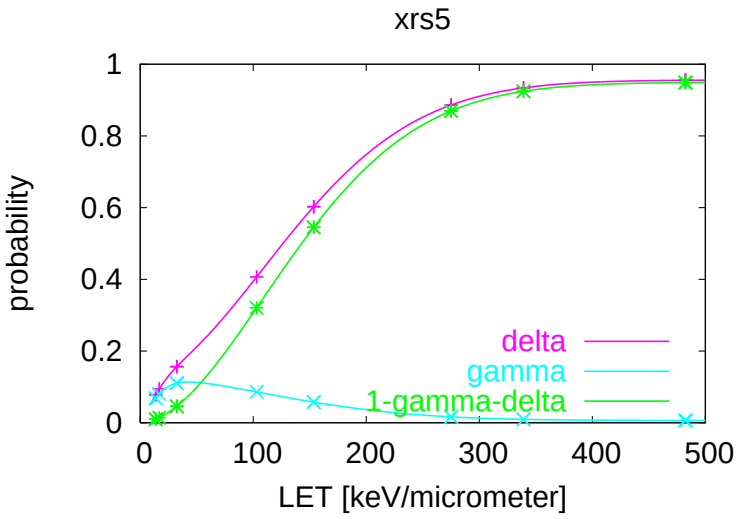

Figure 7.8: Functions $1-\Delta$, $1-\Delta-\gamma$ and γ in dependence on LET; xrs5 cells

In Tables 7.3 and 7.4 the results for damage induction and success repair probabilities are given.

parameter	**value**	**uncertainty**
a_0	0.950	0.3 x 10^{-2}
a_1	0.60 x 10^{-2}	0.3 x 10^{-4}
a_2	1.826	0.9 x 10^{-2}
b_0	0.127	0.4 x 10^{-2}
b_1	0.061	0.003
b_2	1.32	0.08

Table 7.3: Parameters of damage induction probabilities; the values are common to both cell lines

parameter	**value**	**uncertainty**
r_{a0}	0.575	0.2 x 10^{-2}
r_{a1}	1.08	0.01
r_{a2}	3	1
r_{b0}	0.259	0.3 x 10^{-2}
r_{b1}	7	5
r_{b2}	0.000	0.1 x 10^{-2}

Table 7.4: The parameters of repair success probability for CHO-K1 cell line; repair probability is function of LET

The fit is systematic in the sense that for all experimental curves the same parameters a_i, b_i, r_i are used; together 12 parameters. The measurement errors are taken from published experimental data [Weyrather *et al* 1999].

The repair success probabilities in dependence on LET seem to be almost constant (see Figure 7.6). If the calculation was made with only one parameter fitted by MINUIT (i.e. the repair probabilities independent on LET):

$$r_a = r^*_{a0} \qquad r_b = r^*_{b0}, \tag{7.3}$$

the survival curves and damage induction probabilities remain practically unchanged (compare Figures 7.5 and 7.6 with Figure 7.9). In the Table 7.8 and 7.6 values of damage induction probabilities and success repair probabilities r_{a0} and r_{b0} are presented.

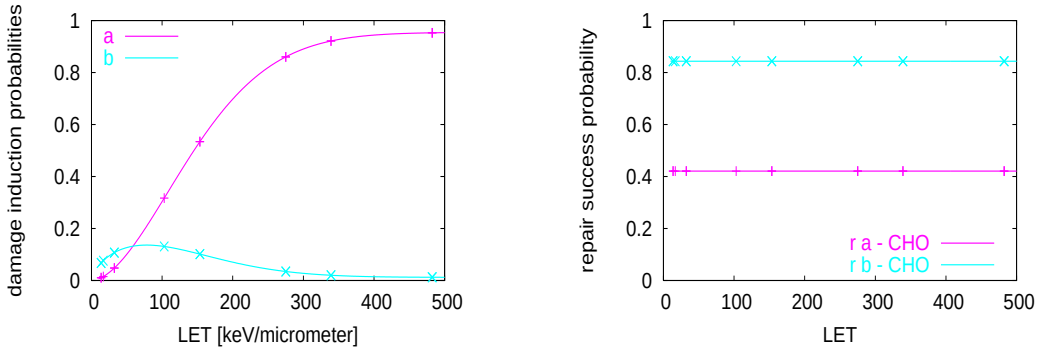

Figure 7.9: Damage induction probability (left) and repair probability (right); repair probability not dependent on LET

parameter	**value**	**uncertainty**
a_0	0.955	0.3 x 10^{-2}
a_1	0.58 x 10^{-2}	0.2 x 10^{-4}
a_2	1.778	0.8 x 10^{-2}
b_0	0.270	0.9 x 10^{-2}
b_1	0.0131	0.6 x 10^{-3}
b_2	0.72	0.01

Table 7.5: The parameters of damage induction probabilities

parameter	**value**	**uncertainty**
r^*_{a0}	0.421	0.002
r^*_{b0}	0.844	0.002

Table 7.6: Parameters of repair success probability for CHO-K1 cell line; repair not dependent on LET

The χ^2 of both calculations are almost the same, too:
χ^2 repair probabilities dependent on LET : 9528
χ^2 repair probabilities independent on LET : 9671

For estimating how different the damage induction probabilities for CHO-K1 and xrs5 cells are, independent fits have been made. In this analysis the values a and b have been fitted independently for individual curves, for both cell lines. It means that every experimental survival curve is fitted by the model (Eq. 5.23) separately, with individual values of a and b. For the sake of simplicity the repair probabilities r_a, r_b are the same for all CHO-K1 cells and for xrs5 the repair is not considered at all. The damage induction probabilities for independent fits together with systematic fits are displayed in Figure 7.10. The individual values of a, b are given in Table 7.7. These values for repair probabilities are: $r_a^* = 0.42$, $r_b^* = 0.84$. These values are almost the same as in the case of systematic fit with repair independent on LET, compare Table 7.6. All values in this analysis were calculated with an accuracy of 0.01. The χ^2 of this independent fit is 7956, approximately about 15 % better then the systematic fit. The Figure 7.10 demonstrates that the a and b in the independent fit have roughly the same behavior as the systematic fit. These findings are in accordance with assumption that the repair ability of the xrs5 cells is very low.

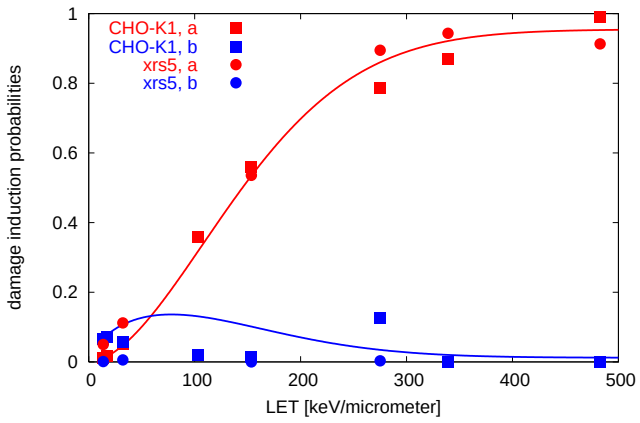

Figure 7.10: Values of a, b in independent fits (points) and their comparison with systematic fit (lines)

cell line	LET [keV/μm]	a	b
CHO-K1	13.7	0.0110	0.0663
	16.8	0.0160	0.0703
	32.4	0.0511	0.0569
	103.0	0.3597	0.0184
	153.5	0.5603	0.0135
	275.1	0.7875	0.1272
	339.1	0.8712	0.0007
	482.7	0.9891	0.0002
xrs5	13.7	0.0498	0.0010
	32.4	0.1119	0.0057
	153.5	0.5357	0.0073
	275.1	0.8948	0.0031
	339.1	0.9435	0.0006
	482.7	0.9129	0.0030

Table 7.7: Values of a and b, independent fits.

Damage induction probabilities

The calculated survival curves (see Figures 7.2 – 7.4) are in good agreement with experimental data. In Figure 7.5 damage induction probabilities in dependence on LET are displayed. It is evident, that for lower LET values ($<$ 50 keV/μm) the probability of creating less severe damage (b) dominates over the probability of forming lethal damage by a single track (a). This finding results from the fact that for low LET the particles transfer to DNA molecule an energy insufficient to forming a severe lesion (complex damage site). With increasing LET (and thus increasing energy given to a cell per unit length) the probability of creating a lethal single particle damage increases. At the LET value of approx. 60 keV/μm the contributions of a and b are equal. From this value the probability of inducing a single particle damage steeply increases, to approximately 300 keV/μm, and from this value more slowly to the probability value of 0.95. The "combined" modified damage probability $b^* = b.(1 - a)$ has the maximum at 60 keV/μm and then decreases to zero. This fact mean, that for these LET values practically every particle traversing

the nucleus has enough energy to create a severe a-type damage.

The experimental curves demonstrate that the steepest slope has the survival curve for LET = 153.5 keV/μm. At this LET value the Relative Biological Efficiency (RBE) reaches the maximum and for greater LET the so-called overkill effect occurs (for more details about RBE and overkill effect see page 14). The RBE in dependence on LET for this data set can be found in [Weyrather *et al* 1999].

Probability of successful repair

As mentioned in section "Assumptions", repair is considered only for wild cell line CHO-K1. The repair success probabilities in dependence on LET are given in Figure 7.6. As shown in this figure, repair success probabilities $r_a(L)$, $r_b(L)$ for CHO-K1 are practically constant. This finding gives the support for the idea that only the first stage in radiobiological mechanism is dependent on physical characteristics of the irradiation (e.g. LET) and the second phase is determined only by biological properties of given cell population [Kundrát 2007]. The difference in repair capability between these cell lines can be visible also in Figures 7.7 and 7.8. For the xrs5 cells, the function γ is identical with modified probability $b^* = b.(1-a)$ and $1-\Delta-\gamma$ coincides with function a.

The cell repair capability is dependent on cell line type, the position in cell cycle (most sensitive are cells in M phase [Steel 1993]), presence of scavenging agents and many others conditions. The most radiosensitive "wild" cells are those with high division and metabolic rate or non-specialized (stem cells). In laboratory it is possible to prepare cell lines with well defined type of radiosensitivity (like xrs5 mutant in this analysis).

Theoretically, the $r_a(L)$ and $r_b(L)$ are dependent only on the intrinsic cell characteristic. Therefore it is possible to say that CHO-K1 cells succeed in repairing approximately 42 % of the a-type damage and 84% of the b-type damage not repaired by xrs5 cells (see Tab. 7.4). The a-type damage involves lethal single particle lesions, like complex damage sites (a group of double-strand breaks and other lesions), while the b-type damage encompasses the less severe lesions (some types of double-strand breaks, misrejoining of double-strand breaks); see DNA lesion classification on page 68.

7.2 Comparison of different models

The aim of this section is to compare various models used currently in radiobiology. For this purpose we have chosen the generally used Linear Quadratic model, the Probabilistic Two-stage model proposed in the Institute of Physics and the Local Effect Model proposed in the GSI center in Germany. The models have been compared by fitting the same experimental data set (chinese hamster ovary cells CHO-K1). The theoretical survival curves obtained from these three models are shown and the goodness of fits is discussed.

7.2.1 Cells

The experimental data was taken from [Scholz *et al* 1997]. The experiments were performed by W. Weyrather with CHO cells grown as monolayers in culture flasks; the further details about cells and their processing were not published. It has been assumed that cells have the same properties as CHO cells used in previous section "7.1 - Study of cellular repair". This assumption is corroborated by the fact that in both cases the measurements were performed by the same authors (W. Weyrather, M. Scholz). Nevertheless, even when the experiments were done with the same cell line and the equal physical parameters of carbon beam, the survival curves are slightly different (see Figure 7.18 on page 102). This discrepancy may be the result of different growth conditions of the cultures, differences in irradiation or diverse data processing and survival scoring.

7.2.2 Characteristics of compared models

The already mentioned models have been used: Linear Quadratic model, Local Effect Model and Probabilistic two-stage model. Very brief characteristics of these models:

Linear Quadratic model
In the Linear Quadratic model (LQ) the survival of irradiated cells is given by

$$S = e^{-\alpha D - \beta D^2}, \tag{7.4}$$

where α, β are parameters. This approach represents continuously bending curves. Further details about this model can be found on page 53.

Local Effect Model
The Local Effect Model (LEM) is based on the presumption that the biological effect of irradiation is given locally as a function of the local dose

deposited by charged particle tracks [Scholz and Kraft 1996]. The inputs for this model are x-ray survival curves, the radial dose distribution inside the track and geometrical parameters of cell nucleus. The LEM theoretical curves are taken from [Scholz *et al* 1997] and they have not been calculated by the author of this thesis. Further details about the Local Effect Model can be found on page 57.

Probabilistic two-stage model
The Probabilistic two-stage model (P2S) describes the damage induction caused by radiation and also repair processes in cells. The P2S model enables to distinguish and describe two various types of lesions - lethal damage formed by a single track and less severe damage, where only combination of at least two events may be lethal. Further details about Probabilistic two-stage model can be found on page 66.

7.2.3 Results

In Figures 7.11 and 7.12 the theoretical and experimental survival curves for CHO-K1 fitted by the probabilistic two-stage model are shown. The damage induction probabilities a, b and the modified probability $b^* = b.(1-a)$ and also the repair probabilities $r_a(L)$ and $r_b(L)$ in dependence on LET are displayed (Figures 7.13 and 7.14). In Figure 7.15 the functions $1-\Delta$, $1-\Delta-\gamma$ and γ in dependence on LET are shown. For calculations of the average number h_D of particles traversing the chromosomal system (see Eq. (5.3)) the published value of nucleus area has been used [Weyrather *et al* 1999]: $\sigma_{CHO} = 107{,}8\ \mu^2$.

For the sake of simplicity, it has been supposed that geometrical effective cross section of the chromosomal system σ is equal to whole nucleus area.

In Figures 7.16 and 7.17 the comparisons between theoretical curves obtained by LQ model, P2S model and LEM for several different LET values are presented.

Survival curves

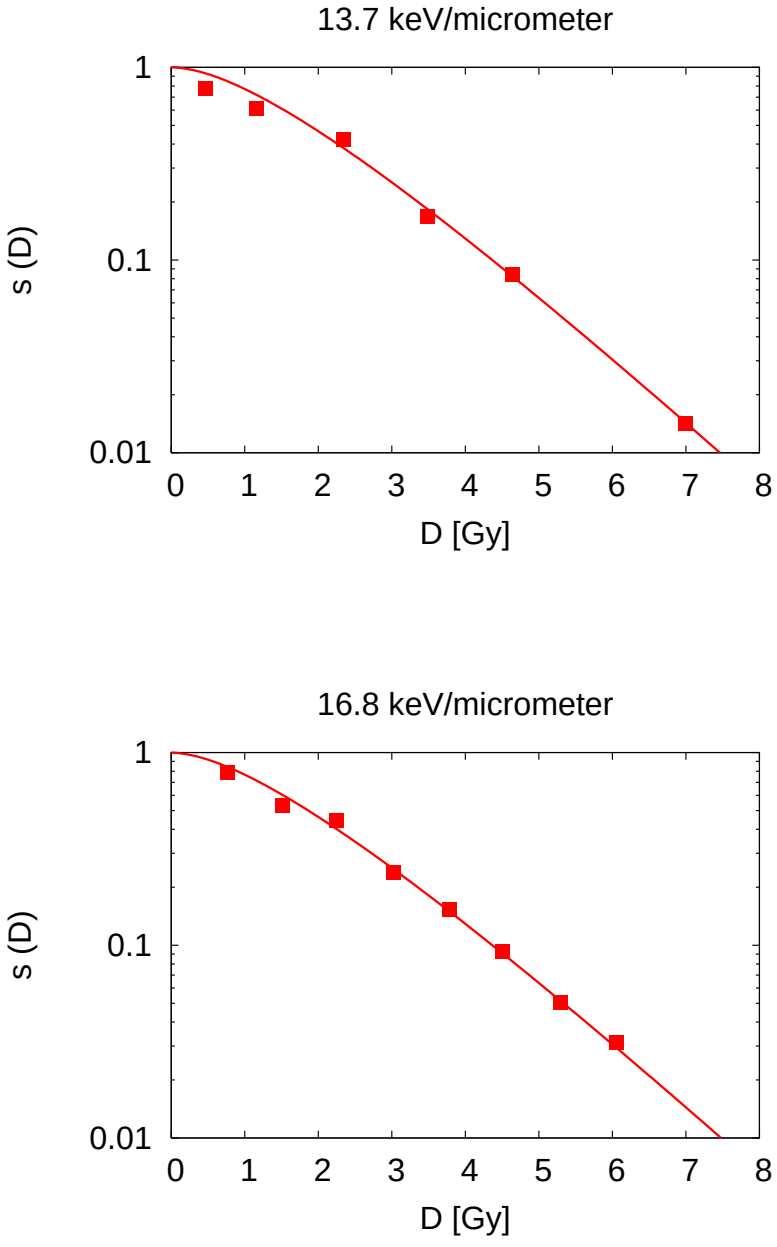

Figure 7.11: Survival curves for CHO-K1 cells irradiated by 13.7 and 16.8 keV/μm C ions, fitted by the P2S model

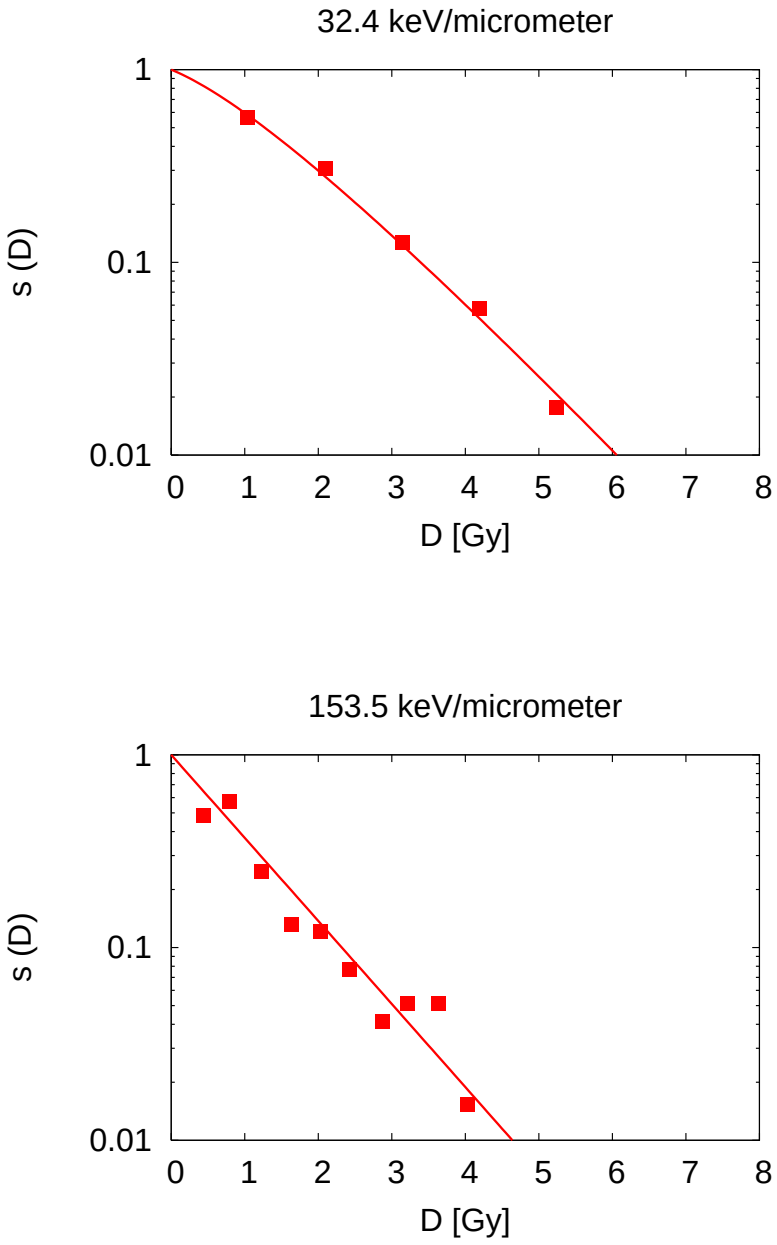

Figure 7.12: Survival curves for CHO-K1 cells irradiated by 32.4 and 153.5 keV/μm C ions, fitted by the P2S model

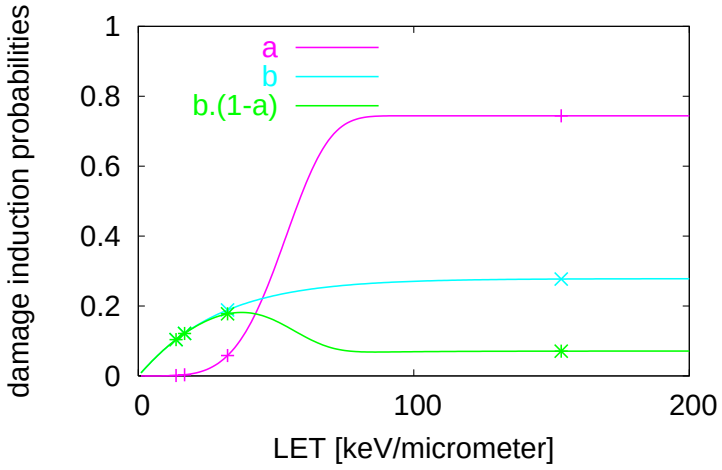

Figure 7.13: Damage induction probabilities in dependence on LET.

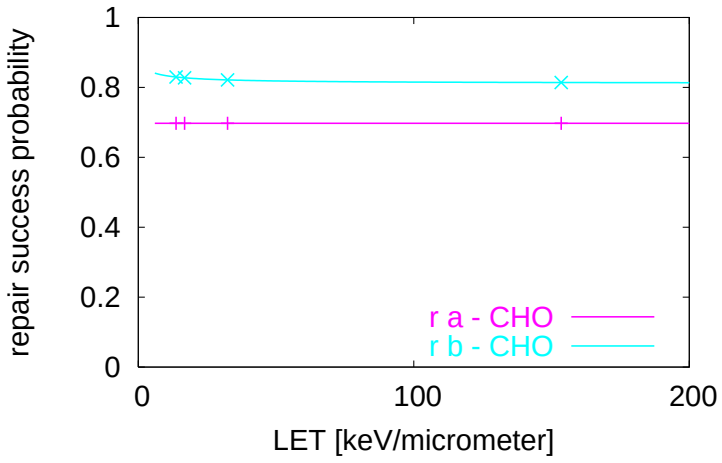

Figure 7.14: Success repair probabilities in dependence on LET.

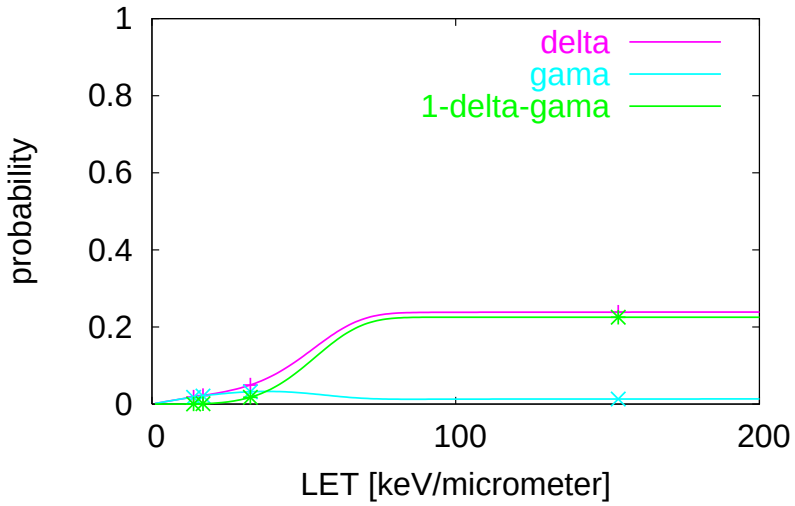

Figure 7.15: Functions $1 - \Delta$, $1 - \Delta - \gamma$ and γ in dependence on LET.

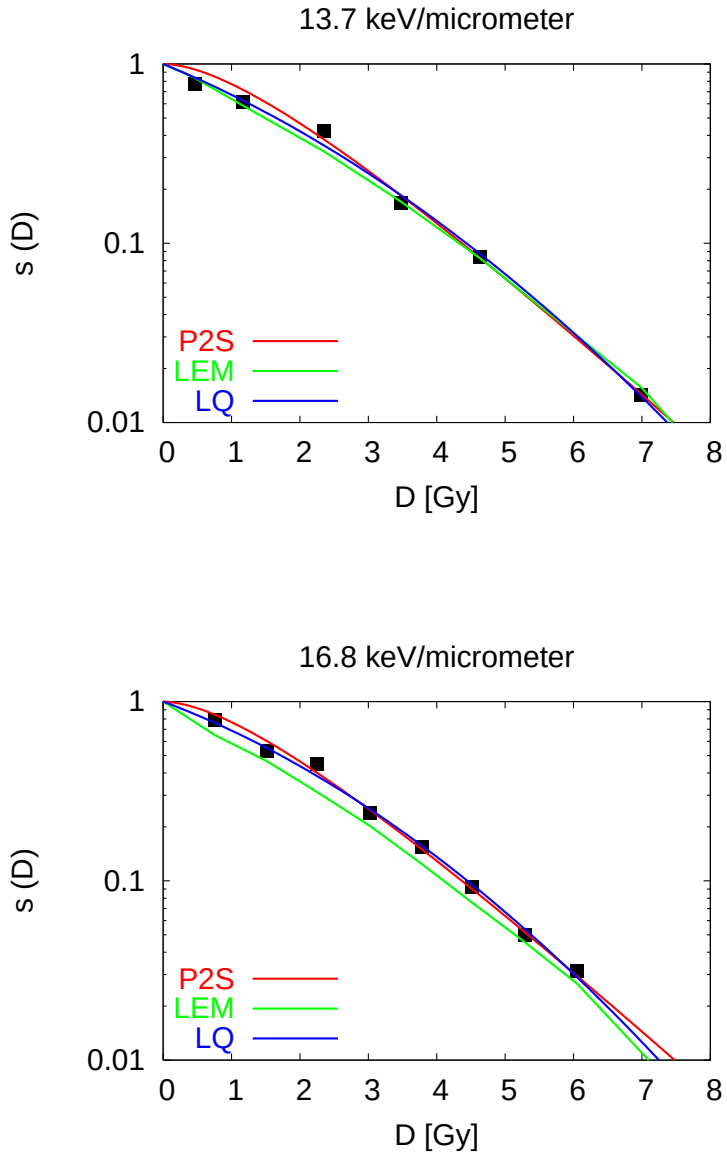

Figure 7.16: Comparison of P2S model (in red), LQ model (in blue) and LEM (in green); the survival curves for CHO-K1 cells irradiated by 13.7 and 16.8 keV/μm C ions

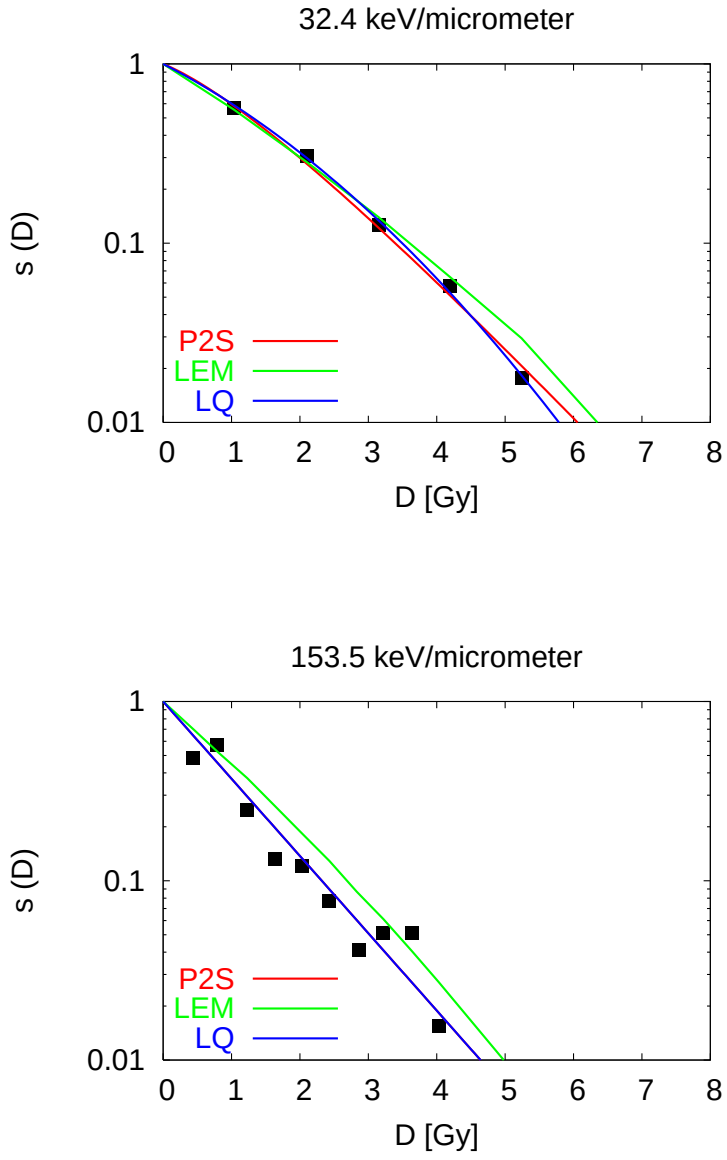

Figure 7.17: Comparison of P2S model (in red), LQ model (in blue) and LEM (in green); the survival curves for CHO-K1 cells irradiated by 32.4 and 153.5 keV/μm C ions. In the lower graph the red line coincides with the blue one.

The Probabilistic two-stage model fit

The experimental data has been fitted by minimization routine MINUIT. For calculation of cell survival the Eq. (5.23) has been used. The fit is systematic, for all four experimental curves the same parameters a_i, b_i, r_i has been used. In Table 7.8 the results for parameters of damage induction and success repair probabilities are given.

parameter	**value**	**uncertainty**
a_0	0.75	0.07
a_1	0.0186	0.5 x 10^{-3}
a_2	4.9	0.3
b_0	0.334	0.3 x 10^{-2}
b_1	0.028	0.6 x 10^{-3}
b_2	1.04	0.05
r_{a0}	0.30	0.03
r_{a1}	3	2
r_{a2}	0.7	0.2
r_{b0}	0.19	0.5 x 10^{-2}
r_{b1}	1.6	0.2
r_{b2}	0.3	0.02

Table 7.8: Parameters of damage induction probabilities and repair success probabilities; repair is dependent on LET

The CHO cells were irradiated by beams with the same LET values as cells in previous Section "Study of cellular repair". Nevertheless, the damage induction probabilities and success repair probabilities are not exactly the same. This fact is caused by slight differences in experimental curves in both measures, compare Figure 7.18. This figure shows, that especially the fourth curve (LET value 153.5 keV/μm) is different in measurement by [Scholz *et al* 1997] than in measurement performed by [Weyrather *et al* 1999]. As mentioned above, the differences in measurements may be result of different growth conditions of the cultures, differences in technique of irradiation or discrepant data processing and survival scoring.

The damage induction probabilities show the same trend as in Section "Study of cellular repair": for low LET the probability of creating less severe

damage (b-type) dominates over the probability of forming lethal damage by a single track (a-type); compare Figure 7.13.

The repair success probabilities r_a and r_b are shown in Figure 7.14. Again, the curves are almost constant. This finding gives support for the idea mentioned in previous analysis that repair success is determined only by biological properties of a given cell population.

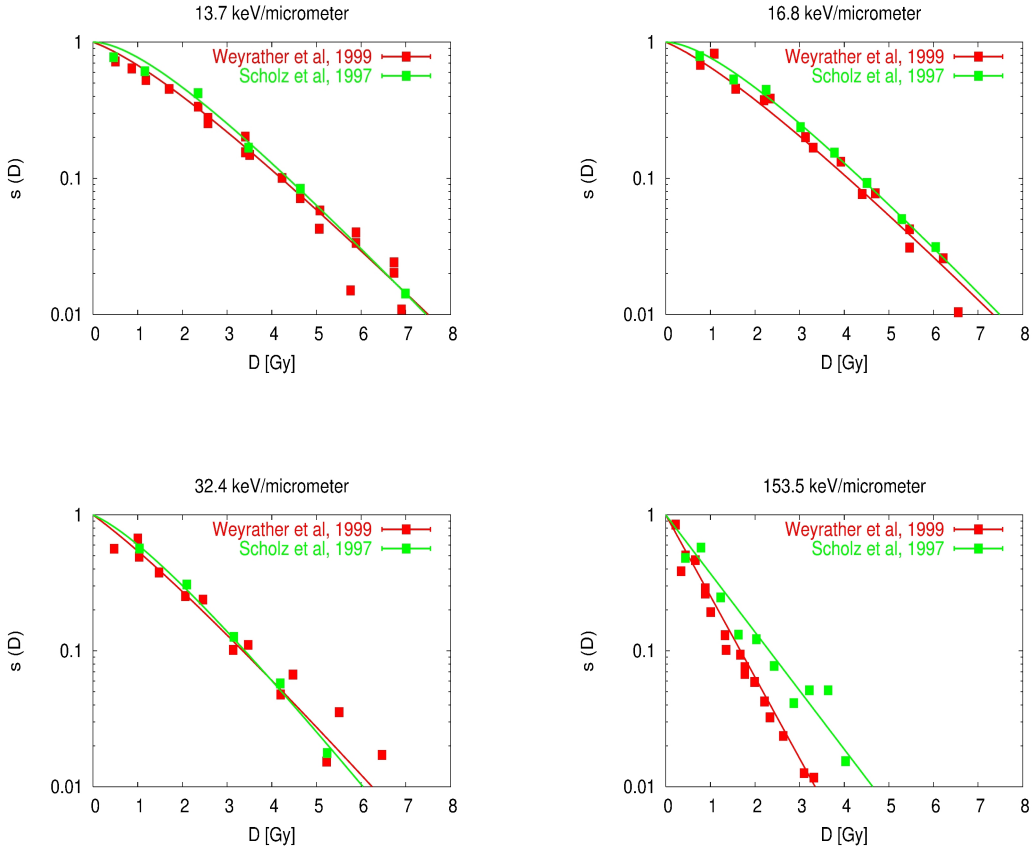

Figure 7.18: CHO-K1 cells: comparison of survival curves for equal values of LET; P2S fit.
Experimental data taken from [Weyrather *et al* 1999] (in red) and from [Scholz *et al* 1997] (in green).

The Linear Quadratic model fit

The cell survival after irradiation was calculated from equation

$$S = e^{-\alpha D - \beta D^2}, \tag{7.5}$$

where α, β are parameters unique for all curves (therefore, for calculating was used 8 parameters). The parameter values are given in Table 7.9.

LET [keV/μm]	α	β
13.7	0.3607	0.0358
16.8	0.3301	0.0421
32.4	0.4495	0.0599
153.5	0.9923	0.0000

Table 7.9: Parameters α, β in linear-quadratic fit

The Local Effect Model fit

The Local Effect Model fit was adapted from [Scholz *et al* 1997] by data digitizing program WinDIG (for details about the programm, see page 76).

The comparison of fits

The goodness of fit of a mathematical model characterizes how well it represents experimental data. Measures of goodness of fit usually describe the discrepancy between values acquired by the experiment and the values obtained by a given model. For describing the goodness of fit, the reduced χ square weighted by measurement uncertainties has been used:

$$\chi^2(\alpha) = \sum_{i=1}^{n} \frac{f_i - e_i}{\sigma_i^2}, \tag{7.6}$$

where the square of difference between theoretical and experimental value is in the numerator and the uncertainties of the measurement are in the denominator. The value of χ^2 was calculated directly by routine MINUIT (for further details, see chapter "Methods of calculation" on page 75).

The comparison of Linear Quadratic model, Local Effect Model and Probabilistic two-stage model is given in Figures 7.16 and 7.17. In Table 7.10, χ^2 values for each survival curve and a sum of them are displayed.

From this table follows that the fourth curve has the biggest χ^2 for all models. This finding is given by fact that the experimental values of this curve are relatively scattered in comparison to other curves. For this curve, all fits are almost linear (on semi-logarithmic scale), but the LEM fit lies

curve	**LET [keV/μm]**	χ^2		
		LEM	LQ	P2S
1	13.7	52	35	55
2	16.8	237	27	26
3	32.4	180	9	34
4	153.5	1599	663	662
$\Sigma \quad \chi^2$		2068	733	777

Table 7.10: χ^2 of different fits for single curves and general χ^2

more outside the experimental points than P2S and LQ fits (see Figure 7.17) and therefore the χ^2 of the Local Effect Model for this curve is relatively high.

Generally speaking, the goodness of fit was the best for the Linear Quadratic model; the Probabilistic two-stage model shows similar results. The disadvantage of the LQ model and to a certain extent also the P2S model is that they are only descriptive, whereas the LEM may be regarded as a predictive model. On the other hand, the P2S model involves also the repair processes that are included neither in the LQ nor in the LEM. The P2S model may be in a manner regarded as partially predictive as it relates all parameters in a systematic way.

A similar comparison of different radiobiological models for cells irradiated by B ions can be found e.g. in [Hollmark *et al* 2007], where descriptive models like LQ model, Repairable-conditionally repairable damage model (RCR), P2S model and predictive models like Track structure theory (TST) and LEM model are compared.

7.3 Inactivation effect of different types of ions

In this analysis the cell inactivation in dependence on LET and ion species to assess the differences in the biological effects will be discussed. The difference in inactivation effect is caused by differences in track structure that result from the different energy deposition pattern for various ions.

For this study the published data [Tsuruoka *et al* 2005] has been used. The experiments were performed at International Space Radiation Laboratory and Division of Accelerator Physics and Engineering, National Institute of Radiological Sciences, Chiba, Japan.

7.3.1 Cell line

Normal human skin fibroblasts NB1RGB were obtained from the Riken cell bank in Japan (cell No. RCB0222). The basic characteristics of cultivation and qualities of cells are given in Table 7.11. The fibroblast skin cells are depicted in Figure 7.19.

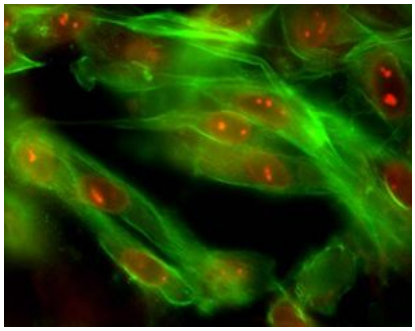

Figure 7.19: Fibroblast skin cells, 1000x zoom.
Picture taken from [http://www.ideum.com/portfolio/zoom_dna].

The cell cultures were irradiated by carbon (290 and 135 MeV/nucleon), neon (230 and 400 MeV/nucleon), silicon (490 MeV/nucleon) and iron (500 MeV/nucleon) ions generated by the Heavy Ion Medical Accelerator in Chiba (HIMAC) at the National Institute of Radiological Sciences (NIRS) in Japan. The physical parameters of beams and dosimetry have been described in [Kanai *et al* 1999]. All irradiations of cells were performed at room temperature [Tsuruoka *et al* 2005]. Experimental data will be given in corresponding figures.

Immediately after irradiation, cells were centerplated onto plastic dishes (diameter 100 mm, Falcon 3003) to produce 60 - 70 colonies per dish for the

Cultivation	
Medium	Eagles minimum essential medium (MEM) with 10% fetal bovine serum During culturing cells were rinsed in calcium- and magnesium-free phosphate-buffered saline (PBS) and exposed to a 0.2% trypsin solution
Atmosphere	95 % air and 5% CO_2
Temperature	37 $^{\circ}C$
Properties of the cells	
Plating efficiency	30 - 40 %
Average nuclear size	172.3 $\pm$ 2.18 μm^2

Table 7.11: Parameters of NG1RGB cells.
The data was taken from [Tsuruoka *et al* 2005].

cell survival assay. The colonies were fixed and dyed with the help of 20 % methanol and 0.2 % crystal violet after 14 days of incubation.

Cell survival was measured using a colony formation assay to measure reproductive cell death. For each dose value, three replicate dishes were used. According to standard procedures, colonies containing more than 50 cells were considered as survivors [Tsuruoka *et al* 2005]. The measurement for each dose was repeated three times.

7.3.2 Carbon ions

In Figure 7.20 the experimental survival curves for NG1RGB cells irradiated by carbon ions with various LET values are shown together with theoretical curves obtained by us. The damage induction probabilities and repair probabilities in dependence on LET are displayed in Figures 7.21 and 7.22. In Figure 7.23 the functions $1-\Delta$, $1-\Delta-\gamma$ and γ in dependence on LET are displayed.

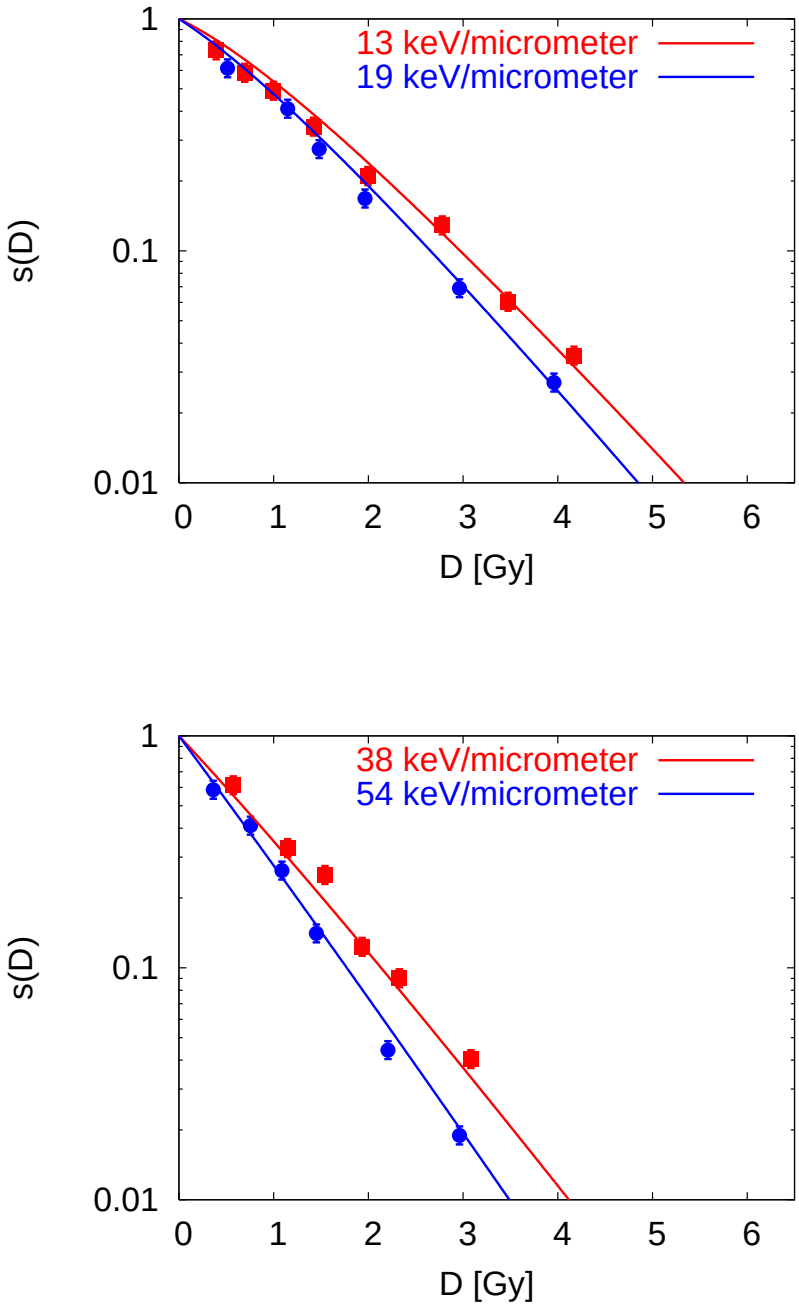

Figure 7.20: Carbon - survival curves for NG1RGB cells irradiated by 13, 19, 38 and 54 keV/μm

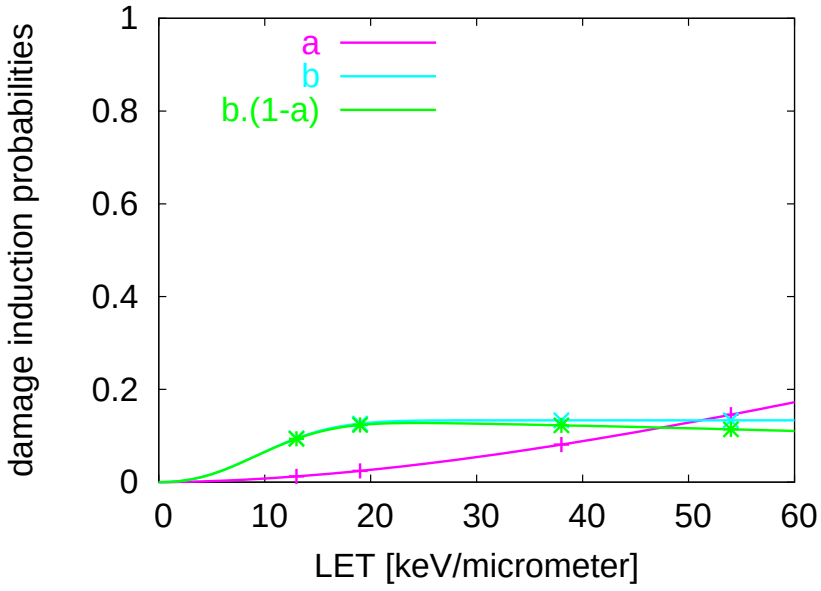

Figure 7.21: Carbon - the damage induction probabilities in dependence on LET

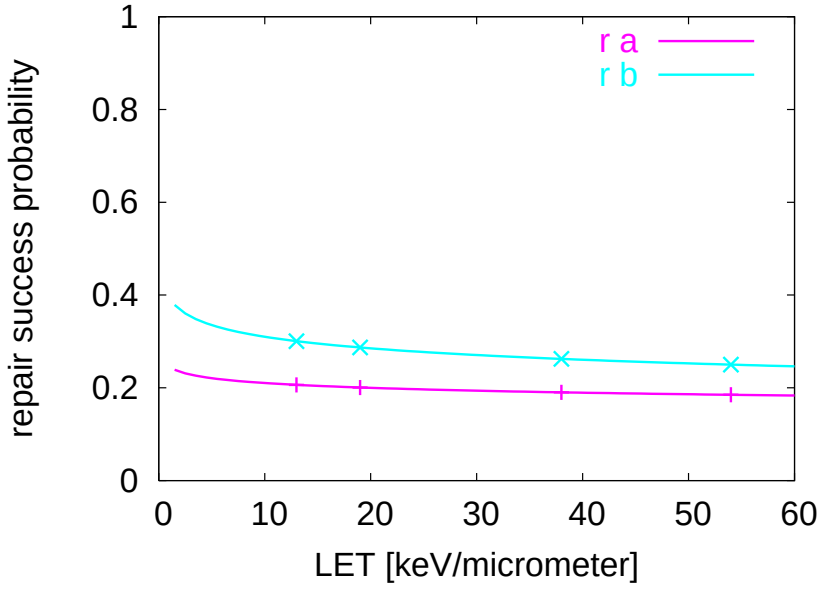

Figure 7.22: Repair success probabilities in dependence on LET

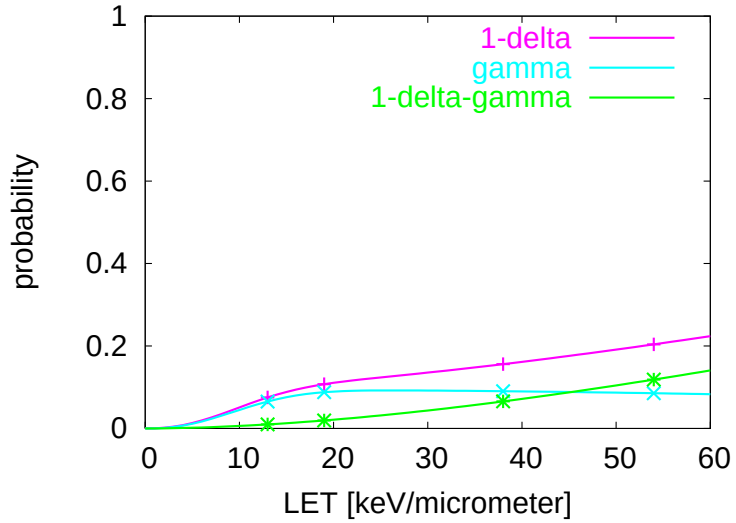

Figure 7.23: Carbon - functions $1-\Delta$, $1-\Delta-\gamma$ and γ in dependence on LET.

7.3.3 Neon ions

In Figure 7.24 the theoretical and experimental survival curves for NG1RGB cells irradiated by neon ions of various LET values are given. The damage induction probabilities and repair probabilities in dependence on LET are displayed in Figures 7.25 and 7.26. In Figure 7.27 the functions $1-\Delta$, $1-\Delta-\gamma$ and γ in dependence on LET are shown.

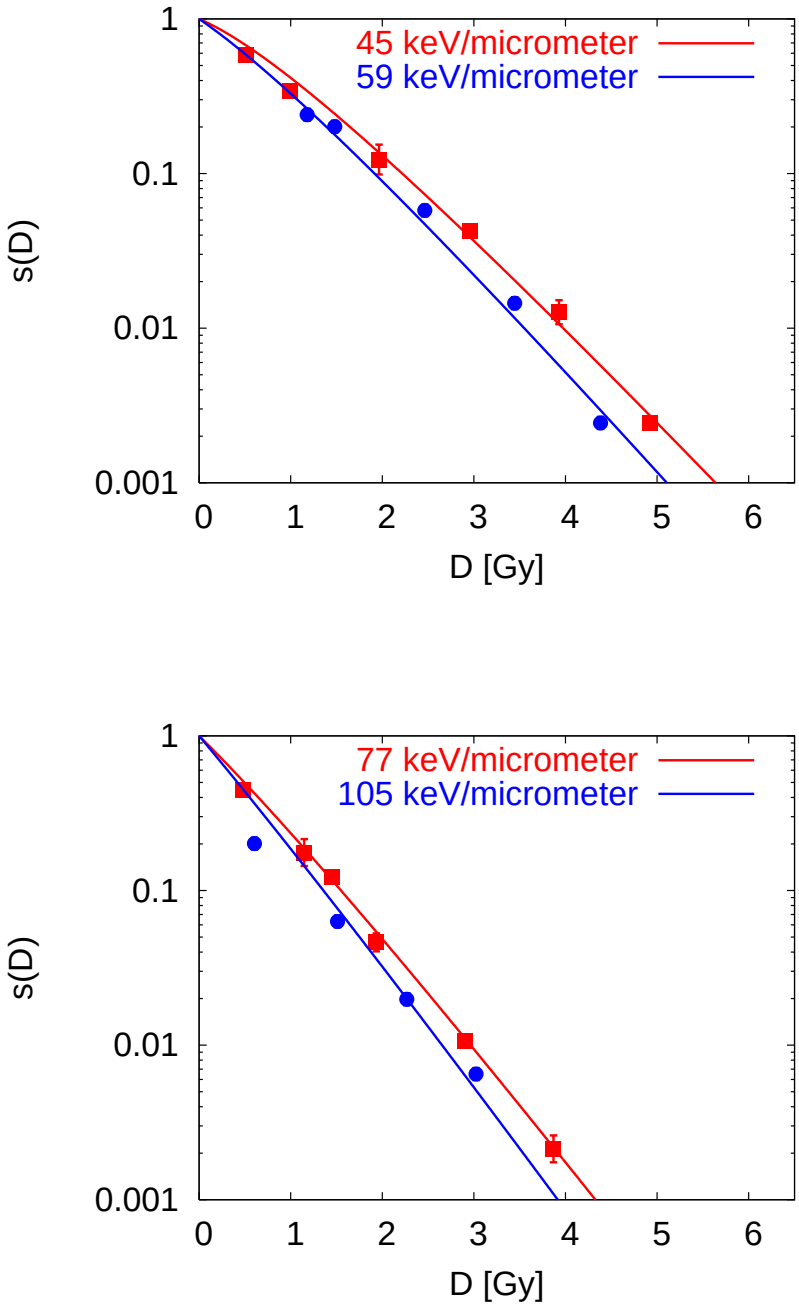

Figure 7.24: Neon - survival curves for NG1RGB cells irradiated by 45, 59, 77 and 105 keV/μm

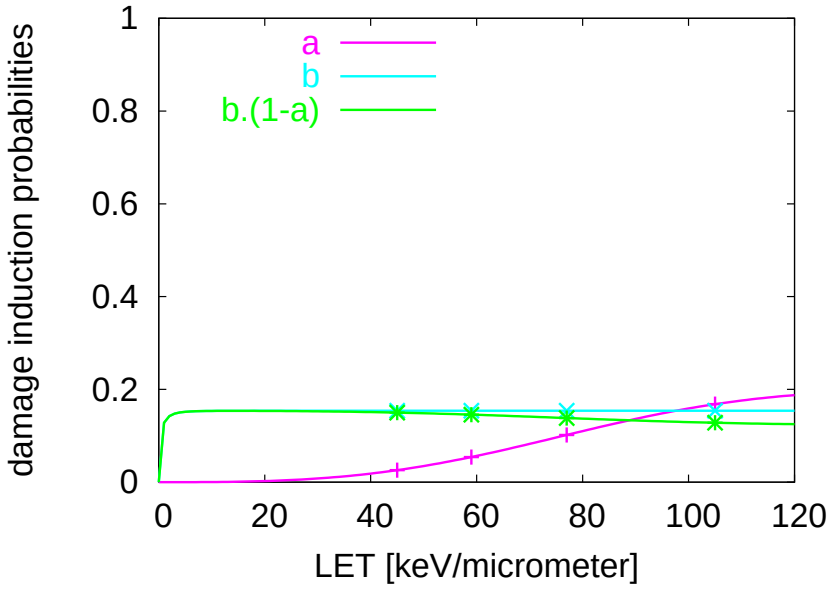

Figure 7.25: Neon - the damage induction probabilities in dependence on LET

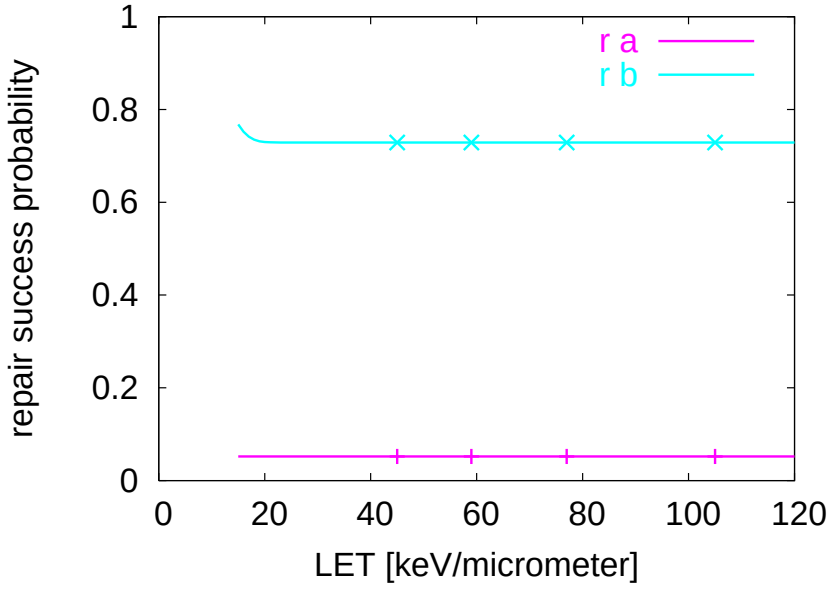

Figure 7.26: Neon - the success repair probabilities in dependence on LET

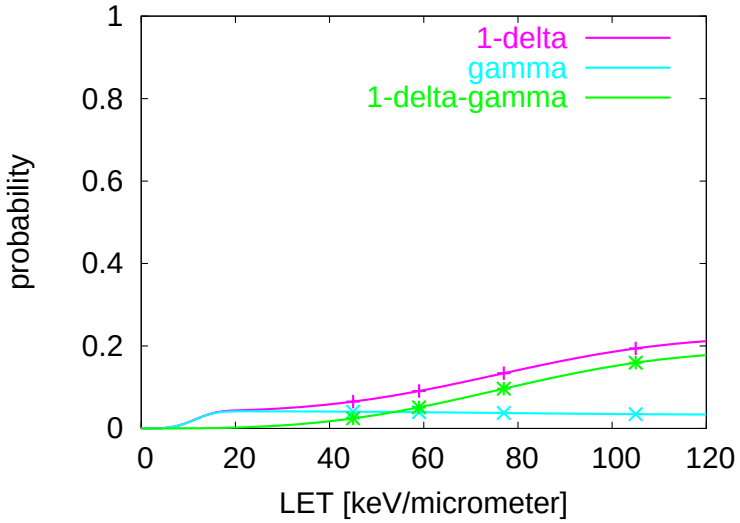

Figure 7.27: Neon - functions $1-\Delta$, $1-\Delta-\gamma$ and γ in dependence on LET.

7.3.4 Silicon ions

In Figure 7.28 the theoretical and experimental survival curves for NG1RGB cells irradiated by silicon ions of five various LET values are presented. The damage induction probabilities *a*, *b* and *b.(1-a)* and repair probabilities in dependence on LET are displayed in Figures 7.29 and 7.30. In Figure 7.31 the functions $1-\Delta$, $1-\Delta-\gamma$ and γ in dependence on LET are shown.

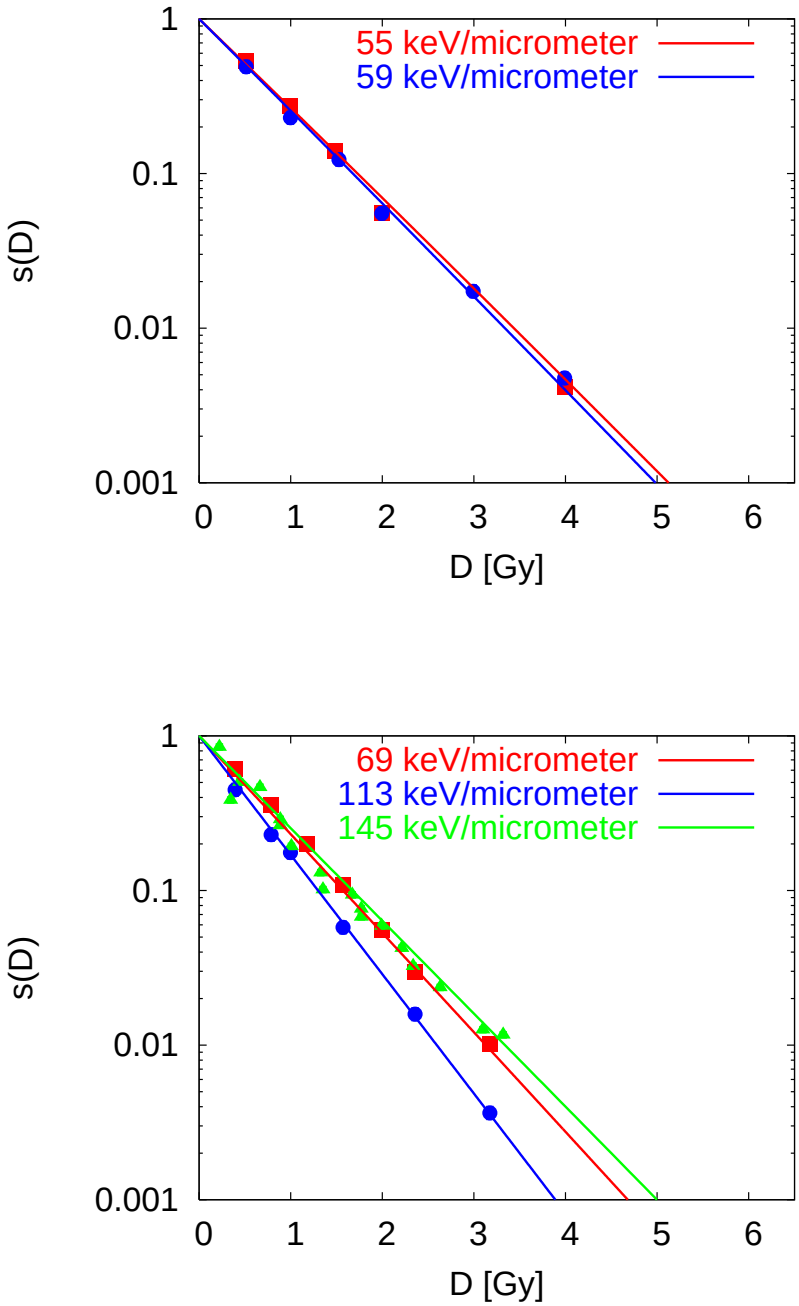

Figure 7.28: Silicon - survival curves for NG1RGB cells irradiated by 55, 59, 69, 113 and 145 keV/μm

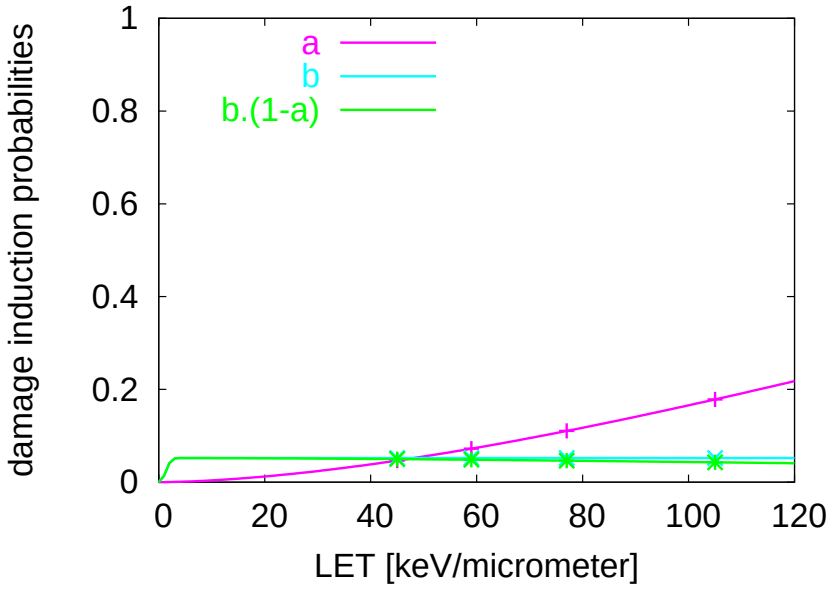

Figure 7.29: Silicon - the damage induction probabilities in dependence on LET

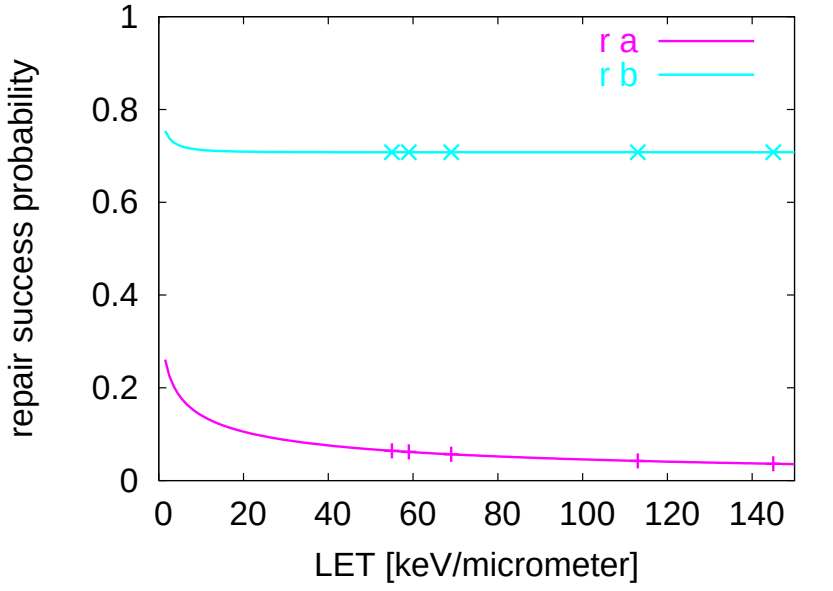

Figure 7.30: Silicon - the repair success probabilities in dependence on LET

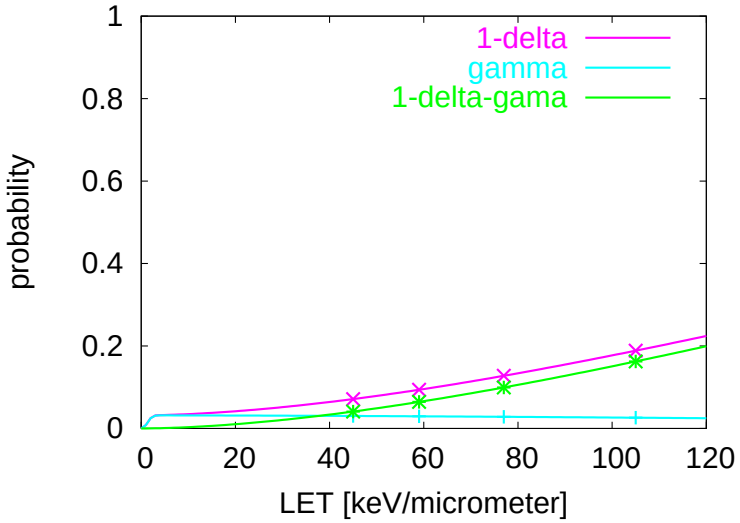

Figure 7.31: Silicon - functions $1 - \Delta$, $1 - \Delta - \gamma$ and γ in dependence on LET.

7.3.5 Iron ions

In Figure 7.32 the theoretical and experimental survival curves for NG1RGB cells irradiated by iron ions of various LET values are shown. The damage induction probabilities and repair probabilities in dependence on LET are displayed in Figures 7.33 and 7.34. In Figure 7.35 the functions $1 - \Delta$, $1 - \Delta - \gamma$ and γ in dependence on LET are demonstrated.

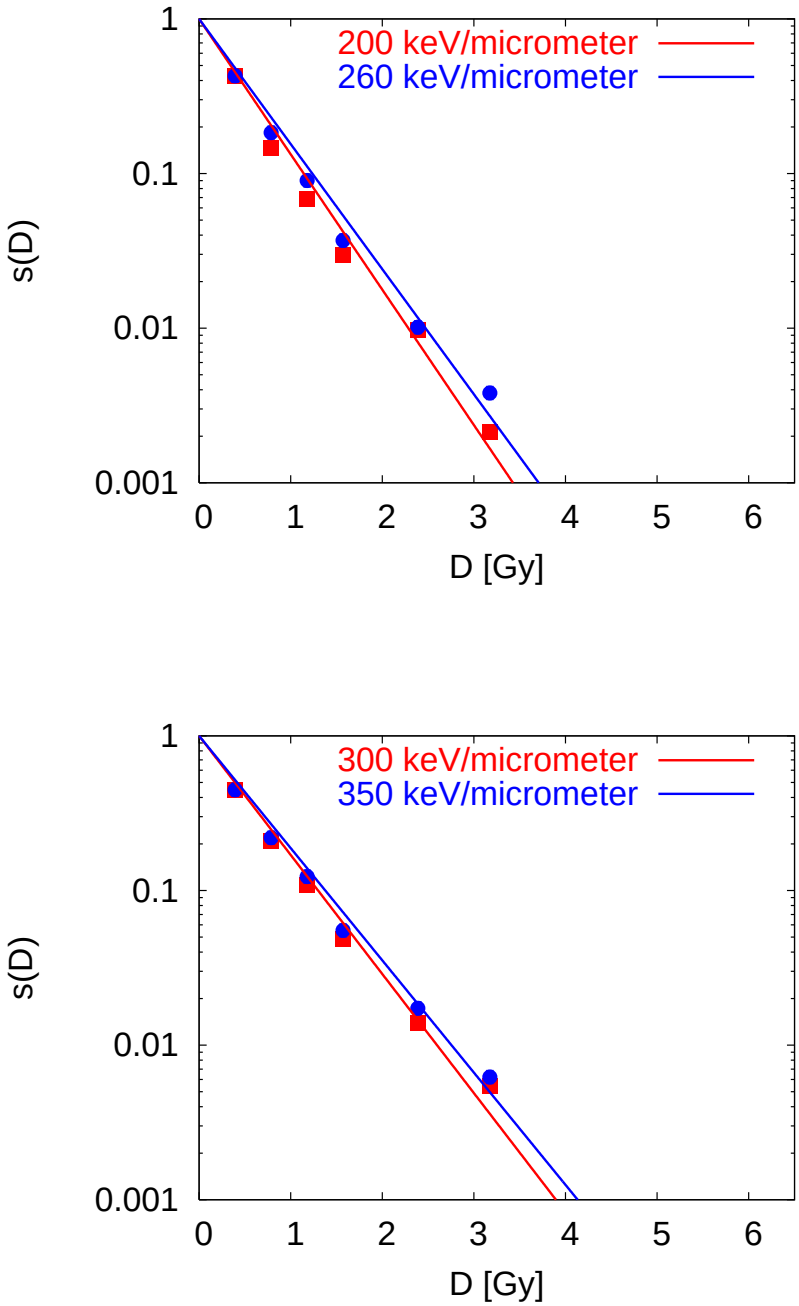

Figure 7.32: Iron - survival curves for NG1RGB cells irradiated by 200, 260, 300 and 350 keV/μm

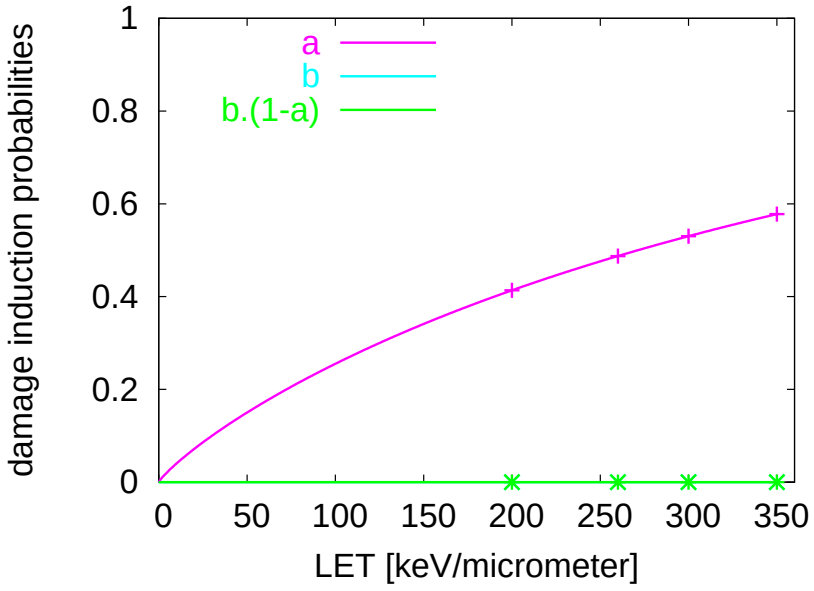

Figure 7.33: Iron - the damage induction probabilities in dependence on LET. The green line coincides with the blue one.

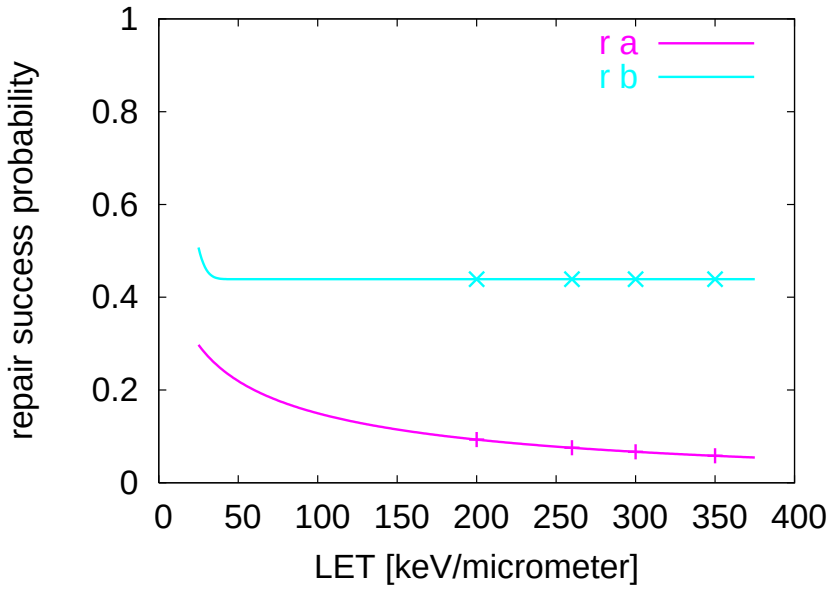

Figure 7.34: Iron - the repair success probabilities in dependence on LET

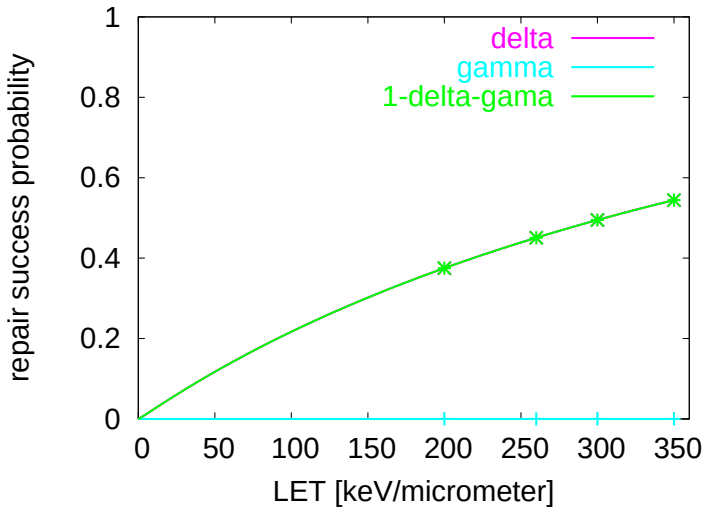

Figure 7.35: Iron - functions $1-\Delta$, $1-\Delta-\gamma$ and γ in dependence on LET. The magenta line coincides with the green one.

7.3.6 Results

As in previous analyses, it has been supposed that geometrical effective cross section of the chromosomal system σ is equal to whole nucleus area. For all calculations of the average number of particles traversing the chromosomal system h_D (Eq. (5.3)), the published value of nucleus area has been used [Tsuruoka *et al* 2005]: $\sigma_{NG1RG} = 172\ \mu m^2$.
The uncertainties of measurements are taken from published experimental data [Tsuruoka *et al* 2005].

Ion type	**The value of χ^2**
Carbon	47
Neon	91
Silicon	41
Iron	164

Table 7.12: The χ^2 obtained for different ions

parameter	**value**	**uncertainty**
a_0	0.83	0.03
a_1	0.72 x 10^{-2}	0.2 x 10^{-3}
a_2	1.79	0.06
b_0	0.13	0.02
b_1	0.08	0.02
b_2	2.3	0.1
r_{a0}	0.56	0.09
r_{a1}	0.07	0.06
r_{a2}	0.73	0.09
r_{b0}	0.9	0.1
r_{b1}	0.2	0.1
r_{b2}	0.1	0.1

Table 7.13: Carbon - the parameters of damage induction probabilities and repair success probabilities; repair regarded as dependent on LET

parameter	**value**	**uncertainty**
a_0	0.2007	0.4 x 10^{-4}
a_1	0.1159 x 10^{-1}	0.1 x 10^{-5}
a_2	3.0429	0.9 x 10^{-3}
b_0	0.1539	0.6 x 10^{-4}
b_1	2.95	0.05
b_2	0.54	0.06
r_{a0}	0.9479	0.2 x 10^{-3}
r_{a1}	1.9312	0.3 x 10^{-3}
r_{a2}	1	3
r_{b0}	0.2711	0.1 x 10^{-3}
r_{b1}	0.079	0.006
r_{b2}	3	2

Table 7.14: Neon - the parameters of damage induction probabilities and repair success probabilities; repair regarded as dependent on LET

parameter	**value**	**uncertainty**
a_0	0.99	0.01
a_1	0.3 x 10^{-2}	0.2 x 10^{-3}
a_2	1.47	0.04
b_0	0.02	0.08
b_1	0.5	0.3
b_2	0.8	0.6
r_{a0}	0.99	0.04
r_{a1}	3	1
r_{a2}	0.19	0.07
r_{b0}	0.3	0.2
r_{b1}	3	1
r_{b2}	0.4	0.9

Table 7.15: Silicon - the parameters of damage induction probabilities and repair success probabilities; repair regarded as dependent on LET

parameter	**value**	**uncertainty**
a_0	1.0	0.1
a_1	0.24 x 10^{-2}	0.3 x 10^{-3}
a_2	0.86	0.4 x 10^{-1}
b_0	0.95	0.9 x 10^{-1}
b_1	0.8 x 10^{-4}	0.3 x 10^{-4}
b_2	2.5	2
r_{a0}	1.0	0.2
r_{a1}	0.7 x 10^{-1}	0.5 x 10^{-1}
r_{a2}	0.3	0.1
r_{b0}	0.6	0.6
r_{b1}	0.5 x 10^{-1}	0.2 x 10^{-1}
r_{b2}	2.5	2

Table 7.16: Iron - the parameters of damage induction probabilities and repair success probabilities; repair regarded as dependent on LET

In Table 7.12 the χ^2 for all four survival curves are given. The presented figures shows that the theoretical fits are in good agreement with experimental data.

In Tables 7.13, 7.14, 7.15 and 7.16 the parameters of damage induction probabilities and repair probabilities for carbon, neon, silicon and iron ions irradiation are displayed.

Damage induction probability

In Figures 7.21, 7.25, 7.29 and 7.33 damage induction probabilities a, b and the modified probability $b^* = b.(1-a)$ in dependence on LET are displayed. In all cases for low LET values the probability of creating a less severe damage (b) dominates over the probability of forming lethal damage by a single track (a). For lower LET radiation the particles do not impart enough energy to the target to cause a severe damage. The probability of creating a severe single particle damage increases with increasing LET. The LET value where these probabilities are equal is for all ions lower than 100 keV/μm. The highest value is for neon ions, approximately 90 keV/μm, and lowest value occurs for iron ions, where it is practically zero.

In survival curves for cells irradiated by silicon and iron, *the overkill effect* occurs apparently. The survival curve for 145 keV/μm silicon is markedly less steep than the curve for 113 keV/μm. For iron ions, the steepest curve is even the curve with the lowest LET - that mean that all LET values lie behind the RBE maximum. The position of the Relative Biological Efficiency (RBE) maxima in dependence on LET for various ions can be found in [Kraft 2001].

Repair success probability

From Figures 7.22, 7.26, 7.30 and 7.34 the similar results follow as in previous sections: First, repair success probabilities $r_a(L)$ and $r_b(L)$ are practically constant (independent on LET), and second, the repair probability of "combined" damage $r_b(L)$ dominates over the repair probability of single-particle damage $r_a(L)$ in all cases. The first finding again validates the idea that only the first stage in radiobiological mechanism depends on physical properties of the irradiation (e.g. LET) and the second phase is given only by biological characteristic of cells. The value of $r_a(L)$ remains between 0.05 and 0.15 for all four data sets. On the other hand, the value of r_b(L) varies to a large extent. This finding follows from the fact, that practically in all cases the corresponding probability of creating b-type (less severe) damage is very small. This is also the reason why big errors occurs in calculation of the parameters r_{a0} – r_{a2} and r_{b0} – r_{b2}.

Chapter 8

Discussion

In previous chapter the basic characteristics of DNA damage induction and also the cellular repair for various cell lines irradiated by different ion species of various energies were derived. The discussion about the particular results is given in corresponding sections in preceding chapter. The general findings are summarized in further text.

For all analyzed data sets we have shown both the damage induction probabilities a, b and the modified probability $b^* = b.(1-a)$ and also the repair success probabilities $r_a(L)$ and $r_b(L)$. The functions $1-\Delta$ (creation of unrepaired a- or b-type damage), γ (formation of unrepaired b-type damage) and $1-\Delta-\gamma$ (creation of unrepaired a-type damage) in dependence on LET are given in corresponding figures, too.

In the analysis "Study of the cellular repair" repair capacities of two cell lines, wild CHO-K1 cell line and their repair deficient CHO mutant, xrs5, have been compared. It has been assumed that the damage induction probabilities for both severe single particle and less severe "combined" damage to chromosomal DNA are equal for wild CHO-K1 and for mutant xrs5 line. The results show how the Probabilistic two-stage model represents the fact that the wild type CHO-K1 cells are capable to repair quite large amounts of lesions not repaired by radiosensitive xrs5 cells (compare Figure 7.6). For the sake of simplicity, repair processes that are common for both cell lines have been comprised directly in the damage induction probability, i.e. only unrepaired lesions for xrs5 cells are taken into account.

The analysis "Comparison of different models" gives a confrontation between the Linear Quadratic model (LQ), Local Effect Model (LEM) and Probabilistic two-stage model (P2S). All models represent the shape of survival curves quite satisfactorily, the best results gives the LQ model and similarly the P2S. The LEM theoretical curves lie more outside the experi-

mental points than the other two fits. The LQ model and to a certain extent also the P2S model are only descriptive models, on the other hand the LEM may be considered as a predictive model. The LEM requires the radial dose distribution, the sensitive volume V and geometrical parameters of the cell nucleus and x-ray survival curve for calculating the number of lethal events and event density. The LQ model needs no cell parameter, the fit is given only by two parameters α and β for each survival curve. For the P2S model it is necessary to know the geometrical effective cross section of the cell nucleus and the LET of irradiation beam; the calculation is made with 6 parameters for damage induction and 2 or 6 parameters for repair (depends on type of repair parametrization) for each set of survival curves with the same kind of ion and cell line. In the P2S model also takes the repair capability of given cell line into account.

The study "Inactivation effect of different types of ions" describes the differences in the radiobiological mechanism for diverse ion species. For the analysis, the normal human fibroblast NG1RGB irradiated by carbon, neon, silicon and iron has been used. On the survival curves of cells irradiated by silicon and iron ions the overkill effect is observable.

Generally, in all performed analyses, similar findings have been observed:

- For lower LET values (generally for LET < 70 keV/μm) the probability of creating less severe damage (b) is greater than the probability of forming lethal damage by a single track (a). For low LET the particles cause less severe damage to DNA and with increasing energy given to a cell nucleus the probability of creating a lethal single particle damage increases. The less severe damage is also more likely repaired by cell enzymatic repair mechanisms.

- The repair probability of less severe "combined" b-type lesions dominates over the severe single particle a-type damage for all analyzed survival curves. This finding validates the fact that the less severe damages are repaired by the cell repair mechanism more likely than the more severe lesions.

- The probability of successful repair is practically independent on LET. That leads to the conclusion that only the first phase of radiobiological mechanism is dependent on physical parameters of the irradiation and the consequent stage is determined only by biological characteristics of cells. The Eq. (5.24) is not very suitable for describing the constant function, and especially parameters $r_{2,3}$ are therefore calculated with big uncertainties.

In testing the Probabilistic two-stage model on the basis of experimental data it is difficult to quantify precisely the damage induction and corresponding repair. That is given by fact that in all analyzed experiments the cell survival was measured using a colony formation assay to measure reproductive cell death. This mean that all repair processes were finished and the outcome of irradiation is determined by both the damage induction and repair mechanisms. For individual cell lines the results demonstrate that cell repair is not dependent on LET and to a certain extent on the particle used in irradiation. The first possibility to solve the problem is analyzing wild cells and their repair deficient mutant. On the supposition that these cell lines did not differ in the induced DNA damage and the difference in response to irradiation is caused only by their different repair capacities, it is possible to obtain damage induction probability without influence of repair processes. This approach was used for the CHO-K1 cells in this work. The second possibility is to use the data sets where repair processes were disabled (for this purpose the irradiation on ice is being used). These data sets are available for x-rays irradiation [Roos *et al* 2000], but not for protons and ions. For further developing the model, the data sets for various cell lines and different ions are needed.

Chapter 9

Conclusion

The Probabilistic two-stage model is a realistic model that describes the radiobiological effects of charged particles and represents the given experimental cell survival curves consistently and systematically. In the model, the "first stage" means physical and chemical phase of the radiobiological mechanism, the impartation of the energy to the chromosomal system and forming the damages. The "second stage" involves the biological phase of radiobiological effect., i.e. in particular the repair processes. The model quantifies two different types of lesions, a severe damage formed by a single particle and less severe damage, where combination of at least two events may be lethal.

The Probabilistic two-stage model has been used for analyzing several published data sets, for Chinese hamster cell lines with different radiosensitivity (data from [Weyrather *et al* 1999]) and for normal human fibroblast cells (data from [Tsuruoka *et al* 2005]). The theoretical curves are in good agreement with experimental data.

For further develop the model and increase its predictive power, two major fields seems to be important: (i) taking into account the microdosimetric approach, especially track-structure models and (ii) involving the biological models of repair.

The analyses presented in this work have indicated the importance of involvement the repair processes in cells into the model. Nevertheless, for the detailed study of cellular repair, special experiments are needed, preferably data sets where the repair processes are disabled during and after irradiation together with their comparison with cells irradiated in normal conditions. The involvement of the ion species (the proton number of the ion) into the calculations seems to be interesting, too. These motives will be studied in the future.

The present development in the field of hadron therapy accents the demand for realistic description of radiobiological mechanisms in cells after irradiation by charged particles. A significant way how to understand better the fundamental radiobiological mechanisms is to involve the physical processes on the level of interactions of atoms and charged particles as well as the chemical reaction between DNA and irradiation induced radicals and finally the biological mechanisms like enzymatic repair. The mathematical models in radiobiology should be able to represent both the qualitative and quantitative characteristics of experimentally observed behavior of the irradiated cells.

The present results accent the needfulness for further research of detailed radiobiological models, which should reflect the various effects of damage induction and repair processes in cells and tissues.

Part III

Appendices

Appendix A

Hadron therapy centers in the world

At present, there are many proton therapy centers in the world and several facilities which offer treatment by ions (usually carbon). Worldwide more than 50,000 cancer patients have been treated by proton therapy up to now and several thousands of patients by carbon therapy. This chapter provides a brief summary of these centers, forthcoming as well as already working. Very detailed information about particle therapy centers can be found e.g. in [http://ptcog.web.psi.ch].

Europe

Proton Therapy Center, Paul Scherrer Institute (PSI)
Villigen, Switzerland

The PSI was opened in 1984 and it has specialized for treatment of the eye tumors with the OPTIS facility. In collaboration with Hôpital Opthalmique of the University of Lausanne approximately 4800 patients have been treated by proton beam. In more than 98 % of cases tumor was cured or its growth was stopped. In more than 90 % of cases the eye could be saved. By the end of 2007 the unique PSI compact gantry was used to treat 320 patients with brain, skull-base or spinal cord tumors and abdominal sarcomas.

At an early date, the new Gantry 2 with new scanning features will be ready for patient treatment. Gantry 2 will provide new scanning features such as organ motion scanning during irradiation. The Gantry 2 is designed

specifically for the implementation of new advanced parallel beam scanning techniques. The new system shall be capable of providing multiple target repainting, without increasing beam size or treatment time.

Source: http://p-therapie.web.psi.ch/e/index.html

Centre de Protonthrapie Orsay, France

First experiments with the proton beam in cancer treatment were done in 1987. Four years later, in January 1991, the Orsay Proton Therapy Center (CPO) was established. The center encompasses a hospital unit with exclusive use of the synchrocyclotron for eye and intracranial tumors. Currently, a large-scale renovation is processing and is scheduled to end in 2010. The goal is to double the number of patients the Proton Therapy Center can treat nowadays.

Source: http://www.protontherapie-orsay.fr

Centre of Oncology Clatterbridge, UK

The Douglas Cyclotron Unit started in 1989 and it is the only proton therapy facility of its kind in the United Kingdom. This center is specifically concerned with treating cancers within the eye. The most common lesions treated are choroidal melanomas. In recent years, however, this has been extended to include choroidal haemangiomas, iris melanomas and conjunctival melanomas.

Source: http://www.ccotrust.nhs.uk/patient/treatment/cyclotron.asp

Biophysics and Therapy Centre, GSI Darmstadt, Germany

The GSI center in Germany is the only carbon therapy facility in Europe. It has been started in 1997 and up to now it has been used to treat almost 400 patients with tumors in the head or neck region. Subsequent monitoring of patients at GSI over a five-year period revealed that the growth of the tumors was stopped in 75 - 90 % of the patients, depending on the type of tumor. New clinical studies are focused to the treatment of the vertebral

column tumors and prostate cancer. The new approach to the treating moving organs is also under development at GSI. GSI plans the new accelerator Facility for Antiproton and Ion Research (FAIR) for the research with ion and antiproton beams.

Source: http://www-aix.gsi.de/%7Ebio/home.html

Heidelberg Ion Therapy Center (HIT) Heidelberg, Germany

An ion-beam radiotherapy center is under construction at the Heidelberg University Medical Center in collaboration with GSI Darmstadt. The clinical operation will start in 2008, and it is supposed that more than 1,000 patients will be treated here per year.

HIT uses a synchrotron to accelerate protons, carbon ions or even other ion. Patients will be treated in two fixed beam treatment rooms and one gantry room.

Source: http://www.klinikum.uni-heidelberg.de (in german)
Source: http://www.medical.siemens.com/

CATANA, INFN Catania, Italy

In present time, CATANA (Centro di AdroTerapia e Applicazioni Nucleari Avanzate) is the actually unique proton therapy facility in Italy. There is a 62 MeV proton beam, produced by a Superconducting Cyclotron (SC). The main interest of CATANA center is the study and the application of protons for the treatment of shallow tumors such as uveal melanomas and subfoveal macular degenerations. Moreover, other less frequent lesions like choroidal haemangioma, conjunctiva melanoma, eyelid tumors and embryonal sarcoma are treated.

Source: http://web2.lns.infn.it/CATANA/CATANA/default.htm

Rinecker Proton Therapy Center (RPTC) Munich, Germany

The Rinecker Proton Therapy Center (RPTC) has been designed to provide radiotherapy for tumours in all parts of the body for approx. 4,000 patients

a year. There are four gantries equipped with patient couches, with adequate options for movement to allow all the tumors that occur in the body and the fixed beam for precision irradiation of the eye, brain and facial tumors.

Source: http://www.rptc.de/english/index.htm

Centro Nazionale di Adroterapia Oncologica (CNAO)
Pavia, Italy

The centre is currently being built in Pavia and its start up is scheduled for the end of 2008. In this center synchrotron 400 MeV/u with three horizontal and one vertical beam will be built up.

Source: http://www.cnao.it/

Asia

HIMAC
Chiba, Japan

The National Institute of Radiological Sciences (NIRS) started cancer therapy in 1961 using x-rays and gamma rays. Fast neutron beam therapy using a cyclotron and proton therapy were introduced in 1975 and 1979, respectively. Charged particle therapy was started in 1994 and by March 2006 it had been used to treat more than 2,800 patients.

There are three treatment room, with one horizontal, one vertical and one with both horizontal and vertical beam. The NIRS, in collaboration with external research institutes and universities, is currently developing new technologies including laser acceleration and conducting research and development on therapeutic systems small enough to install in existing hospitals.

Source: http://www.nirs.go.jp/ENG/research/charged_particle/index.shtml

Proton Medical Research Center
Tsukuba, Japan

The University of Tsukuba started proton clinical studies in 1983 using a synchrotron constructed for physics studies at the High Energy Accelerator

Research Organization (KEK). A more than 700 patients were treated at this facility from 1983 to 2000.

In 2000, Proton Medical Research Center (PMRC) was built near to the University Hospital. PMRC is equipped with a synchrotron and two rotating gantries. Clinical treatment in PMRC was started in September 2001. Up to 2008, approximately 1500 of patients were treated in this new facility. PMRC focuses mainly on liver cancer, lung cancer, prostate cancer, esophageal cancer and brain or skull base tumors.

Source: http://www.pmrc.tsukuba.ac.jp/engRadiotherapy.html

America

Loma Linda University Proton Therapy Center
USA

The Loma Linda proton therapy facility, opened in 1990, was the first hospital-based proton treatment facility worldwide (until 2003, it was the only one in USA). Loma Linda University Medical Center attends to treatment of wide variety of tumors, such as tumors of brain and base of skull, chordomas and chordosarcomas, pelvis cancers and as well as pediatric cancers.

Source: http://www.protons.com/index.html

The Northeast Proton Therapy Center at The Massachusetts General Hospital
Massachusetts, USA

The Northeast Proton Therapy Center (NPTC) is located on the main hospital campus of the Massachusetts General Hospital. The proton beam is divided to three treatment rooms; two of them are equipped by gantries.

*Source:*http://neurosurgery.mgh.harvard.edu/ProtonBeam/NPTCbrochure.pdf

Appendix B

List of abbreviations

BED – Biologically Effective Dose

BER – Base-Excision Repair

BNCT – Boron Neutron Capture Therapy

CSDA – Continuous Slowing Down Approximation

CT – Computed Tomography

D – dose

DSB – Double Strand Break

EDT – Extrapolated Tolerance Dose

ICRU – International Commission on Radiological Units

IGRT – Image-guided radiation therapy

IMRT – Intensity-modulated radiation therapy

IMPT – Intensity-modulated proton therapy

LEM – Local Effect Model

LET – Linear Energy Transfer

LPL – Lethal and Potentially Lethal model

LQ – Linear-Quadratic (model)

NER – Nucleotide Excision Repair

NHEJ – Non Homologous End Joining

MMR – Mismatch Repair

MRI – Magnetic Resonance Imaging

OER – Oxygen Enhancement Ratio

PET – Positron Emission Tomography

P2S – Probabilistic two-stage model

RBE – Relative Biological Efficiency

SCGE – Single Cell Gel Electrophoresis

SOBP – Spread Out Bragg Peak

SSA – Single Strand Annealing

SSB – Single Strand Break

TLK – Two-Lesion Kinetic model

List of Figures

List of Tables

Bibliography

[Adams 1973] Adams GE: Chemical radiosensitization of hypoxic cells. Br. Med. Bull 29, 48–53 (1973)

[Adams 1977] Adams GE: Hypoxic cell sensitizers for radiotherapy. Cancer 6, 181–223 (1977)

[Ahnström *et al* 1981] Ahnström G, Erixon K: Measurement of strand breaks by alkaline denaturation and hydroxylapatite chromatography. EC Friedberg and PC Hanawalt (ed)., DNA Repair. Dekker: New York, 403–418 (1981)

[Alberts *et al* 2002] Alberts B, Johnson A, Lewis J, Raff M, Roberts K, Walter P: Molecular Biology of the Cell. Garland Science, New York, 4th ed. (2002)

[Alpen 1998] Alpen EL: Radiation biophysics. Academic Press, San Diego, second edition (1998)

[Alper *et al* 1956] Alper T, Howard-Flanders P: Role of oxygen in modifying the radiosensitivity of E.colli. Nature 178, 978–979 (1956)

[Ambrose et Hounsfield *et al* 1973] Ambrose J, Hounsfield G: Computerized transverse axial tomography. Br J Radiol. 46 (542), 148–149 (1973)

[Arena 1971] Arena V: Ionizing Radiation and Life. C.V. Mosby, St. Louis, USA (1971)

[Attix 1986] Attix FH: Introduction to Radiological Physics and Radiation Dosimetry. John Wiley and Sons, Germany (1986)

[Barendsen *et al* 1966] Barendsen GW, Koot CJ, Van Kersen GR, Bewley DK, Field SB, Parnell CJ: The effect of oxygen on impairment of the proliferative capacity of human cells in culture by ionizing radiations of different LET. Int. Journal of Radiation Biology Relat Stud Phys Chem Med 10: 317–327 (1966)

[Barendsen 1982] Barendsen GW: Dose fractionation, dose rate, and isoeffect relationships for normal tissue responses. International Journal of Radiation Oncology, Biology and Physics 8, 1981–1997 (1982)

[Barendsen 1990] Barendsen GW: LET dependence of linear and quadratic terms in dose-response relationships for cellular damage: correlations with the dimensions and structures of biological targets, Radiation Protection Dosimentry, 31, 235–239. (1990)

[Baumstark-Khan *et al* 2000] Baumstark-Khan C, Hentschel U, Nikandrova Y, Krug J, Horneck G: Fluorometric Analysis of DNA Unwinding (FADU) as a Method for Detecting Repair-induced DNA Strand Breaks in UV-irradiated Mammalian Cells. Photochemistry and Photobiology 72 (4), 477-484, (2000)

[Bethe 1930] Bethe H: Zur Theorie des Durchgangs schneller Korpuskularstrahlung durch Materie, Ann. Phys. 5,325-400 (1930)

[Beuve *et al* 2007] Beuve M, Colliaux A, Testa E: Theoretical limits of LEM, Proceedings of Ion Beams in Biology and Medicine (39. Annual Conference of the German-Swiss Association for Radiation Protection and 11th Workshop of Heavy Charged Particles in Biology and Medicine), 204–208. (2007)

[Birnboim 1990] Birnboim HC: Fluorometric analysis of DNA unwinding to study strand breaks and repair in mammalian cells, Methods Enzymol.,186, 550–555 (1990)

[Birren *et al* 1993] Birren B, Lai E: Pulsed field electrophoresis: A practical guide. Academic Press, San Diego, USA (1993)

[Bloch 1933] Bloch F: Bremsvermogen von Atomen mit mehreren Elektronen, 2.Phys., 8-L, 363–376 (1933)

[Bradley and Kohn 1979] Bradley M, Kohn KW: X-ray-induced DNA double-strand break production and repair in mammalian cells as measured by neutral filter elution. Nucleic Acids Res. 7: 793-804 (1979)

[Caldecott 2004] Caldecott KW: Eukaryotic DNA Damage Surveillance and Repair, Landes Bioscience and Kluwer Academic, New York, USA (2004)

[Carle *et al* 1986] Carle GF, Frank M, Olson MV: Electrophoretic separation of large DNA molecules by periodic inversion of the electric field. Science 232, pp. 65–68 (1986)

[Carlsson 1978] Carlsson GA: Basic Concepts in Dosimetry. A Critical Analysis of the Concepts of Ionizing Radiation and Energy Imparted, Radiation Research 75: 3, 462–470 (1978)

[Chadwick *et al* 1973] Chadwick KH, Leenhout HP: A molecular theory of cell survival. Physics in Medicine and Biology 18, 78–87 (1973)

[Chatterjee and Holley 1993] Chatterjee A, Holley WR: Computer simulation of initial events in the biochemical mechanisms of DNA damage. Adv. Radiation Biol. 17, 181–226 (1993)

[Chirikjian 1997] Chirikjian JG, Collier BG: Detecting sequences or point mutation(s) in polynucleotide targets - using a nucleic acid repair enzyme, also for use in vitro mutagenesis, pattented by TREVIGEN, INC, Patent Numbers: WO9640902-A; EP832210-A; WO9640902-A1; AU9662527-A; US5656430-A; EP832210-A1; JP11506932-W; EP832210-B1; DE69633723-E; DE69633723-T2 (1997)

[Chu 1990] Chu G: Pulsed-field electrophoresis: theory and practice. In Methods: A Companion to Methods of Enzymology. Pulsed-Field Electrophoresis (B. Birren and E. Lai, eds.) Vol. 1, No. 2, 129-142, Academic Press, San Diego, USA (1990)

[Cooper 2000] Cooper GM: The Cell: A Molecular Approach, Sinauer Associates, Inc.,Boston, USA (2000)

[Cornforth *et al* 1987] Cornforth MN, Bedford JS: A quantitative comparison of potentially lethal damage repair and the rejoining of interphase chromosome breaks in low passage normal human fibroblasts. Radiat Res 111: 385–405,(1987)

[Cox *et al* 1973] Cox R, Damjanov I, Abanobi SE, Sarma DSR: A Method for Measuring DNA Damage and Repair in the Liver in Vivo, Cancer Research 33, 2114–2121, (1973)

[Cucinotta *et al* 2008] Cucinotta FA, Pluth JM, Anderson JA, Harper JV, O'Neill P: Biochemical kinetics model of DSB repair and induction of gamma-H2AX foci by non-homologous end joining. Radiat Res. 169(2): 214–22 (2008)

[Curtis, 1986] Curtis SB: Lethal and Potentially Lethal Lesions induced by radiation - A Unified Repair Model, Radiation Research, 106, 252–270. (1986)

[Dale 1985] Dale, RG: The application of the linear-quadratic dose effect equation to fractionated and protracted radiotherapy. British Journal of Radiology 58, 515–528. (1985)

[Darzynkiewicz *et al* 2006] Darzynkiewicz Z, Huang X, Okafuji M: Detection of DNA strand breaks by flow and laser scanning cytometry in studies of apoptosis and cell proliferation (DNA replication). Methods Mol. Biol. 314: 81–93 (2006)

[Didenko *et al* 2004] Didenko VV, Minchew CL, Shuman S, Baskin DS: Semi-artificial Fluorescent Molecular Machine for DNA Damage Detection. Nano Lett., 4 (12), 2461–2466, (2004)

[Dikomey *et al* 1986] Dikomey E, Franzke J: Three classes of DNA strand breaks induced by X-irradiation and internal beta rays. Int. Journal of Radiation Biology, 50, 893–908 (1986)

[Dikomey *et al* 1998] Dikomey E, Dahm-Daphi J, Brammer I, Martensen R, Kaina B: Correlation between cellular radiosensitivity and nonrepaired double strand breaks studied in nine mammalian cell lines. Int. J. Radiat Biol 73 269-278 (1998)

[Etter 1990] Etter DM: Structured FORTRAN 77 for Engineers and Scientists, 3rd ed., The Benjamin/Cummings Publishing Company (1990)

[Ewing 1998] Ewing D: The oxygen fixation hypothesis - A reevaluation. American Journal of Clinical Oncology - Cancer Clinical Trials 21 (4), 355–361 (1998)

[Featherstone and Jackson 1999a] Featherstone C, Jackson SP: Ku, a DNA repair protein with multiple cellular functions? Mutation Research - DNA repair 434: 1, 3–15 (1999)

[Featherstone and Jackson 1999b] Featherstone C, Jackson SP: DNA double-strand break repair, Current Biology, 9: 20, R759–R761 (1999)

[Feng *et al* 1996] Feng L, Romanienko PJ, Weaver DT, Jeggo PA, Jasin M: Chromosomal double-strand break repair in Ku80-deficient cells. Proc. Natl. Acad. Sci. USA, 93, 8929–8933, (1996)

[Galvin *et al* 2004] Galvin JM, Ezzell G, Eisbrauch A, Yu C: Implementing IMRT in clinical practice: A joint document of the American Society for Therapeutic Radiology and Oncology and the American Association of Physicists in Medicine, International Journal of Radiation Oncology Biology Physics 58 (5), 1616–1634 (2004)

[Gervais *et al* 2006] Gervais B, Beuve M, Olivera GH, Galassi ME: Numerical simulation of multiple ionization and high LET effects in liquid water radiolysis, Radiation Physics and Chemistry, 75: 4, 493–513 (2006)

[Goodhead *et al* 1979] Goodhead DT, Thacker J, Cox R: Effectiveness of 0.3 keV carbon ultrasoft X-rays for the inactivation and mutation of cultured mammalian cells. International Journal of Radiation Biology 36, (2) 101–115 (1979)

[Gray *et al* 1953] Gray LH, Conger AD, Ebert M, Hornsey S, Scott OCA: The Concentration of Oxygen Dissolved in Tissues at the Time of Irradiation as a Factor in Radiotherapy. British Journal of Radiology 26 (312): 638-648 (1953)

[Hall 2003] Hall EJ: The Bystander Effect, Health Physics 85:31-35 (2003)

[Hall *et al* 2006] Hall EJ, Giaccia AJ: Radiobiology for the Radiobiologist, Lippincott Williams and Wilkins, USA (2006)

[Hianik *et al* 2006] Hianik T, Wang X, Andreev S, Dolinnaya N, Oretskaya T, Thompson M: DNA-duplexes containing abasic sites: correlation between thermostability and acoustic wave properties. Analyst, 131, 1161–1166 (2006)

[Holley and Chatterjee 1996] Holley WR, Chatterjee A: Clusters of DNA induced by ionizing radiation: formation of short DNA fragments. I. Theoretical modeling. Radiat Res. 145(2): 188–199 (1996)

[Hollmark *et al* 2007] Hollmark M, Beuve M, Edgren MR, Elsässer T, Kundrát P, Meijer AE, Rodriguez-Lafrasse C, Scholz M, Waligórski MPR, Gudowska I: A comparison of radiobiological models for light ion therapy. // The 11th Workshop of Ion Beams in Biology and Medicine, 25-29 September 2007, Heidelberg, Germany, ISSN 1013–4506, 47, (2007)

[Hromčíková 2003] Hromčíková H: Počítačová simulace postupnych fází radiobiologického mechanismu v buňkách a tkáních, diploma thesis, Faculty of Mathematics and Physics, Praha (2003)

[Hromčíková *et al* 2007] Hromčíková H, Kundrát P, Lokajíček M: Detailed analysis of the response of different cell lines to carbon irradiation. Radiat. Prot. Dosim., 122, 1–4, 121–123, doi:10.1093/rpd/ncl477 (2007)

[Hounsfield *et al* 1973] Hounsfield GN: Computerized transverse axial scanning (tomography). 1. Description of system. Br J Radiol. 1973 46 (552), 1016–1022 (1973)

[ICRP 1992] ICRP Publication: Relative Biological Effectiveness (RBE), Quality Factor (Q), and Radiation Weighting Factor (w_R), International Commission on Radiological Protection (1992)

[ICRU 1980] ICRU: Radiation Quantities and Units. Report 33. Washington, DC, International Commission on Radiation Units and Measurements, (1980)

[ICRU 1993] ICRU: Stopping Powers and Ranges for Protons and Alpha Particles. Report 49. Washington, DC, International Commission on Radiation Units and Measurements, (1993)

[Ikpeme *et al* 1995] Ikpeme S, Löbrich M, Akpa T, Schneider E, Kiefer J: Heavy ion-induced DNA double-strand breaks with yeast as a model system, Radiat Environ Biophys. 34(2): 95–99 (1995)

[Iliakis and Kurtzman 1991] Iliakis G, Kurtzman S: Mechanism of radiosensitization by halogenated pyrimidines: bromodeoxyuridine and beta-arabinofuranosyladenine affect similar subsets of radiation-induced potentially lethal lesions in plateau-phase Chinese hamster ovary cells, Radiat Res. 127: 1, 45-51 (1991)

[Iliakis *et al* 2004] Iliakis G, Wang H, Perrault AR, Boecker W, Rosidi B, Windhofer F, Wu W, Guan J, Terzoudi G, Pantelias G: Mechanisms of DNA double strand break repair and chromosome aberration formation. Cytogenet Genome Res. 104(1-4): 14–20 (2004)

[Iyer *et al* 2006] Iyer R, Pluciennik A, Burdett V, Modrich P: DNA mismatch repair: functions and mechanisms, Chem Rev 106: (2), 302-323 (2006)

[Judas *et al* 2001] Judas L, Lokajíček M: Cell inactivation by ionizing particles and the shapes of survival curves. Journal of Theoretical Biology 210 (1), 15–21 (2001)

[Kanai *et al* 1999] Kanai T, Endo M, Minohara S, Nirahara N, Koyama-Ito H, Tomura H, Matsufuji N, Futami Y, Fukumura A, Kawachi K: Biophysical characteristics of HIMAC clinical irradiation system for heavy-ion therapy. Int. J. Radiat. Oncol. Biol. Phys. 44, 201-210 (1999)

[Kerr *et al* 1972] Kerr JF, Wyllie AH, Currie, AR: Apoptosis: a basic biological phenomenon with wide-ranging implications in tissue kinetics. Br J Cancer 26(4): 239-57 (1972)

[Klaude *et al* 1996] Klaude M, Eriksson S, Nygren J, Ahnstrm G: The comet assay: mechanisms and technical considerations. Mut. Res. 363: 89–96 (1996)

[Kohn *et al* 1973] Kohn KW, Grimeg-Ewig RA: Alkaline elution analysis, a new approach to the study of DNA single-strand interruptions in cells. Cancer Res. 33: 1849-1853, 1973

[Kraft *et al* 1999] Kraft G, Scholz M, Bechthold U: Tumor therapy and track structure. Radiation and Environmental Biophysics 38 (4), 229–237 (1999)

[Kraft 2001] Kraft G: Tumor therapy with heavy charged particles, Progress in Particle and Nuclear Physics, 46 (2): (2001)

[Kraft 2007] Kraft G: Heavy Ion Tumor Therapy - From the Scientific Principles to the Clinical Routine, Nuclear Physics News, 17 (1), 24–29 (2007)

[Kronenberg *et al* 1995] Kronenberg A, Gauny S, Criddle K, Vannais D, Ueno A, Kraemer S, Waldren CA: Heavy ion mutagenesis: linear energy transfer effects and genetic linkage. Radiat Environ Biophys. 34(2): 73–78 (1995)

[Kundrát 2004] Kundrát P: Mechanism of biological effects of accelerated protons and light ions and its modelling. Doctoral thesis, Charles University in Prague, Faculty of Mathematics and Physics (2004)

[Kundrát *et al* 2005] Kundrát P, Lokajíček M, Hromčíková H: Probabilistic two-stage model of cell inactivation by ionizing particles; Physics in Medicine and Biology, 50, 1433–1447 (2005)

[Kundrát 2006] Kundrát P: Detailed analysis of the cell-inactivation mechanism by accelerated protons and light ions. Physics in Medicine and Biology, 51, 1185–1199 (2006)

[Kundrát 2007] Kundrát P: personal discussions, unpublished (2007)

[Kundrát 2008] Kundrát P: Detailed probabilistic modelling of cell inactivation by ionizing radiations of different qualities: The model and its applications, Appl Radiat Isot., in print, PMID: 18684633, doi:10.1016/j.apradiso.2008.06.014 (2008)

[Löbrich *et al* 1995] Löbrich M, Rydberg B, Cooper PK: Repair of x-ray-induced DNA double-strand breaks in specific Not I restriction fragments in human fibroblasts: joining of correct and incorrect ends, Proc Natl Acad Sci U S A. 92(26): 12050–12054 (1995)

[Lodish *et al* 2004] Lodish H, Berk A, Matsudaira P, Kaiser CA, Krieger M, Scott MP, Zipursky SL, Darnell J: Molecular Biology of the Cell, WH Freeman: New York, NY. 5th ed. (2004)

[Lokajíček 1981] Lokajíček M: Mathematical and physical models of the biological effect of ionizing particles on cells and tissues. Internal report of Institute of Physics, AVCR, Prague, report FZU-81-5 (in czech) (1981)

[Lokajíček 1986] Lokajíček M: Biophysical mechanism of cell inactivation by ionizing particles. Internal report of International Centre for Theoretical Physics, IC/86/399 (1986)

[Lokajíček *et al* 2000] Lokajíček M, Barilla J: The role of Oxygen in DNA Damage by Ionizing Particles. Journal of Theoretical Biology, 2007, 405–141 (2000)

[Majno *et al* 1995] Majno G, Joris I: Apoptosis, oncosis, and necrosis. An overview of cell death. American Journal of Pathology, Vol 146, 3–15, (1995)

[Mazeron 2005] Mazeron JJ: Brachytherapy: a new era, Radiotherapy and Oncology 74 (3), 223–225 (2005)

[McCracken 1961] McCracken DD: A Guide to Fortran Programming, Wiley (1961)

[Michael *et al* 1973] Michael BD, Adames GE, Hewitt HB: A post-effect of oxygen in irradiated bateria: a submillisecond fast mixing study. Radiation Research 54: 239–251 (1973)

[Milner *et al* 1987] Milner AE, Vaughan ATM, Clark IP: Measure of DNA Damage in Mammalian Cells Using Flow Cytometry. Radiat. Research 110, 108-117, (1987)

[Montour *et al* 1974] Montour JL, Wilson JD, Rogers CC, Theus RB, Attix FH:, Biological Characterization Of a High-Energy Neutron Beam For Radiation-Therapy, Cancer, 34 (1), 54–64 (1974)

[Morris 1991] Morris JH: Boron Neutron Capture Therapy , Chemistry in Britain, 27 (4), 331–334 (1971)

[Mothersill *et al* 1997] Mothersill C, Seymour CB: Medium from irradiated human epithelial cells but not human fibroblasts reduces the clonogenic survival of unirradiated cells: Possible evidence of a bystander effect. Int J Radiat Biol 71:421427; (1997)

[Mothersill *et al* 2001] Mothersill C, Seymour CB: Review: radiation-induced bystander effects: past history and future perspectives. Radiat Res 155: 759-767. (2001)

[Nagasawa and Little 1981] Nagasawa H, Little JB: Induction of chromosome aberrations and sister chromatid exchanges by X rays in density-inhibited cultures of mouse 10T1/2 cells. Radiat Res. 87(3): 538–551 (1981)

[Nelder and Mead 1965] Nelder JA, Mead R: A simplex method for function minimization. Comput. J. 7, 308 (1965)

[Olinski *et al* 1992] Olinski R, Nackerdien Z, Dizdaroglu M: DNA-protein cross-linking between thymine and tyrosine in chromatin of gamma-irradiated or H2O2-treated cultured human cells. Arch Biochem Biophys. 297(1): 139–143 (1992)

[Petry 1923] Petry E: Zur Kenntnis der Bedingungen der biologischen Wirkung der Rontgenstrahlen. Biochem Zeitschrift, 135, 353 (1923)

[Phillips 1977] Phillips TL: Chemical modification of radiation effects, Cancer 39: 2 (Suppl) 987–998 (1977)

[van der Plaats 1969] van der Plaats: Medical x-ray technique, Centrex Publishing Company, Eindhoven, third revised and enlarged edition, The Netherlands (1969)

[Platzman 1953] Platzman R: Conference on basic mechanisms in radiation biology, National Research Council Publication 305. National Academy of Sciences, Washington DC, (1953)

[Politi *et al* 2005] Politi A, Mon MJ, Houtsmuller AB, Hoogstraten D, Vermeulen W, Heinrich R, van Driel R: Mathematical modeling of nucleotide excision repair reveals efficiency of sequential assembly strategies. Mol Cell. 19(5): 679–90 (2005)

[Puck *et al* 1958] Puck TT, Cieciura SJ, Robinson A: Genetics of somatic mammalian cells. III. Long-term cultivation of euploid cells from human and animal subjects. J Exp Med 108 (6): 945–956 (1958)

[Raju *et al* 1987] Raju MR, Carpenter SG, Chemielewski JJ, Schillaci ME, Wilder ME, Freyer JP, Johnson NF, Schor PL, Sebring RJ, Goodhead DT: Radiology of ultrasoft x-rays: I. Cultured hamster cells (V79). Radiation Research 110, 396–412 (1987)

[Randers-Pehrson *et al* 2001] Randers-Pehrson G, Geard CR, Johnson CD, Elliston CD, Brenner DJ: The Columbia University single-ion microbeam. Radiat Res 156: 210-214; (2001)

[Resnick and Martin 1976] Resnick MA, Martin P: The repair of double-strand breaks in the nuclear DNA of Saccaromyces cerevisiae and its genetic control. Mol. Gen. Genet. 143, 119–129 (1976)

[Resnick 1976] Resnick MA: The repair of double-strand breaks in DNA, a model involving recombination. J. Theor. Biol. 59, 97–106 (1976)

[Roos *et al* 2000] Roos WP, Binder A, Böhm L: Determination of the initial DNA damage and residual DNA damage remaining after 12 hours of repair in eleven cell lines at low doses of irradiation, Int. J. Radiat. Biol. 76: 11, 1493–1500 (2000)

[Rosenbrock 1960] Rosenbrock HH: An automatic method for finding the greatest or least value of a function, Comput. J. 3, 175 (1960)

[Rudinger *et al* 2002] Rudinger G, Blazek ER: Fluid Mechanics of DNA Double-Strand Filter Elution, Biophysical Journal, 82, 19-28 (2002)

[Rydberg 1975] Rydberg B: The rate of strand separation in alkali of DNA of irradiated mammalian cells. Radiat. Research, 61, 274–287 (1975)

[Sachs *et al* 1997] Sachs RK, Hahnfeld P, Brenner DJ: Review The link between low-LET dose-response relations and the underlying kinetics of damage production/repair/misrepair. Int. J. Radiat. Biol, 72, 4, 351–374 (1997)

[Saraste *et al* 2000] Saraste A, Pulkki K: Morphologic and biochemical hallmarks of apoptosis. Cardiovasc Res 45(3): 528–537 (2000)

[Setlow 1966] Setlow JK: Photoreactivation, Radiation Research Supplement, Vol. 6, Structural Defects in DNA and Their Repair in Microorganisms, Proceedings of a Conference on Radiation Microbiology, University of Chicago, Chicago, Illinois, October 18-20, 1965, 141–155 (1966). Available online at http://www.jstor.org/stable/3583554?seq=1 (cited 28. 8. 2008)

[Semenenko and Stewart 2005] Semenenko VA, Stewart RD: Monte carlo simulation of base and nucleotide excision repair of clustered DNA damage sites. II. Comparisons of model predictions to measured data. Radiat Res. 164(2): 194–201 (2005)

[Semenenko *et al* 2005] Semenenko VA, Stewart RD, Ackerman EJ: Monte Carlo simulation of base and nucleotide excision repair of clustered DNA damage sites. I. Model properties and predicted trends. Radiat Res. 164(2): 180–93 (2005)

[Scholz and Kraft 1996] Scholz M, Kraft G: Track structure and the calculation of biological effects of heavy charged particles. Adv. Space Research, 18, 1/2, 5–14 (1996)

[Scholz *et al* 1997] Scholz M, Kellerer AM, Kraft-Weyrather W, Kraft G: Computation of cell survival in heavy ion beams for therapy - The model and its approximation, Radiation Enviromental Biophysics, 36, 59–66 (1997)

[Scholz and Elsässer 2007] Scholz M, Elsässer T: Biophysical models in ion beam radiotherapy. Advances in Space Research 40, 1381-1391 (2007)

[Steel 1993] Steel GG: Basic Clinical Radiobiology, Edward Arnold Publishers, London 1993

[Stewart *et al* 2002] Stewart RD, Ackerman EJ, Shultis JK, Lei XC: Modeling Bystander Effects Using a Microdosimetric Approach, DOE Low Dose Program Workshop III, Rockville, Maryland, March 24–27, (2002) Available online at http://www.pnl.gov/berc/LowDose/Epub/DOE25Mar2002_bystander.html (cited 20. 9. 2008)

[Stewart 2001] Stewart RD: Two-Lesion Kinetic Model of double-strand break rejoining and cell killing, Radiation research 156, 365–378 (2001)

[Takata *et al* 1999] Takata M, Sasaki MS, Sonoda E, Morrison C, Hashimoto M, Utsumi H, Yamaguchi-Iwai Y, Shinohara A, Takeda S: Homologous recombination and non-homologous end-joining pathways of DNA double-strand break repair have overlapping roles in the maintenance of chromosomal integrity in vertebrate cells, EMBO Journal 17: 18, 5497–5508 (1999)

[Taucher–Scholz 1995] Taucher-Scholz G, Heilmann J, Schneider M, Kraft G: Detection of heavy-ion-induced DNA double-strand breaks using static-field gel electrophoresis. Radiat Environ Biophys. 34(2): 101–106 (1995)

[Thames 1985] Thames HD: An 'incomplete-repair' model for survival after fractionated and continuous irradiations. International Journal of Radiation Biology, 47, 319-339. (1985)

[Thames and Hendry 1987] Thames HD, Hendry JH: Fractionation in Radiotherapy. Taylor & Francis, London (1987)

[Tice *et al* 1991] Tice RR, Andrews PW, Hirai O, Singh NP: The single cell gel (SCG) assay: an electrophoretic technique for the detection of DNA damage in individual cells, Adv Exp Med Biol 283: 157–64 (1991)

[Tice *et al* 1995] Tice RR, Strauss GHS: The Single-Cell Gel-Electrophoresis Comet Assay - A Potential Tool for Detecting Radiation-Induced DNA Damage in Humans, Stem Cells 13: 207–214 Suppl. 1 (1995)

[Tobias *et al* 1979] Tobias CA, Alpen EA, Blakely EA, Castro JR, Chatterjee A, CHen GTY, Curtis SB, Howard J, Lyman JT, Ngo FQH: Radiobiological Basis for Heavy–ion Therapy, in: Treatment of Radioresistant Cancers, eds.: Abe M, Sakamoto K, Phillips TJ, Elsevier 159 (1979)

[Tobias *et al* 1980] Tobias CA, Blakely EA, Ngo FQH, Yang TCH: The Repair-Misrepair Model of cell survival, In Radiation Biology and Cancer Research (R.A. Meyn and H. R. Wihters, Eds.), 195–230, Raven Press, New York. (1980)

[Tobias 1985] Tobias CA: The Repair-Misrepair Model in radiobiology: Comparison to other models, Radiation Research, 104, Suppl. 8, S-77–S-95 (1985)

[Tsuruoka *et al* 2005] Tsuruoka Ch, Suzuki M, Kanai T, Fujitaka K: LET and Ion Species Dependence for Cell Killing in Normal Human Skin Fibroblasts, Radiation Research 163, 494-500 (2005)

[Turner 1995] Turner J: Atoms, Radiation, and Radiation Protection, John Wiley and Sons (1995)

[Uehara and Nikjoo 2006] Uehara S, Nikjoo H: Monte Carlo Simulation of Water Radiolysis for Low-energy Charged Particles, Journal of Radiation Research, 47: 1, 69–81 (2006)

[Ulmer 2007] Ulmer W: Theoretical aspects of energy-range relations, stopping power and energy straggling of protons, Radiation Physics and Chemistry, 76: 7, 1089–1107 (2007)

[Wang *et al* 2006] Wang C-K C, Zhang X: A nanodosimetry-based linear-quadratic model of cell survival for mixed-LET radiations, Phys. Med. Biol. 51, 6087-6098 (2006)

[Ward 1985] Ward JF: Biochemistry of DNA lesions, Radiat Res Suppl. 8: S103–111 (1985)

[Ward 1990] Ward JF: The Yield of DNA Double-strand Breaks Produced Intracellularly by Ionizing Radiation: A Review, Int Journal of Radiation Biology, 57: 6, 1141–1150 (1990)

[Ward 1995] Ward JF: Radiation mutagenesis: the initial DNA lesions responsible, Radiat Res. 142(3): 362–368 (1995). Erratum in: Radiat Res 143(3): 355 (1995)

[Watt 1996] Watt DE: Quantities for dosimetry of ionizing radiations in liquid water, Taylor & Francis, London (1996)

[Weyrather *et al* 1999] Weyrather WK, Ritter S, Scholz M: RBE for carbon track-segment irradiation in cell lines of differing repair capacity; International Journal of Radiation Biology 75, 1357–1364 (1999)

[Wilson *et al* 1946] Wilson RR: Radiological Use of Fast Protons, Radiology 47 (5): 487–491 (1946)

[Wolfram *et al* 2006] Wolfram RM, Budinsky AC, Pokrajac B: Endovascular brachytherapy for prophylaxis of restenosis after femoropopliteal angioplasty: Five-year follow-up - Prospective randomized study, Radiology 240 (3): 878–884 (2006)

[Wulf *et al* 1985] Wulf H, Kraft-Weyrather W, Miltenburger HG, Blakely EA, Tobias CA, Kraft G: Heavy-Ion Effects on Mammalian Cells: Inactivation Measurements with Different Cell Lines, Radiation Research, 104: 2, Part 2: Suppl 8. Heavy Charged Particles in Research and Medicine, S122–S134 (1985)

[Yamashita *et al* 2008] Yamashita S, Katsumura Y, Linc M, Muroyad Y, Miyazakia T, Murakami T: Water radiolysis with heavy ions of energies up to 28 GeV. 1. Measurements of primary g values as track segment yields, Radiation Physics and Chemistry, 77: 4, 439–446 (2008)

[Ziegler 1999] Ziegler JF: The stopping of energetic light ions in elemental matter, J. Appl. Phys/Rev. Appl. Phys., 85, 1249–1272 (1999)

Internet pages

[http://www.uzis.cz] Institute of Health Information and Statistics of the Czech Republic http://www.uzis.cz/ (cited 28. 8. 2008)

[http://www.who.int/en] World Health Organisation http://www.who.int/en/ (cited 28. 8. 2008)

[http://www.radiologyinfo.org] The public information web site developed by the American College of Radiology (ACR) and the Radiological Society of North America (RSNA) http://www.radiologyinfo.org/en/info.cfm?pg=brachy&bhcp=1 (cited 28. 8. 2008)

[http://www-bd.fnal.gov] Fermi National Accelerator Laboratory, Batavia, Illinois, USA http://www-bd.fnal.gov/ntf/what_is/index.html (cited 28. 8. 2008)

[http://www.microscopyu.com] website provided by Molecular Expressions, the Florida State University (FSU), and Nikon, Inc., (Nikon) http://www.microscopyu.com/galleries/fluorescence/ cells/cho/cho.html (cited 28. 8. 2008)

[http://seal.web.cern.ch] Math libraries, CERN http://seal.web.cern.ch/seal/work-packages/ mathlibs/minuit/home.html (cited 28. 8. 2008)

[http://www.medical.siemens.com] Siemens medical web pages, http:/www.medical.siemens.com (cited 28. 8. 2008)

[http://www.werc.or.jp] Wakasa Wan Energy Research Center, Japan http://www.werc.or.jp/english/reseadeve/activities/ therapy/protontherapy/index.htm (cited 28. 8. 2008)

[http://www.bnl.gov] Brookhaven National Laboratory, USA http://www.bnl.gov/medical/NASA/CAD/Bragg_Curves.asp (cited 28. 8. 2008)

[http://www.rndsystems.com] Biotechnological company R&D Systems http://www.rndsystems.com/ mini_review_detail_objectname_MR03_DNADamageResponse.aspx (cited 28. 8. 2008)

[http://ptcog.web.psi.ch] Particle Therapy Co-Operating Group http://ptcog.web.psi.ch (cited 28. 8. 2008)

[http://flickr.com/photos/8928507@N02/2547162058] Photo from Molecular Cell Biology course at MTSU http://flickr.com/photos/8928507@N02/2547162058 (cited 28. 8. 2008)

[http://www.unige.ch] Université de Genève http://www.unige.ch/sciences/chifi/cpb/windig.html (cited 28. 8. 2008)

[http://www.ideum.com/portfolio/zoom_dna] The interactive online exhibit, cooperation with The Tech Museum of Innovation, San Jose, California, USA http://www.ideum.com/portfolio/ 0018_zoom_dna/slides/ zoom_dna_01.jpg (cited 18. 9. 2008)

[http://hacd.jsc.nasa.gov/] Human Adaptation and Countermeasures Division (HACD), National Aeronautics and Space Administration (NASA) Johnson Space Center, Houston, Texas. Cellular and Tissue Response to Radiation Damage:
http://hacd.jsc.nasa.gov/web_docs/radiation/DNADamageLBNL.pdf (cited 26. 11. 2008)